Sediment dispersion from a moving source

A research into the influence of source speed on sediment dispersion during deep sea mining operations using small scale experiments

Koen van Pelt

Delft University of Technology

TU Delft

Sediment dispersion from a moving source

A research into the influence of source speed on sediment dispersion during deep sea mining operations using small scale experiments

by

Koen van Pelt

to obtain the degree of Master of Science
at the Delft University of Technology,
to be defended publicly on tuesday August 22, 2023 at 14:30.

Student number:	5414237	
Project duration:	November 15, 2022 – August 8, 2023	
Thesis committee:	Dr. Ir. R. Helmons,	TU Delft, supervisor
	Dr. Ir. S. Alhaddad,	TU Delft
	MSc. S. Wahab,	TU Delft
	Dr. Ir. P. Wellens	TU Delft

This thesis is confidential and cannot be made public until August 22, 2025.

Cover:	Image generated using the Midjourney A.I. image generation tool
Style:	TU Delft Report Style, with modifications by Daan Zwaneveld

An electronic version of this thesis is available at `http://repository.tudelft.nl/`.

TU Delft

Preface

This thesis marks the end of my education at TU Delft. The topic of Deep Sea Mining has interested me from the start, mainly due to the complexity of the problem and the potential impact that it might have on the environment and society. I am grateful for getting the chance to research this topic and hopefully contribute to the knowledge base regarding the impact of deep sea mining operations. Conducting the experiments was occasionally quite demanding; however, witnessing tangible results and the ability to discern trends made the effort all the more gratifying.

I want to thank Dr. Ir. Rudy Helmons for the advice and support he provided during the weekly meetings and for providing support during my experimental process. I would also like to thank MSc. Shaheen Wahab for the help during the meetings, experiments and for providing company in the lab. I would also like to thank Ed Stok and Andre van den Bosch for helping build up my experimental setup and for always being available for questions and problem solving. I would also like to thank S. Alhaddad for his feedback and help during experiments and meetings.

Lastly, I would like to thank my parents and friends for their support during my thesis, as well as for helping out with experiments and proofreading.

Koen van Pelt
Delft, August 2023

Summary

Extracting valuable materials from the deep sea holds immense potential in addressing humanity's short- and long-term goals, especially concerning the current climate crisis. One potential resource are polymetallic nodules which can be found in abyssal planes in the deep sea. One promising method for mining polymetallic nodules, which are potato-sized accumulations of metal laying on top of the seabed, involves the use of a seabed mining tool (SMT) to collect nodules from the deep seabed and transport them to a surface vessel where they are processed. During the nodule collection process, sediment is inadvertently collected as well. The excess of water and sediment which is separated in the SMT from the nodules and then discharged, leads to the creation of sediment plumes. More knowledge on responsible mining practices that minimize environmental impacts caused by sediment plumes is needed before commercial exploitation of the deep sea can begin. Higher concentrations of suspended particles resulting from the mining process can have a detrimental effect on the ecosystem, making it a significant concern. At the TU Delft dredging laboratory sediment plumes can be created in an experimental setup that allows for research into the influence of different input variables. For this research the experimental setup was extended to include a moving cart that allows for research into the influence of the SMT driving over the seabed. Understanding this parameter is essential, as recent studies have shown that a source velocity can have a significant influence on the generation of turbidity currents. However, the only existing research into source velocities employed dye mixtures rather than actual sediment particles, calling for further investigation to bridge this knowledge gap.

In this research experiments were conducted with the aim of researching optimal source velocities and release conditions that minimize sediment plume spreading during deep sea mining operations. To research this a test setup was created in the TU Delft dredging laboratory where a sediment mixture could be discharged from a moving source. The source velocity, mixture concentration, outflow geometry and discharge velocity could be altered to research the influence of each individual component. To research the influence of these parameters, various measurements were taken, i.e., ultrasonic velocity profiling was used to obtain velocity profiles of turbidity currents, a sediment trap was designed to provide an insight into sedimentation and video footage was obtained for visual inspection of the experiments. The experimental setup consists of a 25m^3 modular tank on which a moving cart was mounted. A vertical construction reaching into the water connected the cart to a setup on which different diffusers could be mounted from which a sediment mixture could be discharged. The sediment mixture, consisting of glass beads suspended in water, was mixed and kept suspended in a separate mixing tank. In total 18 experiments were conducted to capture the influence of the concentration and cart velocity.

The obtained results were analysed to find relations between the input variables and the created sediment plumes. During the experiments the sediment flux was kept equal to allow for research mainly looking at the influence of source velocity on the creation of sideways propagating turbidity currents. For lower source velocities the observed trends were as expected based on previous research. One main result was that a distinction can be made between the scenarios with the highest source velocities and other velocities. For the higher range of source velocities, a new regime was observed in which a turbidity current could not be observed, the sediment was suspended higher in the water column which in a real deep sea mining situation could lead to the sediment entering a passive transport phase. A second observation showed that none of the experiments demonstrated the turbidity current advancing in front of the impingement zone which in a DSM situation would lead to less interaction between the SMT and sediment plume.

Contents

List of Figures

List of Tables

Nomenclature

Abbreviations

Abbreviation	Definition
ISA	International Seabed Authority
DSM	Deep Sea Mining
CCZ	Clarion Clipperton Zone
TMC	The Metals Company
EEZ	Exclusive Economic Zone
ECS	Extended Continental Shelf
UNCLOS	United Nations Convention on the Law Of the Sea
SMT	Seabed Mining Tool
ZFE	Zone of Flow Establishment
ZEF	Zone of Established Flow
ADV	Acoustic Doppler Velocimetry
UVP	Ultrasonic Velocity profiling

Symbols

Symbol	Definition	Unit
g	Gravitational constant	m/s^2
g'	Reduced gravity	m/s^2
u	Velocity	[m/s
u_B	Buoyancy Velocity	m/s
u_C	Collector velocity	m/s
u_a	Ambient fluid velocity	m/s
Re	Reynolds number	-
Ri	Richardson number	-
Fr	Froude number	-
U_o	Discharge velocity	m/s
L_m	Model length	m
L_{fs}	Full scale length	m
Q_o	Volume flux	m^3/s
M_o	Momentum flux	m^4/s
B_o	Buoyancy flux	m^4/s^3
u_*	shear velocity	m/s
L_b	Buoyancy length scale	m
v_t	Settling velocity	m/s
R_{sd}	relative submerged density	kg/m^3
ρ	Density	kg/m^3
β_{nr}	Rousse number	-
μ	Kinematic viscosity	m^2/s
λ	Geometric scaling factor	-
λ_v	Velocity ratio	-
β	Spreading angle after discharge	°
α	Spreading angle after impingement	°

1 Introduction

Extracting valuable materials from the deep sea could be of significance for achieving humanity's short- and long-term goals related to the current climate crisis. Performing heavy industrial work on the seabed could however be detrimental to the ocean's ecosystem in many ways, of which most unknown. In this chapter the context for this thesis will be set. First background information will be provided on Deep Sea Mining (DSM). This background information will include the general concept of DSM, the current state and the environmental impact. Using this background information a problem analysis will be given including the problem description, research objective and related research questions.

1.1. Background

DSM includes all mineral resource extraction from the deep sea. Currently three DSM deposits have been identified/researched; the mining of metals from hydrothermal vents, mining cobalt-rich crusts, and mining polymetallic nodules [1]. The latter has been most thoroughly investigated and commercial exploitation is expected to commence in the near future, leading to a large interest from commercial and non-commercial entities in the possible impact of this DSM method.

1.1.1. Business case

On the seabed of a large section of the Pacific, potato-shaped accumulations of metals can be found. These "polymetallic nodules" are the result of the accumulation of metal particles grouping together at a rate of $\approx$ 1 mm per million years. The nodules are of interest because they contain manganese (20-30%), iron (5-25%) and copper (0.2-1.2%). Other materials of economic interest are also present at lower quantities [2]. Polymetallic nodules are typically found in deep-sea environments, particularly in areas with high levels of nutrients and low levels of oxygen, such as the Pacific Ocean's Clarion-Clipperton Zone (CCZ) (see figure 1.1), a stretch of the ocean of roughly 5 million km^2. Commercial parties are interested in extracting the polymetallic nodules from the deep sea for several reasons;

1. The metals found in polymetallic nodules can be of great importance for technologies used in the energy transition from fossil fuels to renewables.
2. DSM would provide a new primary source of critical raw materials, such as rare earth elements and precious metal, that are in high demand. This could help to reduce dependency on certain countries for these resources, potentially leading to increased economic and political stability.
3. Problems occurring in terrestrial mining operations, such as child labour and deforestation, could be mitigated.

Deep sea mining is a relatively new industry and is still in its infancy. Since the late 20th century, the number of companies involved in DSM activities has been steadily growing. A recent (Nov 2022) sea trial conducted by a partnership of ALLSEAS and The Metals Company collected 4500 tonnes of nodules at a rate of 86.4 tonnes/hour [3]. These operations also led to backlash from non-governmental organizations such as Greenpeace [4]. Several nations have also expressed concern, with the French government proposing an altogether ban on DSM and the German government asking for a pause on

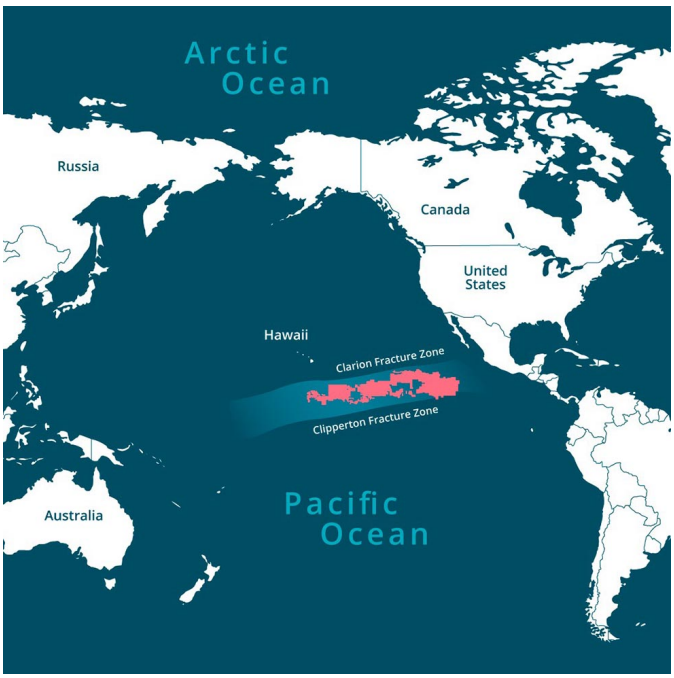

Figure 1.1: Location of the Clarion-Clipperton zone [7]

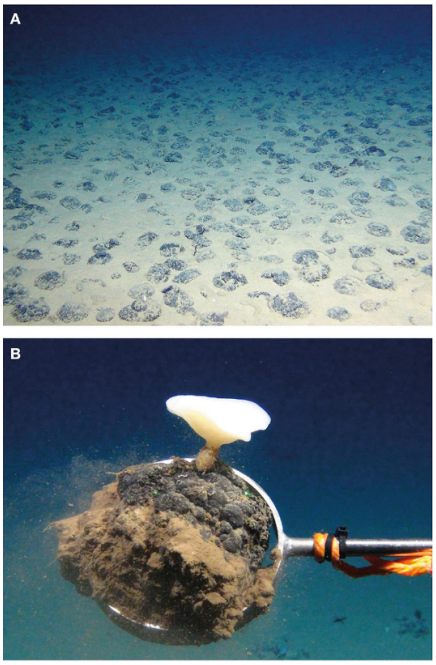

Figure 1.2: A: Scattered Nodules on seabed
B: Nodule with biological growth [8]

the commencement of commercial nodule extraction until the environmental impact is better understood [5][6]. All materials that can be found outside of the Economic Exclusive Zone (EEZ) and outside of the Extended Continental Shelf (ECS) of sovereign states, including the CCZ, are considered a common good. According to the United Nations Convention on the Law Of the Sea (UNCLOS) the resources to be found in the Deep sea are considered a 'common heritage of humankind'. In order to ensure fair distribution and stewardship of the oceans, the International Seabed Authority (ISA) was established.

1.1.2. Polymetallic nodule harvesting

Since the late 70s, various countries and companies have attempted various methods and equipment to collect polymetallic nodules from the seabed [9]. The designs have since then converged into one commonly used setup containing several stages:

1. A remote-controlled collector vehicle on the seabed (see figure 1.3)
2. A system transporting the nodules vertically, often using either a riser pipe using hydraulic transport or airlift
3. A surface vessel from where the offshore operations are led and on which the nodules are dewatered

Figure 1.3: Envisioned collector vehicle Blue Nodules [10]

Various concepts for collector vehicles exist, which mainly vary in the method of picking the nodules from the seabed. There are three different types of collecting methods; mechanical, hydraulic, and hybrid [11]. Mechanical systems are comparable to the systems installed in combine harvesters, this system has high efficiency paired with low reliability. The hydraulic systems use water jets or the Coandă effect to lift nodules, which gives a higher reliability. The hybrid systems use a combination of water jets with mechanical components. Depending on the collecting mechanism an amount of surrounding (unwanted) sediment is collected. This sediment is, after separation from the nodules, discharged through the back of the collector vehicle. The dimensions of the vehicle differ for each concept. A concept developed by Blue Nodules has a vehicle width of 16 m moving at a velocity of 0.5 m/s. In figure 1.3 an illustration of the collector vehicle from blue nodules is given. In this figure, the nodules enter on the left using a hydraulic collecting system. Then the nodules are separated from the sediment and excess of entrained water and transported through the riser system. The sediment is discharged through the pathway displayed with blue arrows in figure 1.3 [12].

1.1.3. Environmental impact

Whilst DSM could be beneficial in some areas, it also has the potential to have significant negative impacts on the environment. The deep sea is a harsh environment with no sunlight, extreme temperatures, high pressure, and low oxygen levels. Due to the lack of light, most of the organisms living there rely on chemosynthesis instead of photosynthesis for energy. Most of the organisms found in the deep sea are unknown to science. During the drafting of UNCLOS, the abyssal planes were assumed to be low in ecological value. Since then, a small number of studies were conducted that have found high biodiversity in the CCZ, and more research is needed to get an actual view of the ecosystem in the deep sea. As an indication of the knowledge available, a field study by Amon et al. (2022) found that over 50% of ecological specimens encountered in the CCZ over 2 cm in size were of a species not yet discovered [13].

There are several ways in which the deep sea ecosystem could be impacted by DSM operations. Local effects, such as light and noise pollution, can have an impact on benthic organisms [14]. Another environmental problem, potentially impacting the largest area, is the collection and consequent discharging of surrounding sediment during nodule collection, which will create sediment plumes. When the small sediment particles are suspended, they can travel over large distances due to ocean currents. The fauna in the area is not accustomed to higher sediment levels, and the increased concentrations can have an impact by burying organisms and disrupting respiratory processes of marine fauna, which will have an impact on their chemosynthesis processes. Lastly, locally, at the mining site, DSM operations will destroy the ecosystem by removing nodules and thereby disrupting a part of the deep sea ecosystem. It is unknown to what extent and on what timescale fauna will recover in a mined area. However, it is expected to require a time period in the order of decades [15][8]. One example of this is a study conducted by Stratmann et al. researching an area where DSM trials were conducted 26 years prior. They concluded that, at present, the ecology had yet to recover to pre-mining levels [16]. Aware of these problems, a consortium of European countries/companies designed a vehicle for which calculations and tests were conducted. The consortium, Blue Nodules, has the aim of designing a sustainable DSM operation. They concluded that most sediment settled in the mining area, small concentrations of finer particles were found to travel much greater distances [10]. The concentration measured was close to the background sediment deposition in the CCZ.

1.2. Problem statement

Whether DSM operations should commence is highly debated. One of the main arguments by opponents of DSM is the potential impact of sediment plumes on the deep sea ecosystem. Uncertainty on the extent and impact of sediment is a large contributor to the discussion. Within DSM regulators and companies, there is a strong emphasis on minimizing the environmental impact. According to Weaver et al. (2019) the three largest issues facing deep sea mining are [17]:

1. Lack of scientific knowledge of deep-sea ecosystems
2. Lack of knowledge on the performance of new technology
3. Lack of regulatory framework

In an attempt to work on these issues many institutions, among whom TU Delft, have been working together with industry and regulatory bodies. One research area at TU Delft includes small-scale experimental research into sediment plumes. In an attempt to control/minimize the impact of the sediment plumes research has been conducted on plume generation/spreading and the influence of controllable variables such as sediment concentration, outlet (diffuser) geometry, and diffuser height. At the TU Delft dredging laboratory, research has been conducted using small-scale experiments on the following three variables;

1. Different diffuser geometries [18]
2. Diffusor height on the SMT [19]
3. Volumetric concentration of discharge mixture [20]

The small-scale experiments were conducted using a 25m^3 tank located at the dredging laboratory at TU Delft as seen in Figure 1.4. In these experiments, sediment discharge from a static source was investigated. Due to a short experiment duration (± 3 per day) many experiments can be conducted, which allows for researching the influence of different input variables.

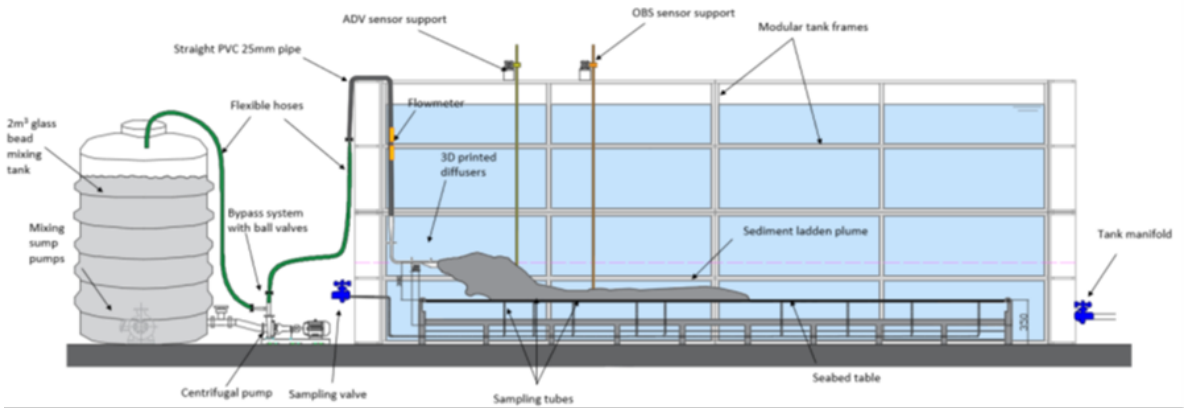

Figure 1.4: Experimental setup dredging laboratory [18]

When researching sediment plume characteristics, it is important to know which parameters are of importance. Oullion et al. (2023) suggest that there are three competing processes that influence sediment plume creation during the discharge phase [21]:

1. The turbulent wake produced by the collector vehicle
2. The turbulent jet produced by the discharge outflow
3. The negative buoyancy of the discharge

The preceding small-scale experiments were used to research plume creation based on the turbulent jet and the negative buoyancy aspects. In order to incorporate first process, the turbulent wake, a moving source has to be created in the experiment setup. Another aspect of interest is the characteristics of the plume with different initial horizontal velocities. All research at TU Delft so far has been conducted using a stationary outflow, which is not representative of the real-life situation in which a collector vehicle is discharging a mixture whilst driving on the seabed. The research on moving systems is limited, with one publication by MIT in which a combination of numerical simulations and small-scale experiments were conducted on the influence of the source speed and buoyancy velocity on sediment plume behaviour [22]. The influence of the source speed was researched by changing the ratio of buoyancy velocity (u_b) and source velocity (u_c). In this, the buoyancy velocity represents the velocity at which sediment plumes move when in a plume state. Ouillion et al. (2023) determined that in a collector system with a width of 10 m and a velocity of 0.5 m/s, the ratio of the background flow speed to the plume centerline speed (u_c/u_b) will significantly influence plume spreading. Their findings suggest that the source speed is a key factor to consider in the design and operation of collector vehicles. To arrive at this conclusion, the researchers conducted experiments in a towing tank equipped with a traversing setup that discharged a dense dye mixture as depicted in Figure 1.5. A camera setup was used to gather data on the geometry of the sediment plumes following discharge.

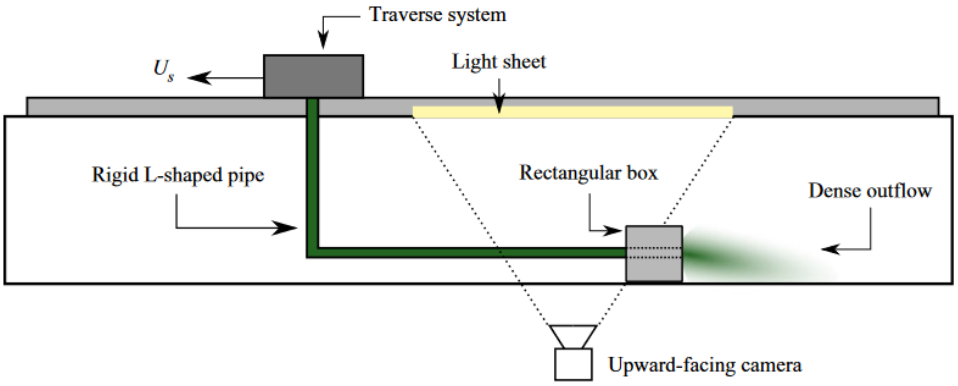

Figure 1.5: Experimental setup used by Oullion et al [22]

Figure 1.6 shows a set of results obtained using the experimental setup used by Oullion et al. From figure 1.6 it can be observed that a decrease in "*a*"(u_c/u_b), i.e. when the buoyancy velocity relative to the source velocity increases, will result in a higher gradient of plume spreading. The difference in spreading rate could have an impact on the resulting footprint of the sediment plume.

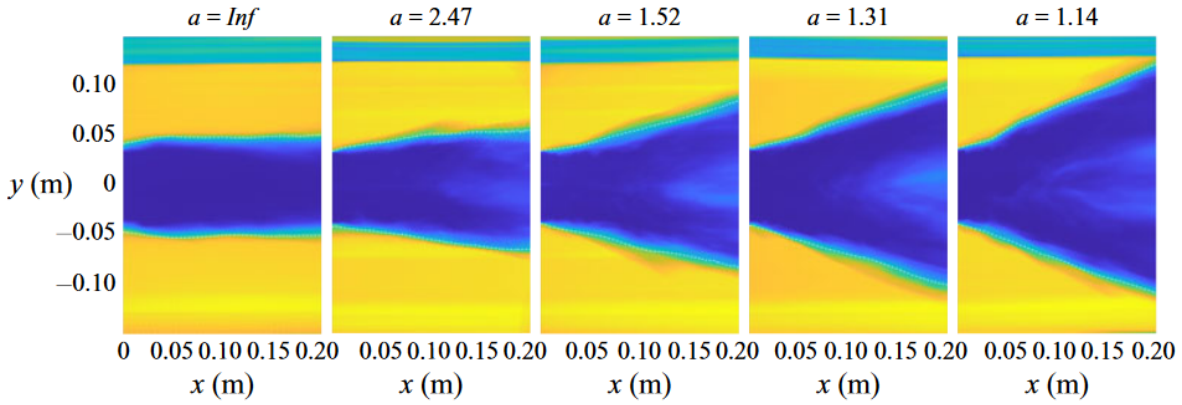

Figure 1.6: Bottom view of experimental tests showing plume front position conducted by Oullion et al. [22]

The research into sediment plume dispersion has been extensive. However, it has mostly been limited to a stationary discharge source, with the exemption of the research conducted by Oullion et al. In order to assess the impact of sediment plumes as accurately as possible it is necessary to model all physical phenomena occurring during DSM operations. The research by Oullion et al. concludes that there are physical phenomena that are based on the velocity of the collector vehicle, which implies that the experiments conducted at TU Delft could be improved. Another gap in the research is that there has been no experimental research into a moving source discharging an actual sediment mixture, the only experiments conducted to date have used a dye and density differences based on salinity. Using dye provides the possibility to research the interaction between the discharged fluid and the ambient fluid, however, a big part of the potential impact of sediment plumes is due to sediment settling.

1.3. Research objective

The goal of this research is to combine the existing knowledge accumulated by the previous small-scale experiments at the TU Delft tank into an experimental setup implementing a moving source. The research objective has been defined as:

> "To find the optimal source velocity and release conditions leading to the least sediment plume spreading during deep sea mining operations using small scale experiments"

The research will consist of small-scale experiments conducted in the dredging laboratory tank. Using a new setup in which a variable source speed can be modelled. During this research experiments will be conducted based on input variables that can be controlled during DSM operations/design:

1. Source velocity
2. Discharge velocity
3. Concentration discharge mixture

The influence of these variables will be researched by measuring several plume characteristics during and after the experiments. The environmental impact of the plumes is largely related to several parameters that are therefore of interest for measurements:

1. Volumetric concentration of discharge mixture
2. Deposition of sediment
    - Footprint [m^2]
    - Deposition [mm]

3. Velocity of sediment plumes
4. Dispersion of suspended sediments

By measuring the deposition characteristics, new data can be gathered regarding sediment plume dispersion with a moving source. Using the moving source setup also provides the opportunity to measure/research new plume characteristics. One of these is that during DSM operations the forward movement of the SMT will create a wake, which will influence the flow behind the SMT, and could therefore also have an impact on the discharged sediment. With this setup, the experiments and simulations conducted by Oullion et al. [22] can be continued by using a sediment mixture instead of dye and by measuring more plume characteristics.

1.4. Research questions

To achieve the research objective, it is necessary to address several sub-questions, which include:

1. What experimental setup would be optimal to investigate plume spreading in a moving source experiment?
2. How will the ratio of source and discharge velocity impact the footprint and deposition of sediment plumes?
3. How can modifying the source velocity, mixture concentration, and discharge velocity be used to reduce the plume dispersion in polymetallic nodule harvesting operations?

A significant part of this research will be designing an experimental setup that can be implemented in the facilities at the TU Delft dredging lab, and that will provide relevant research results. The answer to the first research question will therefore be the overall testing setup and the accompanying experimental matrix. Research question two embodies the core of this research. Using the resulting setup from research question one, results will be obtained which will be analyzed. If results are accurate, conclusions can be made on what parameters influence sediment plume dispersion in what way. The last research question combines the previous research questions. The answer to this question will be advice on how the results obtained by the small-scale experiments could be translated to real-life operations.

2

Literature review

In this chapter, the available theory and research relevant to answering the research questions will be discussed. This chapter will exclusively offer an overview of research available in literature. The chapter will include a review of scaling theory, which is necessary for designing valid experiments. Consequently the available literature on turbidity plumes, the physical phenomena at the center of the experiments, will be discussed. Then research into the wake produced by moving objects will be discussed to provide information useful for answering the research question related to turbulent wakes. Experimental measurement techniques will be discussed in the last section of this chapter to provide more information necessary for designing the final experiments.

2.1. Sediment mixture discharge

Discharging a sediment-laden mixture from an SMT will induce interaction between two different fluids; the ambient fluid and the sediment mixture. A difference in fluid properties such as density, temperature and salinity combined with an initial momentum will result in dynamic interaction between the two fluids. In DSM situations the difference in density will yield a gravity flow, which is defined as a deformation of sediment-water mixture due to applied shear stress (gravity). A distinction can be made between fluid-gravity flow, in which gravity acts on the fluid itself, and a sediment-gravity flow, where gravity acts on the individual particles suspended in the fluid. Shanmugam (2020) identified six types of gravity flows each with separate characteristics, of which the turbidity current describes the DSM situation best. Shanmugan also describes several flow attributes for a turbidity current; the fluid must have a Newtonian rheology, volumetric concentration of $< 9\%$, flow density of $\approx$ 1.1 g/m^3 and deposition by settling [23][24]. In mixtures with a volumetric concentration above 9% the distance between individual particles becomes too small, leading to interaction between particles resulting in a non-homogeneous mixture leading to a grain or debris flow.

Flow of one fluid through another can be generated by either momentum or buoyancy. At discharge, in situations with high discharge velocity, the flow is governed by momentum and called a turbulent jet, during the transition from momentum-driven to buoyancy-driven it is called a buoyant plume and when fully governed by buoyancy it is a turbidity current. The different stages are displayed in figure 2.1. What type of flow occurs after discharge depends on the discharge parameters.

A second distinction can be made between the near-field and far-field regions. The three stages; turbulent/buoyant jet, impingement area, and gravity current, are part of the near-field region. The near-field has a length scale of up to a few hundred meters, with an accompanying time scale of seconds to minutes. For comparison between the momentum and buoyancy-driven phase the Richardson number (equation 2.1) can be used. The Richardson number describes the ratio of buoyancy over shear stress. When Ri > 1 the flow is buoyancy dominated and when Ri < 1 the flow is momentum driven.

$$Ri = \frac{g\Delta\rho/\rho_0 L}{U_0^2} \tag{2.1}$$

In the far-field region the turbidity current, in this stage often called a plume, is mainly influenced by deep-sea environmental characteristics, such as background currents and topology. Far-field plumes typically last days and can be in the length scale of kilometers [25].

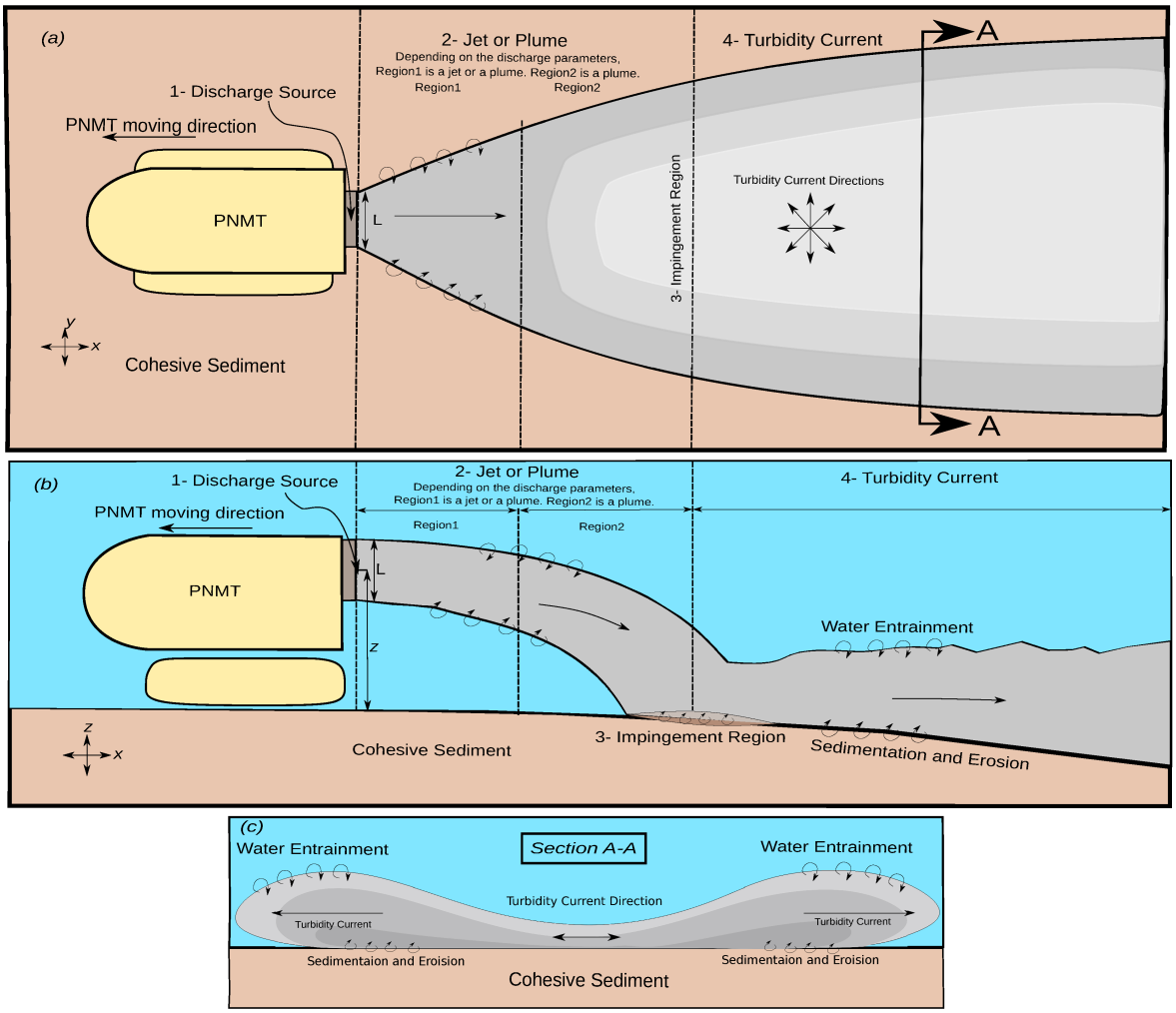

Figure 2.1: Evolution of sediment flow after discharge where (a) provides a top view and (b) a side view [26]

2.2. Scaling theory

When attempting to represent real-life DSM operations using small-scale experiments a scientific scaling approach needs to be used. Scaling is often used to cost-effectively research complex physical phenomena without having to use computational methods or full-size prototypes. When designing a scaled experiment the goal is to reach a certain level of similitude, this similitude can be of geometric, kinematic or dynamic nature. When full similarity is reached the model will provide reliable scaled-down results that can be translated to full-size results. Geometric scaling is satisfied when the ratio of corresponding lengths and angles is equal, this ratio is referred to as the geometric scaling factor λ_L as given in equation 2.2, where L_m is the model length and L_{fs} is the full scale length. Kinematic similarity requires that the motions of the two systems are kinematically similar and dynamic similarity exists when length, time and force ratios are similar [27]. For scaling methods, dimensionless numbers are used. The most common in fluid dynamics are the Froude number and the Reynolds number. The Froude number is defined as the ratio of the flow inertia over the external forces and is defined as in equation 2.3. The Reynolds number is defined as the ratio of inertial forces over the viscous forces and is defined as in equation 2.4. By keeping dimensionless numbers equal there is the ability to produce scaled down experiments whilst maintaining similar flow behaviour. Due to both dimensionless

numbers containing a velocity term, scaling of velocity poses a challenge. If the velocity were to be scaled according to Froude the velocity ratio, λ_v, would be equal to $\sqrt{\lambda_L}$, and for Reynolds scaling $\frac{1}{\lambda_L}$. Obtaining both Froude and Reynolds scaling would require a different viscosity fluid as suggested by Imran et al. [28].

$$\lambda = \frac{L_m}{L_{fs}} \quad (2.2) \qquad Fr = \frac{u}{\sqrt{gL}} \quad (2.3) \qquad Re = \frac{\rho u L}{\mu} \quad (2.4)$$

Starting small-scale experiments should therefore always commence with choosing what scaling approach is to be used. Reynolds scaling is often applied in research into fully-enclosed flows. For physical effects concerning free-surface flows gravity aspects are of importance, therefore most experiments researching sediment flows have used a Froude scaling approach. The aim of this research is to research the spreading of the plume and the physics related to the settling of sediment, experiments using scaling based on the Froude number would be optimal. In research into sediment plumes, the Froude number is often replaced by the densimetric Froude number (see equation 2.5). In this equation, the gravity is replaced by the reduced gravity defined by equation 2.6, where ρ_a is the density of the ambient fluid and ρ is the density of the sediment mixture. The densimetric Froude number gives an indication on whether intertial of gravitational forces are dominant. At a densimetric Froude number above 1 a flow is supercritical, which indicates a flow in which enough energy is present to keep sediment suspended. A densimetric Froude number below 1 indicates that gravity, or negative buoyancy, forces are dominant.

$$Fr = \frac{u}{\sqrt{g'h}} \quad (2.5)$$

$$g' = g\frac{|\rho - \rho_a|}{\rho_a} \quad (2.6)$$

The Reynolds and Froude number describe certain characteristics of a fluid that are of importance to the physical phenomena occurring. Reynolds and Froude both have regimes that can be identified in which the flow has different characteristics. The Reynolds number can give an indication on whether a flow is in turbulent, transitional, or laminar flow. According to White (2016) multiple approximate ranges occur inside pipeline flow, as shown in table 2.1.

$100 < Re < 10^3$	Laminar
$10^3 < Re < 10^4$	Transition to turbulence
$10^4 < Re < 10^6$	Turbulent, moderate Re dependence
$10^6 < Re < \infty$	Turbulent, slight Re dependence

Table 2.1: Reynolds number flow regimes [27]

When the Reynolds number is not correctly scaled it could lead to dissimilarity. Imran et al (2017) researched the limitations of Froude scaling in turbidity current research. In a purely depositional turbidity current scale-invariant results could be obtained. With scale-invariance meaning that the scaling laws and physics do not change [28].

2.3. Near-field flow

After nodules are collected by an SMT nodules and sediment are separated. Sediment, suspended in water, is then discharged from the SMT at a discharge velocity U_D. The discharge can result in a sediment mixture traveling through the ambient fluid with a relative velocity difference. The current DSM plan expects a discharge velocity equal to the forward velocity,U_C, of the SMT. This case would lead to a situation without a momentum-driven phase as the relative velocity of the mixture with the ambient fluid would be zero. The case in which $U_D > U_C$ is still possible and is likely to occur in experiments in which a flow is discharged from a stationary source, or in DSM operations if a higher discharge speed is deemed beneficial. Important conditions describing the outflow characteristics are the momentum flux M_o, Buoyancy flux B_o, volume flux Q_o and reduced gravity. These three variables, assuming that the flow is turbulent, have been found to be governing the dilution of a buoyant jet [29].

$$Q_0 = A \cdot U_D \qquad (2.7) \qquad M_O = Q_O \cdot U_D \qquad (2.8) \qquad B_O = Q_O * g'_O \qquad (2.9)$$

The area between the source and six jet diameters is called the zone of flow establishment (ZFE). The zone of established flow (ZEF) occurs after the ZFE and continues whilst the density decreases (see figure 2.2). In the ZEF the velocity and concentration profile can be represented by equation 2.10 and the length can be approximated as $6.2 \cdot D_o$, with D_o the diameter of a circular orifice [30]. In this equation, w is the velocity with w_m being the centerline value, x the transverse coordinate, and b_w a shape factor.

$$w = w_m f(\frac{x}{b_w}) \qquad (2.10)$$

At the interface with the ambient fluid entrainment will occur. A characteristic length scale can be approximated using natural length scales. By conducting a dimensional analysis Chen found that the momentum length scale L_m, which describes the distance of momentum-dominated flow, can be characterized by equation 2.11 [30][31].

$$L_m = \frac{M^{3/4}}{B^{1/2}} = \frac{M^{1/2}}{u_a} \qquad (2.11)$$

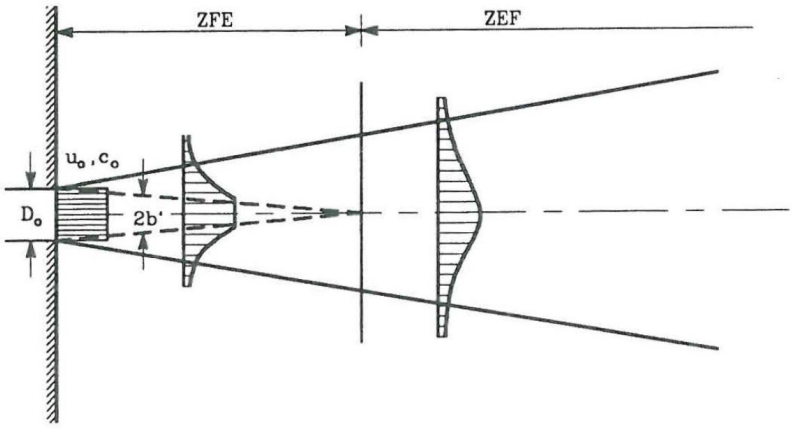

Figure 2.2: Turbulent jet characteristics [30]

Munoz-Royo et al. (2022) conducted research, including in-situ studies using a collector vehicle, and found that the flow near the discharge is dominated by the turbulence induced by the wake of the SMT. The Froude number of the discharge can give an indication of whether wake turbulence dominates negative buoyancy (Fr > 1) or if buoyancy dominates (Fr< 1). Munoz-Royo et al. found that for the collector vehicle used in the research, the densimetric Froude number was $\approx$ 2.3 [32].

2.3.1. Impingement area

In the impingement area, the sediment flow collides with the ocean bed, leading to a wall-bounded flow. The physics occurring in the interface are not studied extensively, most research focuses on the characteristics of the turbulent jet itself and not on the interaction with a horizontal plane. Roberts et al. (1997) describe that the mixing during and after impingement is complex and depending on a range of different physical phenomena; gravitational mixing, entrainment by vortices, and mixing at jet edge [33]. The turbidity current is expected to propagate in all directions through radial spreading. This radial spreading, as displayed in figure 2.3 can be divided into multiple phases as time increases as described by Papakonstantis and Christodoulou (2010) [34];

1. At small time scales, it can be assumed that radial momentum is the dominant variable
2. After some time the radial momentum balances out with the inertial forces which leads to a constant velocity phase
3. Buoyancy takes over as the main driver of propagation.

4. A balance between force due to buoyancy and drag force is reached

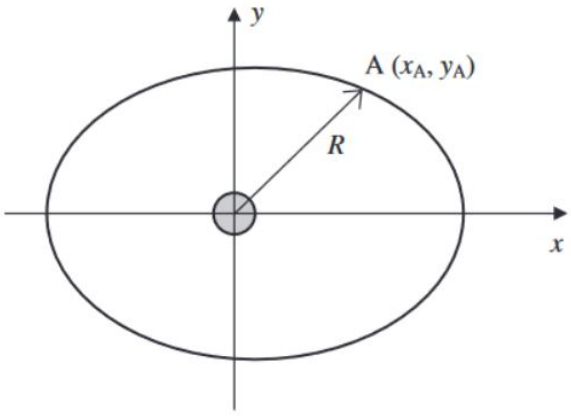

Figure 2.3: Directional propagation of turbidity current [34]

During the propagation and particle settling in the gravity current the Rouse number, β_{nr}, is of interest. β_{nr} is defined as the ratio of settling velocity to shear velocity.

$$\beta_{nr} = \frac{\omega_s}{k \cdot u_* \cdot \lambda} \tag{2.12}$$

In which u_* is the shear velocity, k the von Karman constant, and λ a dimensionless mixing length scale. The Rouse number can give an indication of whether sediment suspension is maintained. When $\beta_{nr} < 1$ the sediment is kept in suspension. The Rouse number can also be used to provide an equation for the sediment concentration over height as given in equation 2.13 [35].

$$\phi = \phi_0 e^{-\beta_{nr} \frac{z}{h}} \tag{2.13}$$

In which h is the flow height and ϕ is the volumetric sediment concentration. Many experiments have been conducted in which velocity and density profiles were created for sediment-laden turbidity currents using experiments. Wells (2021) conducted a review on this research and combined the results of different experiments, which are plotted in figure 2.4.

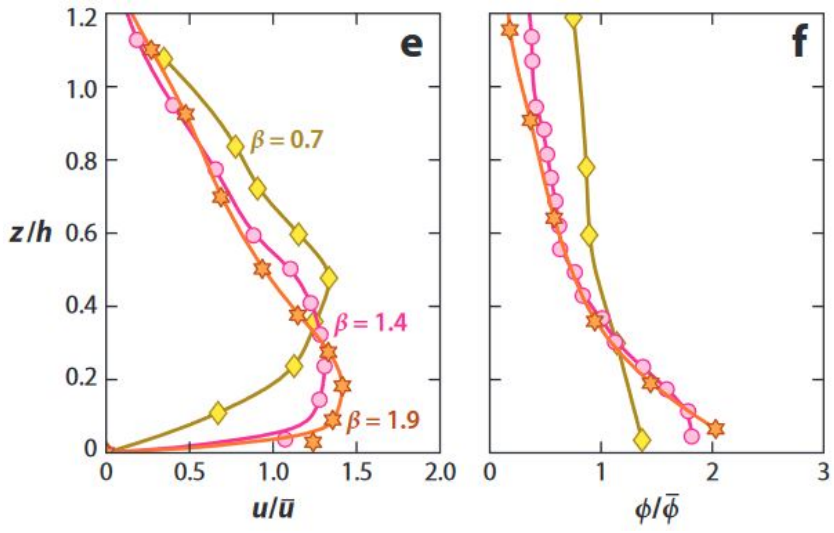

Figure 2.4: Velocity (u) and density (ϕ) profiles [36]. Yellow =[37], orange = [38], Pink =[39]

The state of a turbidity current can also be described by the densimetric Froude number. The Froude number can give an indication of whether a flow is subcritical, critical, or supercritical. Flow velocity

profiles can differ greatly for different Froude number regimes. For turbidity plumes, this difference in regime can have an impact on the suspension of sediment and will have an impact on the sediment deposition [40]. Turbidity currents with supercritical flows have a maximum velocity closer to the seabed, leading to more erosion [41]. Supercritical flow also leads to more mixing with the ambient fluid (entrainment), the mixture being more turbulent, and therefore also ensures a homogeneous mixture [42].

2.3.2. Turbidity current

A flow can be called a gravity current, or plume, when the initial momentum has gone. The parameters which influence the plume are the buoyancy flux, distance, and viscosity [29].As for the turbulent jet, there is a characteristic length scale, L_b, that gives an indication of the distance where the buoyancy-induced velocity has decayed to the ambient velocity [30].

$$L_b = \frac{B}{u_a^3} \tag{2.14}$$

Using gravity surge experiments, Middleton (1993) conducted research into the different aspects of a gravity current; the head, body, and tail. The section propagating into the ambient fluid is referred to as the head of the gravity current. Behind the head, vortices are generated due to velocity shear and ambient fluid. The turbulence induced by the vortices results in entrainment of ambient water into the gravity current, leading to dilution. The dilution rate can be modeled by a dimensionless entrainment ratio. This entrainment ratio is dependent on Re and mainly densimetric Fr. When Fr > 1 entrainment is large, whilst for Fr < 1 entrainment is small and the turbulence due to friction with the seabed is dominant. [42][36].

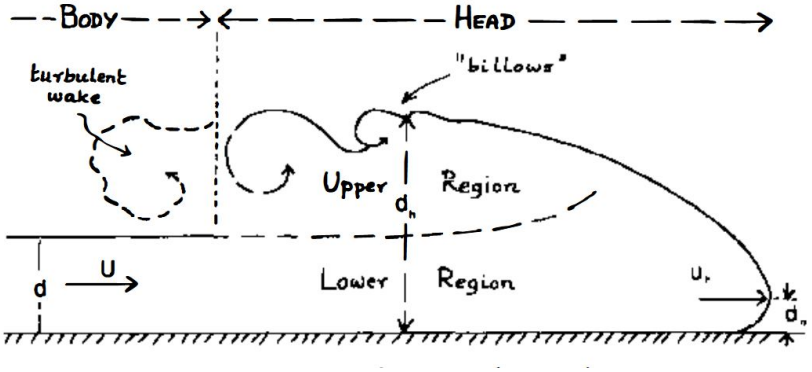

Figure 2.5: Plume characteristics [42]

2.4. Sediment

Whilst harvesting polymetallic nodules using an SMT surrounding sediment is collected. The amount of sediment collected depends on what type of collector system is used, hydraulic or mechanical, and what collector settings are used. The exact amount of sediment ”by-catch” is often not communicated for new collector designs [22]. After harvesting the mixture of water, nodules and sediment is separated in the SMT where-after the nodules, and still a small amount of sediment, are transported upwards through the riser system and the remaining sediment is discharged in the wake of the SMT. The sediment flux in the discharge will be a direct result of the speed, mining width and cutting layer depth. A hydraulic collector used by GSR was found to discharge 12 ± 3 kg/s at a collector speed of $\approx 0.3m/s$ with a collector width of $\approx$ 4m [32]. Burns (1980) calculated, for technology from the 70s, that for a 5000 ton/day production of nodules 35000 mt of sediment will be discharged within 20 m of the seafloor [43].

The sediment surrounding the nodules in the CCZ is a mixture of clay, silt and sand. Several studies have been conducted on sediment compositions and characteristics in the CCZ. Table 2.2 presents the results of several sediment composition studies. Several aspects of the sediment are of interest regarding sediment plumes. The density and shape/size have an influence on the settling velocity of

Name of Sediment Fraction	Diameter Limits (Micro) WRB Classification	GSR Data Average (%)	NTNU Data BC062 (%)	NTNU Data BC064 (%)	IOM Data Average (%)
Clay	<2	12	11.3	14.5	23.24
Silt	2–63	76.2	85.7	82.5	70.36
Sand	63–2000	11.8	3	3	6.13

Table 2.2: Distribution of sediment types in the CCZ [44]

the particles. There are multiple computation methods to calculate the settling velocity for different regimes and particle sizes as desribed by Miedema (2019) [45]:

- Stokes; laminar flow and d<0.01 mm.

$$v_t = 424 \cdot R_{sd} \cdot d^2 \tag{2.15}$$

- Budryck; transition flow, 0.1<d<1 mm.

$$v_t = 8.925 \cdot \frac{(\sqrt{1 + 95 \cdot R_{sd} \cdot d^3}) - 1}{d} \tag{2.16}$$

- Rittinger; Turbulent flow, d>1 mm.

$$v_t = 87 \cdot \sqrt{R_{sd} \cdot d} \tag{2.17}$$

- Zanke; Transitional flow

$$v_t = \frac{10 \cdot v_1}{d} \cdot \left(\sqrt{1 + \frac{R_{sd} \cdot g \cdot d^3}{100 \cdot v_1^2}} - 1 \right) \tag{2.18}$$

In which R_{sd} is the relative submerged density defined by $R_{sd} = \frac{\rho_1 - \rho_a}{\rho_a}$. In figure 2.6 an overview of settling velocities for the different theories is provided.

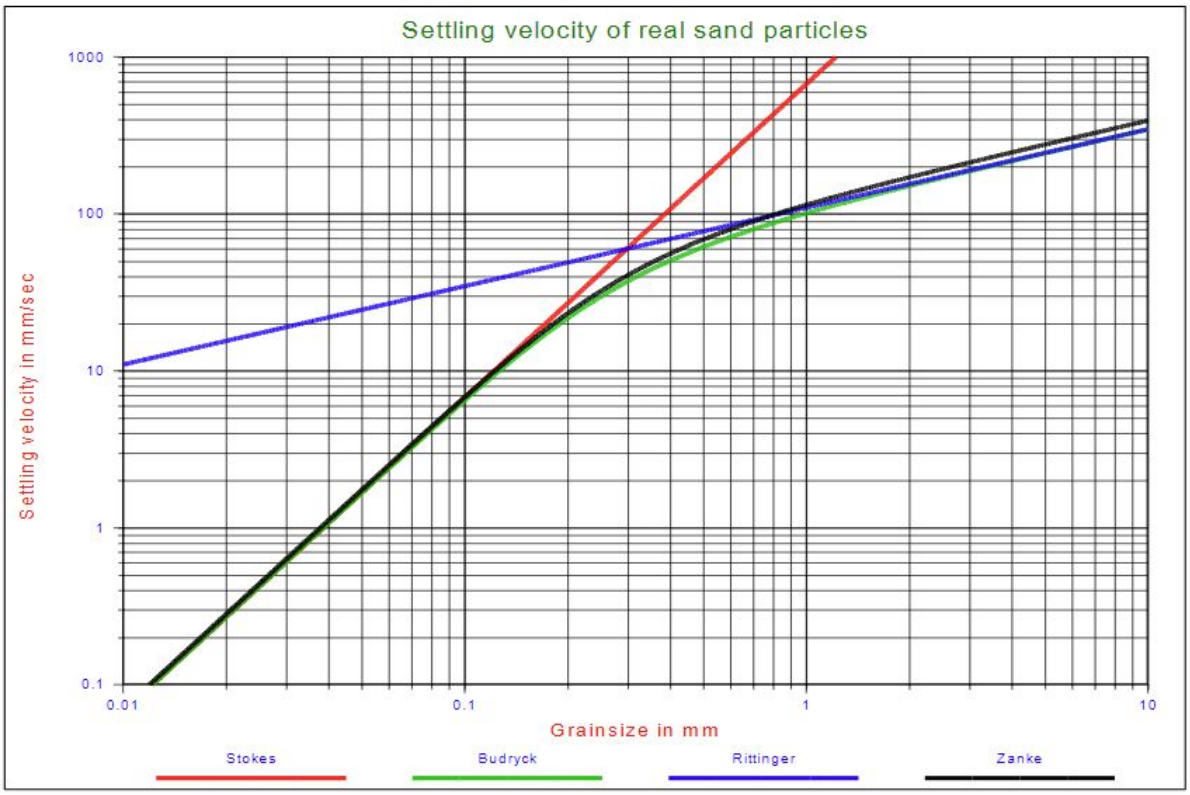

Figure 2.6: Settling velocities for different theories [45]

2.5. Sediment traps

Sediment traps are a measuring method used in the maritime field to measure vertical sediment settling quantities. In turbidity research sediment traps could be of interest when determining the particle deposition. Sediment traps for offshore applications commonly use a conical funnel gathering the settled sediment in a removable tube. Figure 2.7 shows a commonly used sediment trap design. Gardner (1980) divided the designs for sediment traps into five categories; cylinders, funnels, wide-mouthed jars, containers with bodies wider than the mouth and basin-like containers with width much greater than height [46]. For specifically cylinders Gardner (1979) conducted research into what height-to-width ratios would have the highest efficiency and found that in flows of up to 15 cm/s a H/W ratio between 2 and 3 yield the best results. The reasoning for this lays mostly in that traps should be deep enough to prevent eddies from reaching the collected sediment [47].

Figure 2.7: Common sediment trap design [48]

Research has been conducted into the efficiency of sediment traps and the induced flow disturbance. Gardner (1980) conducted research into efficiency of different geometry sediment traps suspended in the water column [46]. The results in efficiency are displayed in figure 2.8. The research shows that cylindrical shapes and segmented boxes performed close to optimal efficiency.

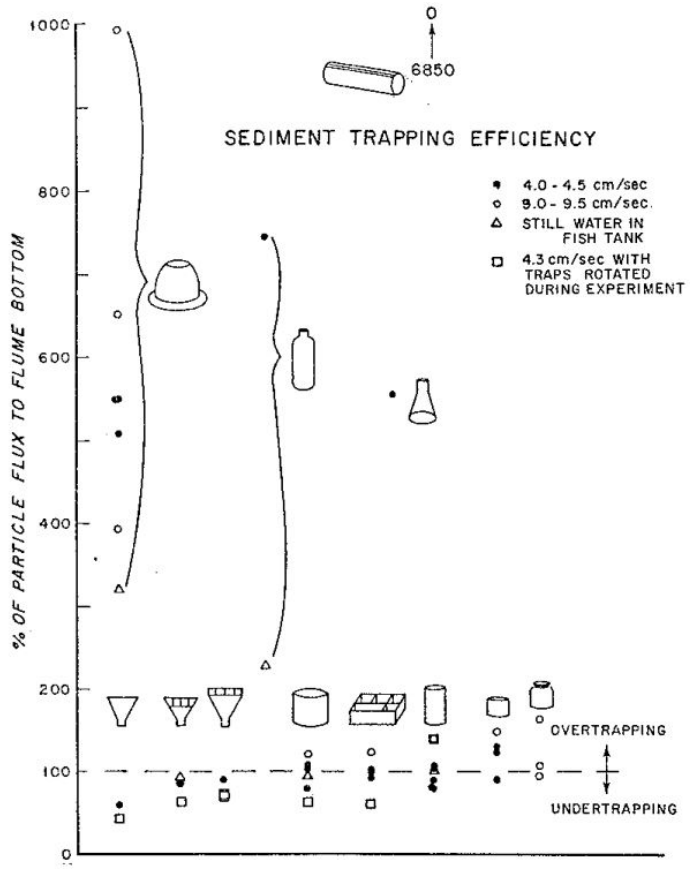

Figure 2.8: Efficiency of different sediment trap geometries [46]

2.6. Discharge from moving sources

DSM-related research into moving source discharges is limited, with the only known published experiments conducted by Oullion et al. which have briefly been discussed in the introduction. Research from other sectors could be of interest, for example the dredging industry. Research conducted by Decrop et al. used experiments to research the discharge of sediment mixtures in a crossflow in an attempt to investigate sediment discharge from a moving dredging vessel. In figure 2.9 the experimental setup used is shown. In the experiments, the relation between background current and discharge velocity was researched. This situation is however more related to a DSM midwater plume discharge and does not include the interaction with the seabed, which is an important factor for SMT discharges. For the experiments in this research, a Froude scaling approach will be used. For the Reynolds number, a minimum value of 4148 was maintained to ensure turbulent outflow at the discharge [49].

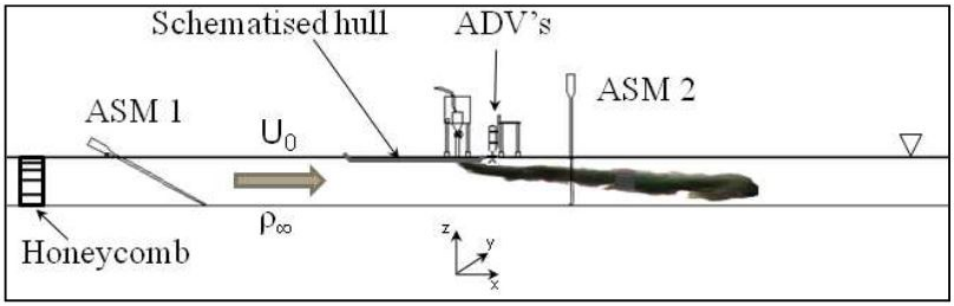

Figure 2.9: Experimental discharge Decrop et al. [49]

The research conducted by Oullion et al. found that the ratio of cart velocity to buoyant velocity had a large effect on the dispersion of the plume. In the research different regimes were found for different

ratios of a (U_c/U_b):

$a \leq 0.63$	Flow spreads radially
$a \geq 0.63$	Supercritical regime is entered, source propagates faster than gravity current.

Table 2.3: Regimes for values of a

When the supercritical regime is entered the sediment plume obtains a wedge shape behind the moving source. Figure 2.10 shows the difference of y_fr, which is the front of the turbidity current, with an increasing value of *a*. In the figure the difference between the two regimes mentioned in table 2.3 can be recognized [22].

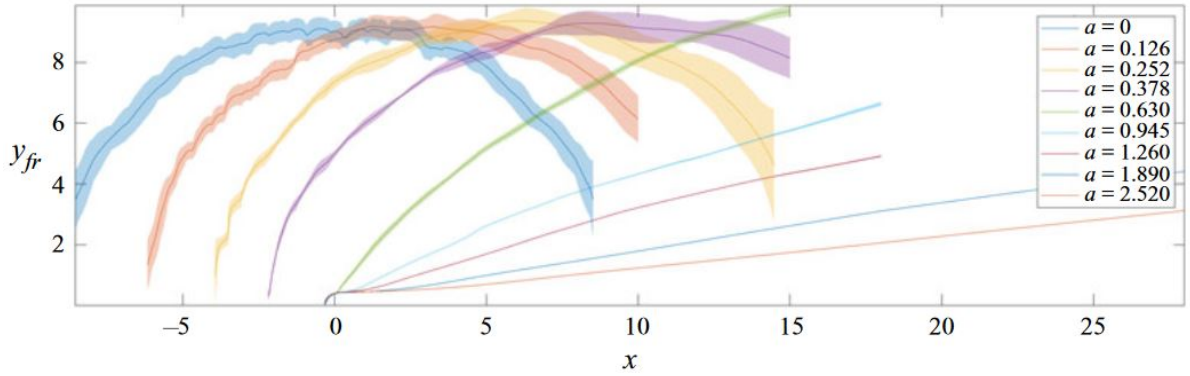

Figure 2.10: Buoyancy front evolution with increasing value of *a* [22]

2.7. Turbulent wake in DSM operations

Sediment plumes are dependent on the velocity profile of the ambient fluid. During DSM operations it cannot be assumed that the ambient fluid is motionless. One reason for this is the wake created by the forward displacement of the collector vehicle. A wake can be described as a region of disturbed flow formed behind a moving object. This disturbance is the result of the changes in pressure and velocity around an object leading to flow separation and turbulence. When considering the wake of a bluff body a distinction can be made between the near wake flow and the far wake flow [50]. Research into object wakes is often not focused on the shape of the wake itself but on the reduction of the hydrodynamical resistance of the object. Hydrodynamical analyses are conducted for new geometries using either small-scale experiments or numerical simulations, with numerical simulations becoming more accurate, cheaper and better suitable for complex structures. Research into the hydrodynamical properties of SMT vehicles has been conducted by Dai et al. (2021). In this study, the flow around an SMT at a velocity of 1.2 m/s was studied [50]. In this section the relevant research into the interaction between the SMT wake and the sediment discharge will be discussed. In this section first, a review of simple geometry and stationary object wakes will be provided, and finally a review of research into the wakes of SMT vehicles will be given.

2.7.1. Simple geometry objects

Researching the wake of objects has been conducted with both numerical approaches and laboratory experiments. Most research has been conducted on simple geometries, with the circular cylinder studied most extensively. For this simple geometry distinct flow regimes could be identified based on the Reynolds number [51]. Rectangular objects located in a flow mounted on a surface have been studied by Castro and Robins (1977). In DSM situations an SMT will be on the seabed leading to other flow behaviour, research into wall-mounted objects could provide flow characteristics similar to what is expected in DSM operations. Castro and Robins found that for a wall-mounted cube the flow returns to initial upstream conditions rapidly. At $x/h = 8.5$, in which x is the length dimension behind the cube and *h* is the cube height, the deviation from the upstream velocity profile was negligible. At $x/h = 4.5$ the difference with upstream velocity profiles was only in the range of a few percent [52]. Research conducted by Banerjee and Singh (2022) found that for rectangular objects a ground vortex can occur due to an occurring low-pressure field (see figure 2.11) [53]. This ground vortex could cause additional sediment suspension in the wake of the SMT.

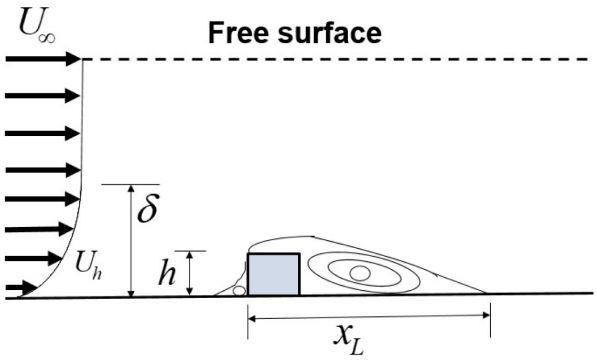

Figure 2.11: Schematic of Wake around a wall-mounted cube [53]

2.7.2. Wake of SMT

Several studies have been conducted focused on hydrodynamical models of an SMT during transit. A study by Dai et al. conducted a Reynolds Stress Model numerical analysis of an SMT [50]. This study did not research the interaction with the plume, however the results showing the velocity distributions could be of value for recognizing specific flow characteristics. Figure 2.12 and 2.13 show the velocity profile and kinetic energy occurring around an SMT at a forward velocity of 1.2 m/s. Some observations can be made regarding these results:

- The ground vortex mentioned by Banarjee and Singh does not lead to high velocities or low pressure fields

- Most energy is located behind the wake at a height of $\approx 2h$
- The peak of kinetic energy is located $\approx$ 1 collector length behind the collector. After this the velocities and kinetic energy decay rapidly

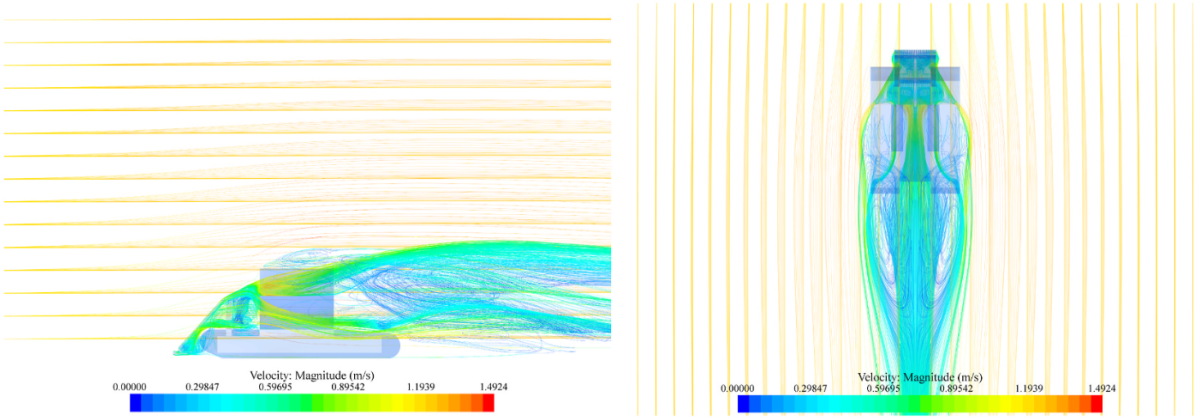

Figure 2.12: Velocity profile around SMT [50]

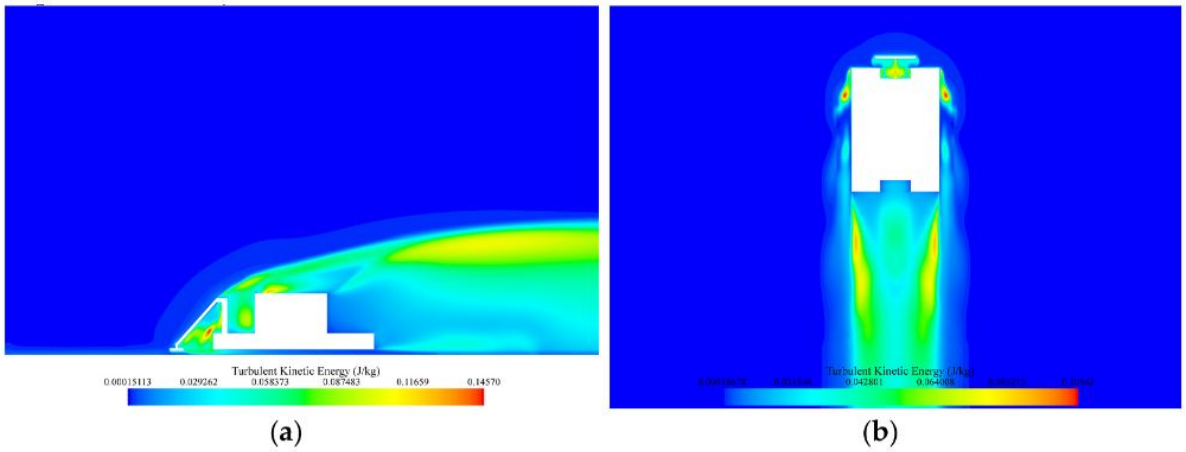

Figure 2.13: Turbulent kinetic energy distribution around SMT [50]

According to Oullion et al. the turbulent wake is characterized by the Reynolds number of the collector vehicle. For an SMT vehicle with dimensions as used by Blue Nodules this would lead to an Re of O($10^6 - 10^7$), which would be supercritical or transcritical flow [44][54]. Studies conducted on rectangular geometries close to a wall only included Re numbers of up to $5.6 \cdot 10^5$ [53]. Rectangular objects not near a surface were studied for Re numbers up to 10^6 by Mannini et al. [55]. A review of research into the subcritical and supercritical flow around objects concluded that supercritical flow around rectangular objects needs further investigation [54]. Research into a full-size collector prototype was conducted by Munoz-Royo et al (2022). For this study a collector vehicle was deployed in the CCZ where DSM operations were tested. Equipment onboard the collector found that the sediment is suspended higher than what would be expected purely from the discharge, they hypothesize that this is likely due to the turbulence generated by the wake of the collector vehicle [32].

2.8. Literature conclusion

Based on the literature gathered in this chapter an updated view of the different research questions can be provided. First, the important takeaways will be summarized. After this, for each research question a review will be given and a first attempt will be made at partly answering the research questions using the information gathered hitherto.

2.8.1. Summary of literature review

A review of literature available on scaling laws and approaches showed that a limited amount of in-depth scaling theory is available. The basics of scaling theory have been established for a considerable time, however detailed information on the scaling of turbidity currents/DSM operations is scarce. Researchers often do not provide a detailed breakdown of an experimental setup and the underlying assumptions. Multiple basic methods for relating scaled experiments to real life are used. For experiments focused on researching the physics of turbidity currents a scaling approach based on the Froude number is best suited. The important non-dimensional numbers; The Densimetric Froude, Reynolds number, and reduced gravity are introduced, and the accompanying regimes for the Reynolds number are provided.

The wake of an object is mostly dependent on the Reynolds number. Several flow regimes can be identified that describe flow characteristics; subcritical, critical, supercritical and transcritical. DSM operations are likely to operate in the transcritical regime. For this regime, only numerical simulations could be found, mainly conducted by Dai et al. It should also be noted that for the other Re regimes there was little information on the geometry of the wake. The research conducted by Dai et al. was not aimed at researching the impact of the wake on sediment plumes, however velocity and kinetic energy contours were provided in the results. The results of this research do provide insight into where the energy in the wake is largest and what the characteristic dimensions of the wake are. Research conducted by Oullion et al found a high level of complexity behind the collector vehicle in experiments conducted with dye. These experiments however were not designed with collector wake in mind and were therefore not similar to the real-life situation. In the in situ experiments conducted by Munoz-Royo it is hypothesized that the turbulence induced by the collector wake can increase the height of the turbidity current.

The processes occurring during the discharge of sediment from a source have been researched extensively. Because the topic is also of interest for other applications, such as wastewater discharges, a large scientific basis has been established. A distinction can be made between the different stages of a sediment discharge; jet/plume, impingement, and turbidity current. Whether the first stage of the discharge is a turbulent jet or a plume depends on the relative velocity with the background current. The flow in a turbulent jet stage is governed by momentum, whilst a plume is governed by buoyancy. The Richardson number gives an indication of whether the flow is buoyancy or momentum driven, with Ri > being buoyancy-dominated and Ri < 1 momentum driven. The discharge of an SMT can be characterized by the momentum flux, buoyancy flux, and volume flux. The length of the momentum-driven phase can be characterized using a momentum length scale which is based on the momentum flux and buoyancy flux.

Once the initial momentum has decayed the flow turns into a gravity current. The characteristic geometry of a gravity current divides the current into a head, body, and tail. The characteristics of turbidity currents have been researched in many experimental setups. Most research show a characteristic velocity and density profile as displayed in figure 2.4. The Rousse number can be used to give an indication of the ratio of settling velocity to shear velocity, which can be of use when determining whether the sediment is kept in suspension. Using this Rousse number an expression was made which describes the sediment suspension over the height of a turbidity current.

Research into sediment traps provides knowledge on experiments and designs. The common use case of a sediment trap is when it is suspended in a water column, for these situations different designs have been subjected to tests, and their efficiency was determined. Research conducted by Gardner concluded that geometries implementing a cylindrical shape have the best sediment trapping efficiency.

A relationship is provided proposing that the height should be more than three times the width. The amount of sediment that will deposit in an area will be impacted by the settling velocity of the particles. The sediment found in the CCZ is a mixture of sand, silt, and clay of which silt is the largest component. Research into sediment characteristics has characterized the distribution of sediment types and the corresponding sizes. Different sediment sizes also lead to different settling velocities. Research into settling velocities has led to multiple equations which apply to different sediment sizes and flow regimes.

Lastly research into sediment dispersion from moving sources was researched. Knowledge on this topic is very limited, with only one research focussed on DSM. One study conducted concluded that the relation between buoyancy velocity and collector velocity will generate different spreading patterns, based on if the ratio is in a supercritical or subcritical regime.

2.8.2. Answers to research question

The information gathered in the literature research can be used to answer the research questions posed in the introduction partially. With this research being focused on conducting experiments it is expected that most questions will not be answerable purely by literature research. Nonetheless, in this section an attempt will be made to answer the first research question. The other research question could not be answered by literature.

What experimental setup would be optimal to investigate plume spreading in a moving source experiment using sediment particles?

The research into scaling laws provides a basis for designing small-scale experiments. Two scaling methods are often used in small-scale fluid experiments; scaling based on the Froude number and based on the Reynolds number. The dimensionless numbers both describe different ratios of forces. Research into turbidity currents is often based on a Froude scaling approach, in which the Froude number is replaced by the densimetric Froude number. Wells (2021) found that the velocity and density profiles of a turbidity current are dependent on the Froude number as displayed in figure 2.4. Research into scaling theory, turbidity currents, and moving sources has also provided information on the different regimes that occur for dimensionless numbers. The main conclusion from the literature research is that conducting experiments in which all scaling laws are applied is not possible. When designing experiments an attempt should be made at ensuring that the processes occurring in the small-scale experiments are in the same ranges. Conducting experiments in which all dimensionless numbers are equal will be impossible, however, analyzing results from experiments that operate in the same dimensionless number ranges can provide relevant information.

3

Methodology

In this chapter the approach for obtaining the desired experimental results will be discussed. First a short explanation of the TU Delft dredging laboratory will be provided to illustrate experimental possibilities. After this, previous research conducted at the Dredging lab will be discussed. Then a detailed explanation of the scaling approach will be provided and the final test matrix will be presented. After this a detailed explanation of the experimental setup will be given, the different measurement techniques will be discussed and a breakdown of the experimental procedure will be given.

3.1. The Dredging laboratory

The dredging laboratory at TU Delft has facilities to conduct experiments focused on sediment transport. Conducting wet experiments is possible in a flume channel, which can be used for lock exchange experiments, and in a larger modular flume experiments can be conducted that require more space. For this research the large tank and accompanying equipment will be used. In this section a short description of the facilities will be given, a more detailed explanation of the final experimental setup will follow later.

Figure 3.1: Dredging lab with modular flume

3.1.1. Modular flume

The largest object in the dredging laboratory is a blue 25 m^3 modular steel flume/tank. The flume's dimensions are displayed in figure 3.2. The longer sides have transparent panels allowing visual measurements during the experiment. The tank is only used for experiments using tap water, making the fluid saline could lead to better experimental however, the deterioration of the steel by salinity makes this option not preferable. This tank can be used for submerged processes, varying from deep sea systems to stone dumping systems. When visual measurements are taken with cameras, a drape can block the natural light in the dredging laboratory. When interaction with a horizontal surface (seabed) is researched a light table can be installed that is 1,85 m in width and 4.6 m in length. This table has light strips that can be used to improve visualisation of experiments. The modular flume is connected to a water supply to fill, and if needed, refresh water in the tank.

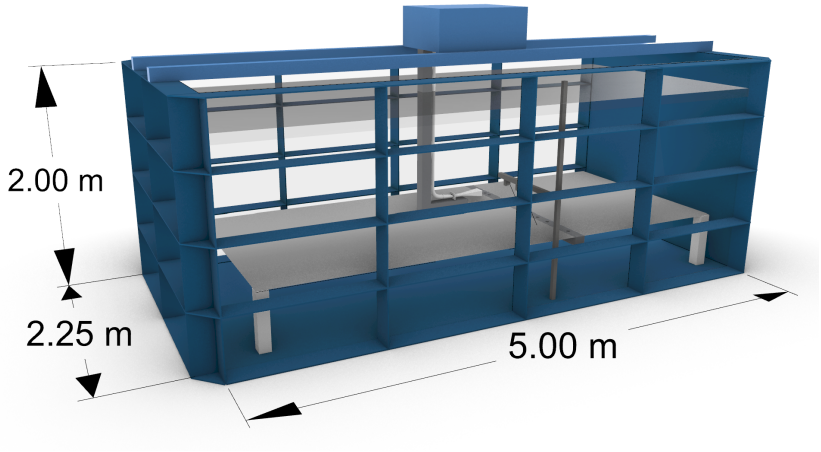

Figure 3.2: Modular flume with dimensions

Sediment mixtures used in experiments can be created using a separate tank as shown in figure 3.7 connected with a flexible pipe to the modular flume. In a transparent tank with inner dimensions of 0.6 m by 0.7 m and a maximum height of 1 meter. In this flume, the sediment particles can be suspended into the fluid using submersion pumps. When placed correctly the submersion pumps will suspend the sediment into the water and maintain a near-homogeneous mixture. The mixing tank discharges through the diffuser into the modular flume.

3.2. Previous work

The Dredging laboratory has been used extensively to research sediment plume behaviour and spreading. Three graduate students from TU Delft conducted research on different parameters. Their work is a good baseline for the design of a new moving test setup. All of these experiments were conducted in the modular flume. All three research objectives were in the context of sediment plume dispersion in DSM operations. A short summary will be given for each research, including the research objective, scaling approach and measurement methodology.

3.2.1. Diffuser geometry

This research conducted by J.O. Rodriguez had the objective of researching different diffuser geometries. A total of three diffusers were tested using visual imagery technology and velocity/concentration profiling using an Acoustic Doppler Velocimeter (ADV) and Optical Back Scatter Sensors (OBS). A Froude scaling approach was used with a geometric scaling factor of 15. Glass beads with a particle size range of 65-105 microns were used. In total 19 experiments were conducted in which velocity and concentration are measured at three locations. To ensure the resemblance of results, one repeat experiment was conducted for each diffuser. [18].

3.2.2. Initial concentration

The research conducted by Y. Wijmans had the objective of researching the influence of the initial concentration of the sediment mixture on the spatial spreading of the turbidity current. Assuming a constant sediment flux and discharge velocity, experiments were designed with the aim of measuring concentration and velocity profiles. Velocity was measured using an ADV, which was also used to determine concentration measurements inside the turbidity current. Three different concentrations were tested: 175, 100 and 25 grams per liter. The results indicated that a higher initial volumetric concentration could prevent spatial spreading. For the experiments, a Froude scaling with a geometric scaling factor of 15 was used [20].

3.2.3. Diffuser height

In this research B.K. Blankenaar used numerical models along with small-scale experiments to conduct research into diffuser height. Video visualization experiments were conducted in combination with concentration and velocity measurements. Two different sediment sizes were tested; 40-70 microns and 65-105 microns. Experiments showed that the smaller size could lead to contamination of the flume after several minutes. The research found that a higher diffuser height leads to more spatial spreading due to a more vertival impact at impingement. A diffuser height of 100 mm at scale was recommended [19].

3.3. Scaling approach

The objective of this research is to research sediment plume spreading, when designing small-scale experiments the physics governing plume spreading should be the main influence for the experiment design. To achieve relevant results, it is necessary to ensure similarity in several aspects. In particular, the discharge of the sediment mixture from the collector vehicle should be turbulent, with a Reynolds number (Re) larger than 4000. Additionally, to maintain similarity in the overall plume process, the densimetric Froude number should be above 1 in order to ensure homogeneous outflow at the diffuser. These conditions help to ensure the proper scaling of the discharge and plume behavior. As mentioned in the literature research, the two relevant non-dimensional numbers are the densimetric Froude and Reynolds number. Because scaling both down is not physically possible in the TU Delft dredging laboratory one approach needs to be selected, either Froude scaling or Reynolds scaling. For experiments aiming to research turbidity current behaviour a Froude scaling approach was found to be optimal. Compared to the Reynolds number, the Froude number gives a better indication of the physical processes occurring in the turbidity plume. In order to scale down the system a real-life SMT was considered with a diffuser width of 1 m and a velocity of 0.5 m/s [10]. It should be noted that this pre-economic SMT does not represent a full scale SMT that would potentially be used in the future. Basing the research on this design however, allows for comparisons to be made with actual DSM operational tests. For this research it is assumed that an SMT used in large-scale DSM operations will consist of multiple smaller diffusers. The variables of the design this research is based on were scaled down using various geometric scaling factors; 1/20, 1/15 and 1/10. For each geometric scaling factor, calculations are made on the flow characteristics for three concentrations. At first, volumetric concentrations of 1, 4, and 7% are considered. Assuming that the sediment flux out of the diffuser is a constant value for all concentrations, the dimensions of the diffuser is calculated. With these dimensions known the criteria for the Reynolds number and Froude number are verified. The criteria which had to be passed are collected in table 3.1.

Re_p > 4000	This criteria makes sure that the flow in the pipeline is fully turbulent
Re_d > 4000	To ensure that at the outflow of the diffuser turbulent flow occurs
Fr_p > 1	This ensures that the correct physical phenomena occur in the turbidity current.

Table 3.1: Flow criteria applied during scaling calculations

After an iterative approach, the choice was made to continue with the 1/20 geometric scaling.

One of the objectives of this research is to use experiments to obtain information on how the turbu-

lent wake behind a DSM vehicle would impact the spreading of sediment plumes. The literature review showed that experiments on turbulent wakes in the correct Reynolds number regime had not been conducted, or have not been published. Calculations on the required test parameters show that maintaining Reynolds similarity between an actual SMT tool and the experimental setup would require high velocities in the range of $U_c > 1.5m/s$. Experiments designed to research the wake are not possible at TU Delft dredging laboratory.

3.4. Experimental setup

Using the equipment available in the lab and building on previous research an experimental setup is designed that allows to conduct experiments. Several adjustments are made to the setup used by previous researchers. In this section, the setup used during the experiments will be described. The base of the experiments will be the same as for the experiments researching sediment plume dispersion from a stationary discharge [20]. The aspects that have been added, or changed will be mentioned. In figure 3.3 an overview of the test setup is provided.

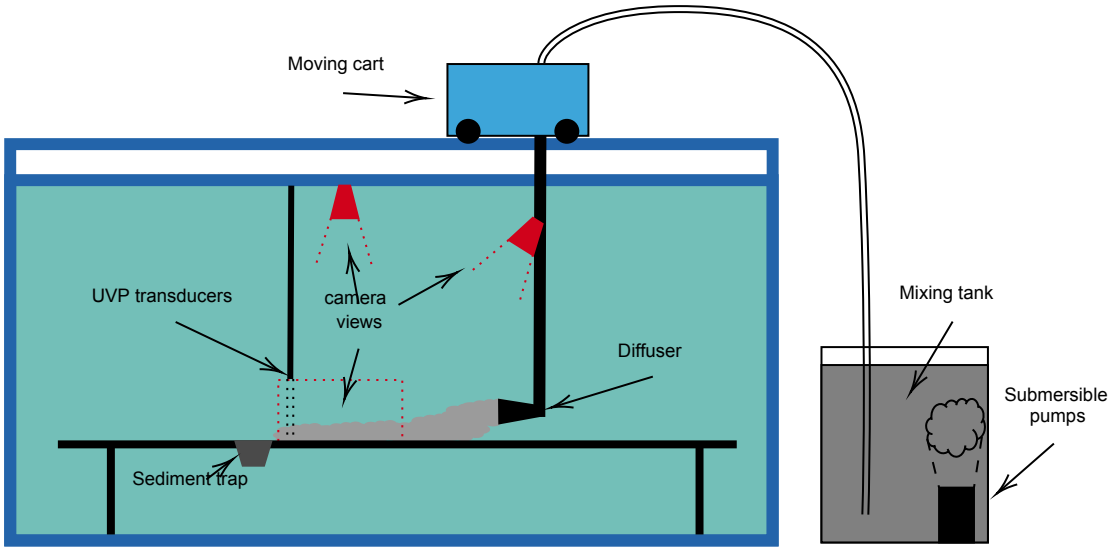

Figure 3.3: Schematic of experimental setup

3.4.1. Moving setup

To add the possibility of experimenting using a moving source, a system is installed with a moving cart on tracks. The cart and tracks are used in previous experiments on smaller flume tanks. The design of this system was optimized for the smaller flume tanks with a small width. For using the cart on the modular flume additional beams were installed which would provide a structurally suitable base for the cart tracks. The moving cart can be controlled using a control panel on which the speed and direction of movement can be controlled. The velocity can be altered using a knob on the control panel. The actual speed could be calculated by measuring the velocity using a preset distance and a stopwatch.

Figure 3.4: Moving cart

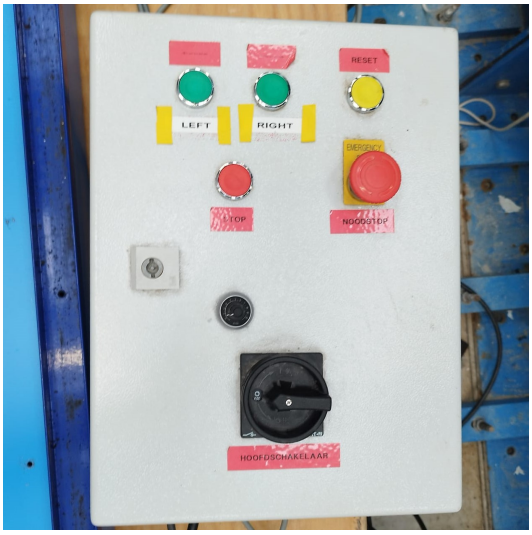

Figure 3.5: Control panel of moving cart

3.4.2. Sediment

The type of sediment that has been used for the previous experiments, and for this one, is glass beads. These glass beads are commonly used for sandblasting applications. The glass beads have a density of 2.46 kg/dm^3. Glass beads are produced in several size distributions. For this research, the glass beads size closest to CCZ sediment dimensions was chosen, with a grain size between 40 and 70 microns. There are significant differences between the sediment used in this research and the actual sediment in the CCZ. The sediment found in the CCZ is cohesive, which will cause the particles to flocculate when suspended. Glass beads are not cohesive, due to this relevant physics will be missing from the experiments. The use of glass beads, however also has advantages, due to the higher density, the total settling time is limited, which increases the amount of experiments that can be performed per day. That flocculation is missing allows for research into the occuring fluid dynamics without influence of flocs. Size measurement distribution measurements were conducted by Blankenaar, the distribution is given in figure 3.6 and a standard deviation of 10% was found [19].

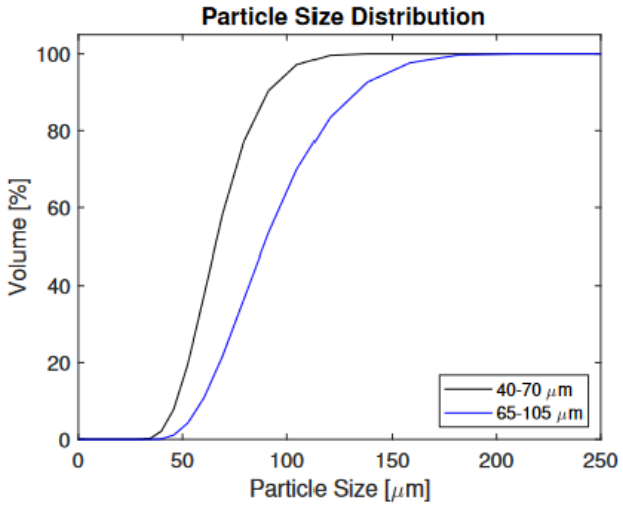

Figure 3.6: Sediment size distribution [19]

3.4.3. Mixing tank

A second smaller tank was used to prepare the sediment mixture used in the experiments (see figure 3.7). This rectangular mixing tank had dimensions of 0.6 width by 0.7 length and 1 meter height and is made of plexiglass to allow for inspection of the mixing process. The desired sediment mixture

combination is achieved by measuring the amount of sediment needed per volume using a balance. For a clearer mixture, the weighed sediment is washed before adding it to the mixing tank to remove floating glass beads and other impurities. Two Einhell clear water submersible pumps with a capacity of 9000 L/h are used to maintain suspension of the glass beads. One submersion pump was placed horizontally and one vertically. The connection between the mixing tank and the experimental setup is through a Marina centrifugal pump with a capacity of 100 L/min. The sediment mixture enters the centrifugal pump through a pipe that is placed roughly 10 cm from the bottom of the tank. The centrifugal has a ball valve that can be used to regulate flow through the hose going into the experimental setup. In between experiments, this pump could also be used to keep the sediment in suspension by adjusting the valves to pump everything back into the mixing tank. To measure the velocity at which the sediment mixture was pumped into the experimental setup a KATFLOW 200 velocimeter was attached onto the hose to obtain velocity readings.

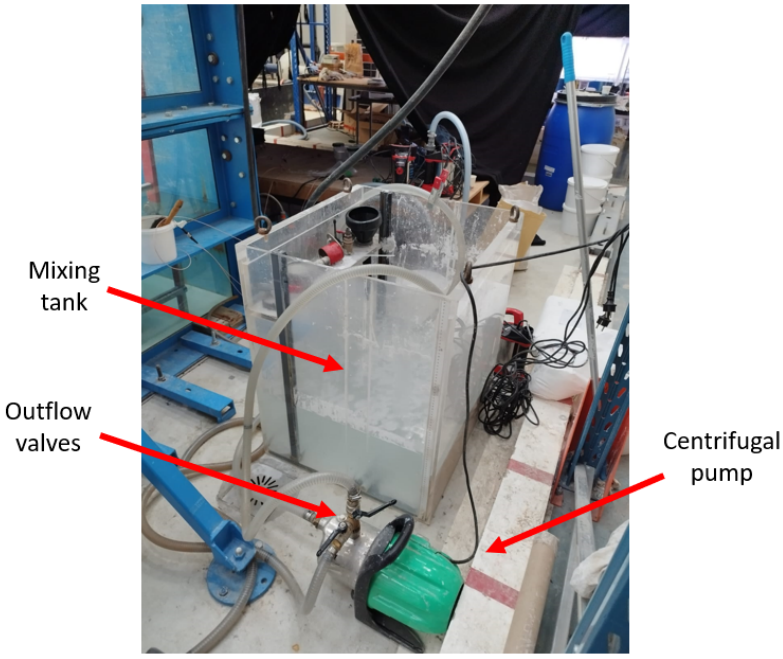

Figure 3.7: Sediment mixing tank and pump

3.5. Diffuser

In the experiments a diffuser will be used to attain the correct discharge parameters. The ”mouth” of the diffuser represents the outflow of an SMT. The width of the diffuser will be the result of the width of an SMT diffuser multiplied by the geometric scaling factor. To maintain a constant sediment flux while varying the concentration, different diffuser designs are used. For the experiment with the lowest concentration, the aspect ratio (width/height) is set to one. Subsequently, the dimensions of the other diffusers are calculated based on the assumption of constant sediment flux. During the design of the diffuser several criteria had to be taken into consideration to reach a homogeneous outflow without separation in the diffuser. The main criterion for this are that all angles inside the diffuser are not larger than 7 degrees, if this criteria were to be met the diffuser would take up too much room in the experimental setup. To keep the length of the difuser minimal, and to comply with the criteria to prevent flow separation, vanes were installed. At first only one horizontal vane was necessary for the diffuser designed for 1 % volumetric concentration. After running some tests in the experimental setup it was found that the outflow was correctly distributed over the height of the diffuser however, the outflow was not correctly distributed over the width of the diffuser, likely due to flow separation. To solve this two vertical vanes were added to both (see figure 3.9) to ensure an evenly distributed outflow over both height and width. The diffusers were produced at TU Delft using an SLS 3d printer. The experimental setup involved connecting the diffuser to a pre-existing duct, which, in turn, was linked to a vertical pipe leading to the moving cart. The height-adjustable vertical pipe was mounted onto the moving cart.

This equipment was previously used in the research conducted into diffuser height influence. This equipment provides flexibility in experimental design, if during experiments problems occur regarding the diffuser height, this can be fixed in little time. The setup also allows for relatively easy deconstruction to change out diffuses between experiments.

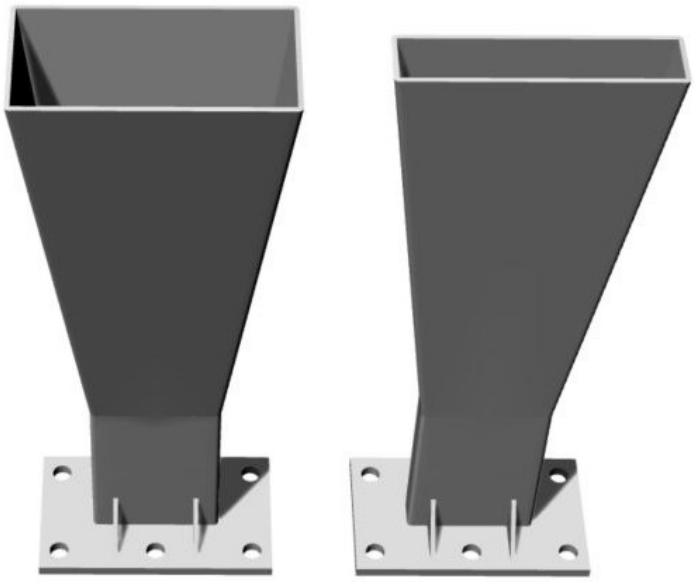

Figure 3.8: Diffusers design for 1% (left) and 3 % (right)

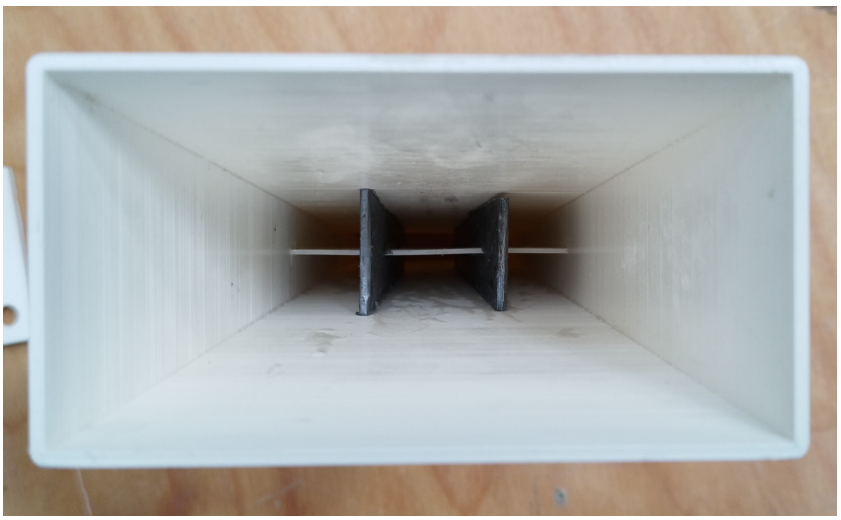

Figure 3.9: Diffuser for 1% with added vanes

3.5.1. Discharge height

The height at which the diffuser is located has been shown to impact the spreading of sediment plumes [19]. Research conducted at the Dredging laboratory focused on diffuser height concluded that with an increasing height more sediment settles closer to the source. However, a lower diffuser height was found to cause more erosion of the nearby seabed. The experiments concluded that the optimal experimental height, leading to the best sediment plume characteristics, is 100 mm [19]. The experiments will be designed with the height, at the center of the diffuser, at 100 mm. The height adjustability of the setup gives the possibility to differ from this height if needed.

3.5.2. Concentration

The concentrations which will be used during the experiments were based on previous studies. One aspect of this research is increasing the practical know-how of the TU Delft when it comes to the dredging laboratory. Previous experiments conducted regarding sediment plumes used three concentrations; 1, 4 and 7%. These values are based on both realistic values in DSM operations and the practical limitations of the experimental setup [20]. Current designs for SMTs use relatively low concentrations in the range of 1%. One method for determining the concentration in the wake, which assumes that the sediment mixture is quickly spread out over the cross-sectional area of the SMT, approximates the calculation as $c_0 = \frac{\dot{m}}{U_c A}$, with $\dot{m}$ being the mass flow, and A being the cross sectional area of the wake close to the SMT. Assuming an average sediment discharge of 12 kg/s this would result in a volumetric concentration of 1.25%[32]. Research suggests that using higher concentrations could minimize the impingement length and the overall impact induced by sediment. Previous graduation research has found results that support this [20]. The results of the research on concentrations combined with the advantage of being able to compare led to the desire to test multiple concentrations, one at 1 %, which is close to realistic DSM conditions, and one higher concentration at 3% volumetric concentration.
To enable online concentration measurements during the experiments, an Acoustic Doppler Velocimeter (ADV) is utilized. A series of calibration experiments were conducted to establish a reliable relationship between the ADV measurements and the concentration. In the calibration experiment, incremental amounts of sediment were added to a bucket containing a known volume of water. To ensure homogeneous suspension of the mixture, a hand mixer was employed. The calibration curve depicted in Figure 3.10 was generated by measuring the noise to signal (NSR) ratio at each process step. The NSR gives the level of unwanted noise compared to the desired signal in the ADV's measurements. A correlation between the NSR and the mixture concentration allows for concentration measurements using the ADV. The calibration curve was used during the experiments to measure the mixture concentration in the mixing tank. For this research all measurements were in the upper section of the calibration curve, removing the need to analyse which concentration led to which SNR value.

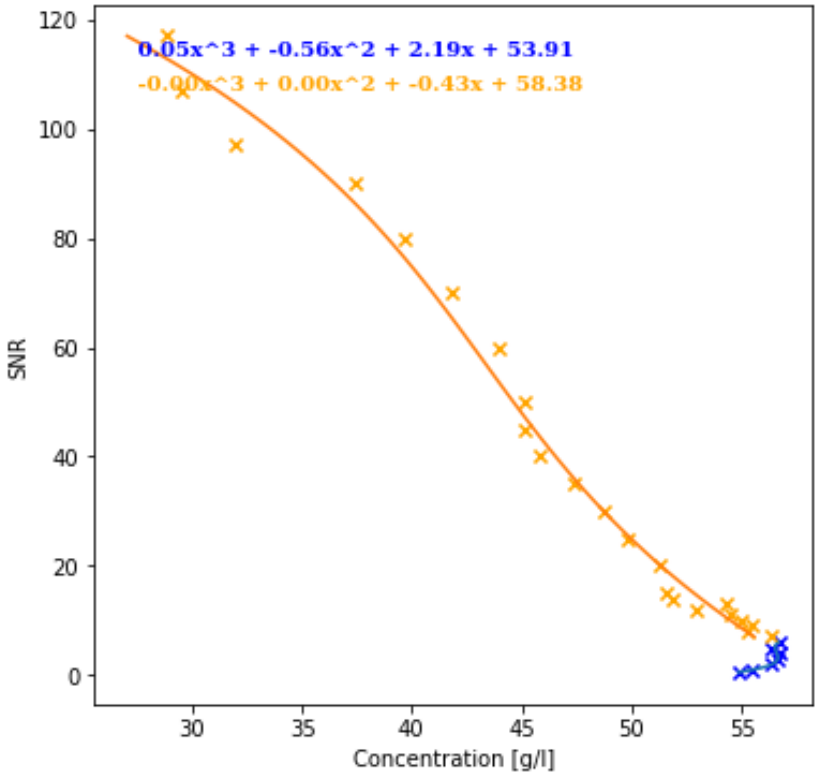

Figure 3.10: Calibration curve ADV

3.5.3. Source velocity

What source velocities to model in the experiments is based on the findings of Oullion et al. [22]. In their research three different regimes are identified for the relation of the source speed and the buoyancy velocity. The first regime; $\frac{U_c}{U_b} < 0.63$ describes the situation in which the speed of the collector vehicle is lower than that of the gravity current. The second situation; $\frac{U_c}{U_b} > 0.63$ describes the situation in which the source propagates faster than the gravity current. The last regime concerns $\frac{U_c}{U_b} > 1$ in which the gravity current propagates in the direction normal of the source. Because this research will be the first to research turbidity currents in a DSM setup using a moving source all three regimes will be researched.

3.6. Test matrix

All information gathered in this chapter has been combined into an experimental setup. In order to use this experimental setup optimally and to obtain relevant results, different experiments will be conducted. The variables which will be researched on their influence on sediment plume spreading are the volumetric concentration, the carriage velocity and the discharge velocity. These two variables will lead to other differences in the experimental setup, such as different diffusers, that are needed in the attempt to maintain similarity in sediment flux. Next to the experiments researching the influence of source velocity, there will be stationary experiments. These stationary experiments will provide the base values for each concentration. In total, 18 experiments will be conducted, the experimental info for the different concentrations are provided in Table 3.2. In chapter 4 an overview is given of all experiments. After getting used to the experimental setup, new insights were gained on what experiments were feasible. One limitation that was not previously considered was the maximum flow rate that could be obtained using the centrifugal pump between the mixing tank and the modular flume. This posed a problem for the experiments planned for a 0.5% volumetric concentration, ultimately leading to the test matrix being changed to replace the 0.5% volumetric concentration experiments with other interesting experiments. Eventually 4 new experiments were added that were designed to research the influence of a critical and subcritical densimetric Froude number on sediment plume dispersal.

3.7. Measurement setup

In order to properly assess the sediment plume behaviour multiple measurement methods will be used. In order to assess the spreading of the sediment plumes three variables will be researched; Concentration, Deposition and velocity. In this section, a measurement approach will be proposed for each variable. What equipment will be used is mostly dependent on availability in the Dredging lab.

3.7.1. Velocity profiling

Several methods exist for measuring velocity profiles, most notably the ADV and the UVP. Ultrasonic velocity profiling (UVP) uses acoustic measurement methods which are able to non-invasively measure suspended flows. The UVP uses transducers that can measure a velocity profile along a line. The transducers transmit pulses of ultrasound, when the pulses interact with particles, in this case sediment particles, a part of the pulse echoes back and is measured by the transducer. Measuring the time delay between pulse transmission and receiving, a Doppler shift can be observed for non-zero velocity particles. Using the sound velocity of the medium the measured Doppler shift can be used to obtain a velocity component [56]. Compared to ADV, a UVP is better at resolving vertical distributions of flow velocity and concentration due to it being able to obtain measurements over a larger depth [57]. Each transducer can be used to measure a separate velocity profile or can be used in duos to ensure synchronization between separate transducer's measurements as displayed in figure 3.3.

In this research, a UVP is used to obtain velocity profile in the direction perpendicular to the direction of the moving cart. Two transducers were mounted in the modular flume above the table using a purpose-built frame. The transducers were placed 30 cm above the table surface in an angle of 45 degrees as depicted in figure 3.11. The distance between the two transducers was 20,5 cm and the distance between the centre of the diffuser and the first transducer was 8 cm. Because the transducers were placed at an angle the locations where the velocity profiles were measured are 38 and 58,5 cm from the centre line of the diffuser.

Volumetric concentration	Density mixture	g'	$\Delta\rho$	Diffuser width [m]	Diffuser height	Hydraulic diameter	Re diffuser	Re pipe	Fr plume
%	[kg/m3]		[kg/m3]	[m]	[m]	[cm]	-	-	-
0,5	1006	0,07	7,30	0,1	0,1	1,80	13416	85412	1,58
1	1013	0,14	14,61	0,1	0,05	0,67	8944	42706	1,58
3	1042	0,43	43,85	0,1	0,017	0,29	3833	14235	1,58

Table 3.2: Experiment characteristics for different concentrations

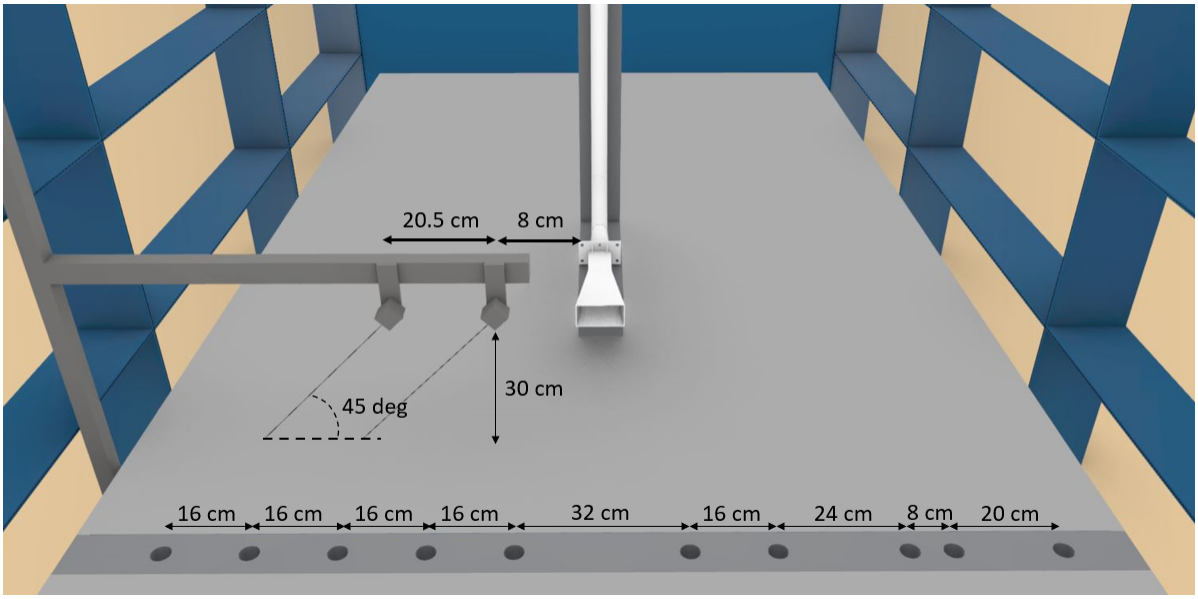

Figure 3.11: Measurement setup including dimensions

3.7.2. Deposition measurements

Being able to obtain deposition measurements can give insights into how different experimental variables influence the footprint and sediment deposition. Previous research at the dredging laboratory used visual imagery technology to measure and visualize a qualitative 2d footprint. Side and top-mounted cameras were used to capture the sediment discharge and the resulting turbidity currents. This allows for visual inspection and measurements of jet/plume physics and allows for comparisons with other qualitative measurements. Using the top view allowed researchers to use post-processing techniques in which a footprint could be determined.

For this research, in which a moving setup will be used, the experiment duration will be significantly shorter compared to previous experiments in the dredging lab. Due to the shorter duration, and the moving setup, a lower amount of deposited sediment is expected compared to a stationary setup. It is expected that the lower deposition leads to challenges in using imagery methods. It should also be mentioned that using the top view cameras could only provide the area contours of the footprint and not the actual layer thickness. In order to perform more accurate measurements, the use of sediment traps is proposed. As discussed in the literature research, sediment traps are currently used for deposition measurements in oceanography.

The sediment traps discussed in the literature research are in practice located above the bed. For the testing setup in the dredging lab a different type of sediment trap was designed. The sediment trap that was implemented in this research consisted of a beam located in the table of the modular tank. The stainless steel frame, depicted in figure 3.12, of the beam can be fitted into the table as depicted in 3.11 so that the surface of the table and the sediment trap are flush. The sediment trap contains holes in which cylindrical glass beakers, with an inside diameter of 38 mm and a total volume of 50 ml, can be positioned as displayed in figure **??**. This beam can be lifted out of the tank in between experiments using ropes that were attached to both sides, after which the individual beakers can be emptied and the settled sediment can be measured.

Figure 3.12: Sediment trap

3.8. Experimental procedure

In order to ensure that all experiments were conducted using the same method a step-by-step plan was drafted to conduct the experimental runs in the dredging laboratory. For all experiments this plan was executed so that the testing setup had similar conditions during all experiments.

1. Install the correct diffuser
2. Create the sediment mixture in the mixing tank. First the mixing tank was filled to the needed height, which was dependent on the volume flow needed in the experiments. With the dimensions of the mixing tank and the water height the needed amount of glass beads could be calculated and weighed using a balance. The sediment was then washed to take out any other material and to remove potential floating glass beads. After this the glass beads were slowly added to the mixing tank whilst the submersion pumps were on. The concentration was measured using the ADV and by taking a test tube sample
3. Input the correct cart velocity using the control panel. Knowing the length of the cart track, the exact velocity could be calculated using a timer.
4. Turn on the three cameras and move cart to starting position
5. Adjust pump valves using the KATFLOW velocity meter to reach desired discharge velocity
6. Turn on UVP and start cart movement
7. Shut off pump when cart reaches end of tank
8. Turn off cameras and measuring equipment
9. Collect sediment measurement from sediment trap

Between the 7th and 8th step a waiting period was needed to ensure that all sediment in the tank was settled. In between the experiments, the table inside the modular flume was cleared of sediment and between experiment sets the mixing tank was cleaned.

4

Results

In this chapter, results obtained from the small-scale experiments will be presented. During the experiments, there were three different types of results: video footage, velocity measurements, and sediment trap sedimentation. First, an overview of the realised experiments will be provided to give an overview of the types of experiment series that have been conducted. After this, for each type of result an overview will be given, more detailed results can be found in the appendices. Information on the exact setup of the equipment used to obtain the results can be found in the previous chapter; methodology. This chapter mainly focuses on the type of results and how they were gathered and processed, an analysis of the results will be provided in Chapter 5

4.1. Realised experiments

Based on the experimental matrix drafted in Chapter 3 a series of experiments, 18 in total, were conducted. There were multiple input variables that differentiated the type of experiment from others: diffuser geometry, cart velocity, volumetric concentration of sediment mixture and discharge velocity. During the experiments the realized values for all input variables were noted or calculated, all input variables for the experiments are gathered and displayed in Table 4.1.

The performed experiments can be grouped into several experiment series. Each series of experiments was designed to provide value on the topics that are to be studied.

1. Set of two series of experiments using two different volumetric concentrations. Each series tested four different values of a; 0.5, 0.75, 1 and 1,5. The first series tested a 1% volumetric concentration using the diffuser designed for this concentration. The second series tested a 3% concentration using the diffuser designed for 3%. In Table 4.1 these are set B and D, respectively.
2. Set of two experiment series testing a volumetric concentration of 0.5%, 1% and 3% in a situation with a different sediment flux by using the diffuser designed for a 1% volumetric concentration. The diffuser and discharge velocity were kept constant. Two values of a, 0.5 and 0.75, were tested for each concentration. In table 4.1 these are sets A, the last two experiments of B and the first two experiments of E.
3. Set of four experiments in which the input variables are changed so that the densimetric Froude number is lowered to a different regime at Fr equal to 1 and 0.6. These experiments were conducted for a volumetric concentration of 1% and 3%. In table 4.1 these are sets C and F.
4. Set of two stationary experiment for a volumetric concentration of 1% and 3%. This is set G in table 4.1.

Set	Exp #	Diffuser	Cart velocity cm/s	Discharge velocity cm/s	Sample conc. g/l	NSR conc. g/l
A	1	1	5.87	13.00	8.14	7.5
	2	1	8.06	13.95	3.42	5
B	3	1	17.8	13.38	24.83	12
	4	1	13.58	14.33	25.85	20
	5	1	6.15	13.95	29.10	14.5
	6	1	9.7	13.63	27.66	20
C	7	1	8.25	8.36	32.76	20
	8	1	6.00	4.71	43.24	20
D	9	3	10.69	14.89	37.88	40
	10	3	16.00	11.88	57.78	65
	11	3	30.30	11.50	41.76	40
	12	3	13.55	13.95	57.56	60
E	13	1	5.95	13.26	56.60	60
	14	1	8.80	13.95	46.95	65
F	15	3	8.20	9.90	54.77	60
	16	3	4.70	5.28	48.82	60
G	17	3	-	12.81	59.24	-
	18	1	-	13.38	27.15	-

Table 4.1: Realized Experimental Data

4.2. Video footage

During the experiments, video footage was obtained using three GOPRO action cameras. Figure 4.1 gives an overview on where the cameras were located. Camera 1 and 2 were placed to have a stationary view of the sediment plume at one location. Camera 3 was attached to the moving setup providing a view of sediment discharge and the sediment plume geometry shortly after discharge. For each view an example is provided in figures 4.2, 4.3 and 4.4.

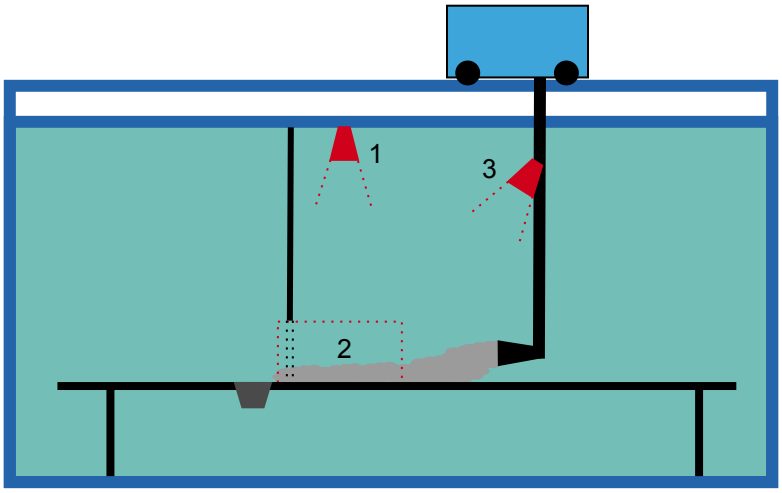

Figure 4.1: Placement of cameras

The top-view perspective (camera 1 in Figure 4.1) offers a comprehensive observation of the sediment plume as it spreads. To capture this footage, a GoPro Hero 11 Black was utilized and attached to the cart track structure using a clamp, positioning the camera just below the water surface. However, due to the experimental nature of the study, the camera had to be manually removed, turned on, and repositioned between experiments. Consequently, the resulting footage from different experiments varied slightly in terms of the viewpoint.

For the side view of the experiments, a GoPro Hero 4 was employed. This camera was placed outside the tank, positioned behind transparant panes of the modular tank. As the camera was located outside the tank, it could capture audio, which was later synchronized with the UVP data. However, it is worth noting that the video quality was lower in comparison to the other cameras used, and the presence of modular tank panes and reduced water transparency caused some footage to appear blurry. The reduced water transparency was due to algae growing in the tank. To keep the growth of algae to a minimum the water in the tank was refreshed whenever possible, due to the large volume of water in the tank this approach was limited. To address this issue, postprocessing software was used to adjust the image contrast, enabling the visualization of sediment plumes, although identifying key characteristics became more challenging.

To provide a camera view moving with the moving setup, a GoPro Hero 9 was mounted on the structure attached to the cart. This camera was positioned just below the waterline to provide an almost top-view perspective of the sediment mixture discharge. However, similar to the other cameras, it had to be removed before each experiment, leading to slight variations in the viewpoint across all experiments. Notably, during the preparation phase, the moving cart was relocated to the opposite side of the tank to initiate the experimental run. This movement occasionally caused the camera to interact with the flexible pipe connecting the diffuser to the mixing tank, resulting in a slight rotation of the camera. To ensure consistency, all images extracted from the camera footage were subsequently rotated to display a uniform view of the discharge.

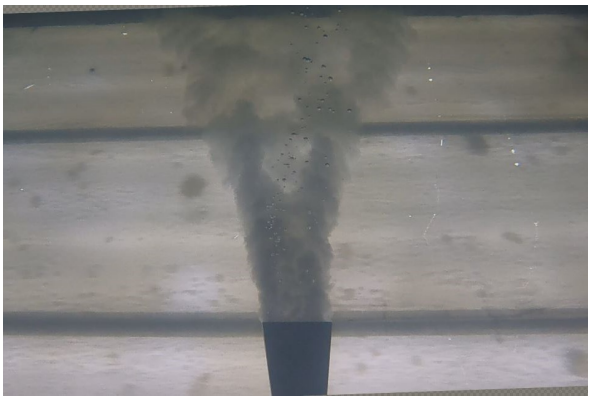

Figure 4.2: Mounted view Experiment 12

Figure 4.3: Top view Experiment 12

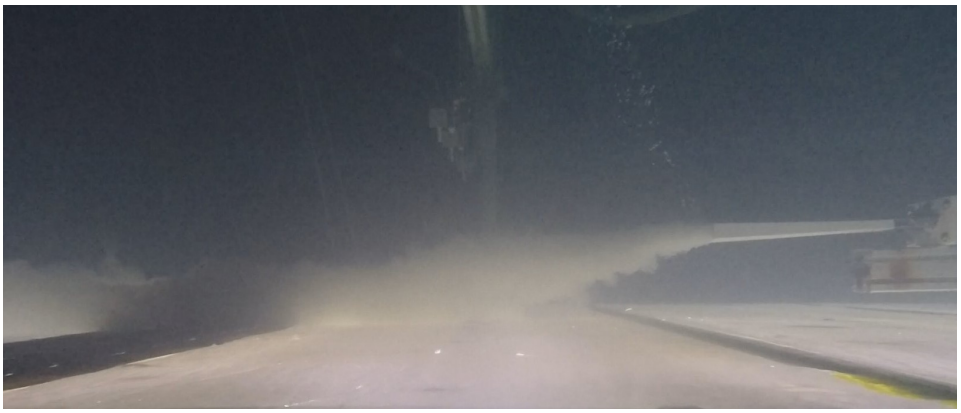

Figure 4.4: Side view experiment 12

The images obtained from the video can be used to obtain three different characteristics of the sediment plume.

1. Distance of impingement. This value can be obtained from the side view as displayed in figure 4.6.
2. Spreading angle before impingement. α in figure 4.5.
3. Spreading angle after impingement. β in figure 4.5

The spreading angles, as shown in Figure 4.5, are utilized for defining the observed characteristics. Table 4.2 presents the gathered angles from all experiments. It is important to acknowledge that these particular characteristics may not be observable in every experiment conducted. In several instances, there is no clear difference between angle α and β, or no angles are apparent at all. Additionally, the concept of impingement length does not apply universally to all experiments. To distinguish between different situations, three labels are employed: clear impingement (CI), no impingement (NI), and a situation where some impingement is observable, although the exact characteristics cannot be determined solely from the experimental data (SI).

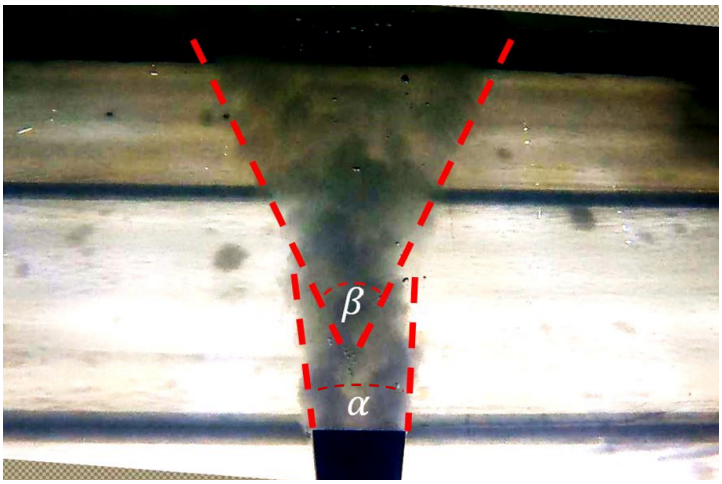

Figure 4.5: Definition of angles α and β in the mounted view

Figure 4.6: Definition of the impingement length

Set	Exp #	Impingement length	α	β
		cm	deg	deg
A	1	70	9	-
	2	84	9	-
B	3	-	7	-
	4	84	9	-
	5	33	9	68
	6	26	9	44
C	7	17	13	54
	8	8	7	100
D	9	28	11	50
	10	50	13	40
	11	-	7	-
	12	28	10	40
E	13	13	9	93
	14	17	7	63
F	15	52	10	50
	16	10	10	80

Table 4.2: Impingement length and spreading angle results

4.3. Velocity profiles

During the experiments velocity profiles were measured using a UVP. Two transducers were placed along a line transverse to the direction of source movement. The quality of the signal obtained by the transducers depends on how dense the occurring gravity currents were. The data measured by the transducers is gathered by the UVP-DUO from Metflow. The settings of the UVP can be altered to best fit the experiments. One of the main considerations to take into account is that the UVP is limited to one transducer collecting data at any moment in time. Because of this limitation the UVP loops through the specified transducers, for each transducer a number of measurements, a block, is gathered after which the UVP switches to the next transducer, where it measures another block. The amount of profile measurements obtained per block can be specified in the UVP-DUO settings, for these experiments a block size of 10 was used. The measurements for every block take up 1.3 seconds. Figure 4.7 shows one measurement obtained during the experiments. The transducers only obtain valuable data when there are sufficient particles to reflect the acoustic signal, when insufficient particles are available, the transducer receives noise. In figure 4.7 it can be seen that valuable data is obtained in the second half of the measurement channel. The channel for measurements was set larger than the actual required size, due to this all data can be removed after roughly 35 cm, which is where the measurement channel crosses the table. The section above the gravity current has to be removed for every measurement individually as the height of the gravity current is a result that is different from experiment to experiment.

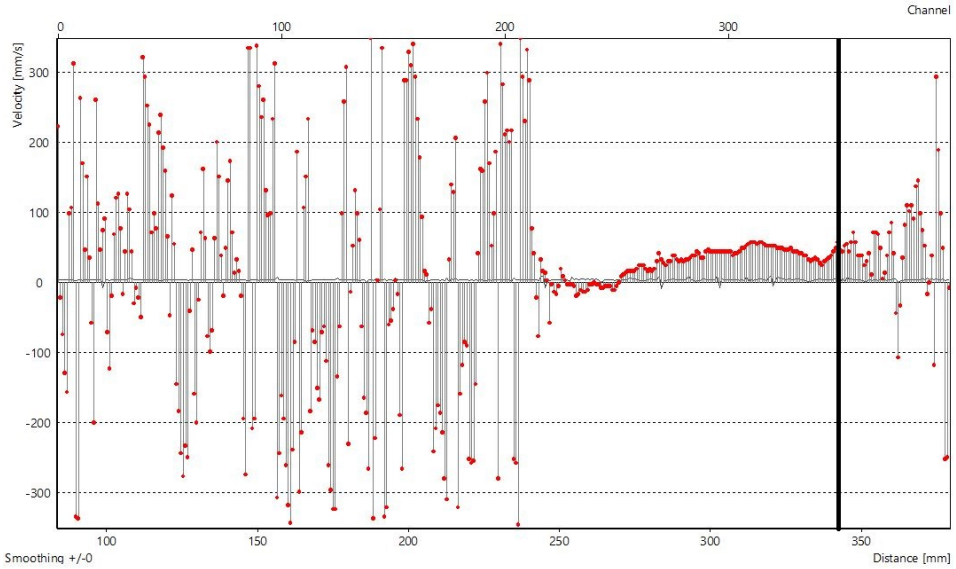

Figure 4.7: Profile as measured and displayed in UVP-DUO software, vertical black line indicating start of table

The obtained velocity profiles collect data instantaneously. The turbulent nature of the turbidity current can lead to big changes in velocity profiles, to decrease the inaccuracy of the velocity profiles due to turbulence multiple velocity profiles can be averaged. For this to be done correctly, the data has to be analysed to ensure that the profile is only averaged over a time period where the same results are expected. As an example there should be no averaging of profiles where only the gravity current head is measured with profiles where the body of the gravity current is measured. Figure 4.8 displays an example for a velocity profile after averaging. The measured velocity profiles were averaged over one block length, which is equal to 1.3 seconds.

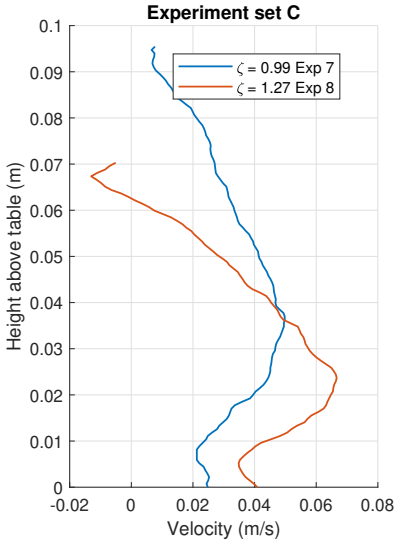

Figure 4.8: Averaged velocity profiles

As can be observed in both figure 4.7 and figure 4.8 the velocity obtained at the table is not equal to zero. The exact reason for this is not known, however the UVP system used showed similar problems in other research. The bottom can be found by finding the location where the velocity starts going to zero. The exact reason for this is not known, however the UVP system used showed similar problems in other research. The location of the bottom can be estimated by finding the location where the velocity starts going to zero and by using the measurements

4.4. Sediment trap

After every experiment the contents of beakers in the sediment trap were transferred to glass test tubes (figure 4.9) which were later analysed. The test tubes were analysed in the laboratory of Deltares in Delft, where a Sartorius balance with a resolution of 0.01 mg was used. The procedure applied to measure the sediment collected by each individual trap to results had the following steps:

1. Measure weight of the individual filter paper.
2. Remove 80% of water from the test tube by pouring out directly. If the test tubes are handled with care the sediment is not resuspended which allows for pouring out the water.
3. Resuspend the resulting water and sediment into a mixture and pour though the filter paper folded into a funnel. Resuspend the resulting sediment in the test tube with demiwater and repeat until the left over sediment is negligible.
4. Transfer all filter papers to an oven tray and store in the oven and remove after 45 minutes.
5. Measure weight of the filter paper including sediment.

Applying this method to all obtained test tubes provides the data as presented in appendix B. These data points can be plotted over the width of the experiment table to provide a profile of settled sediment as seen in figure 4.11.

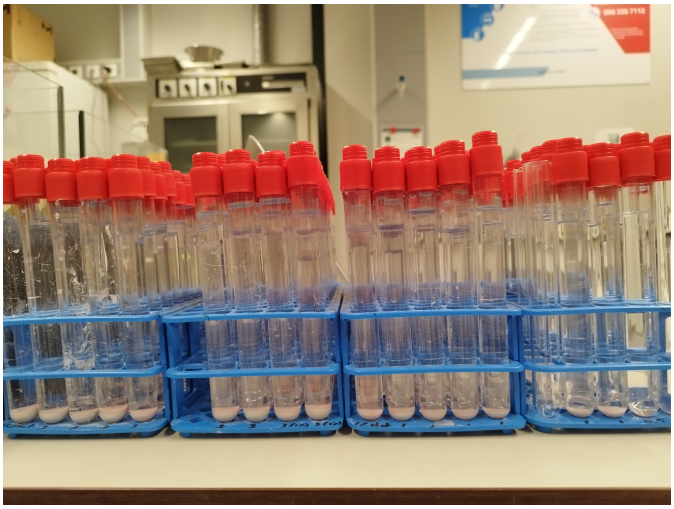

Figure 4.9: Test tubes filled with samples

Figure 4.10: Balance and filters

The resulting data from this is a series of measurements over the width of the table used in the experimental setup. Using these measurements a distribution of sediment settling can be drafted as displayed in figure 4.11. To ensure that the measurement method was sufficiently accurate tests were performed with the filter paper used to filter/weight the sediment.

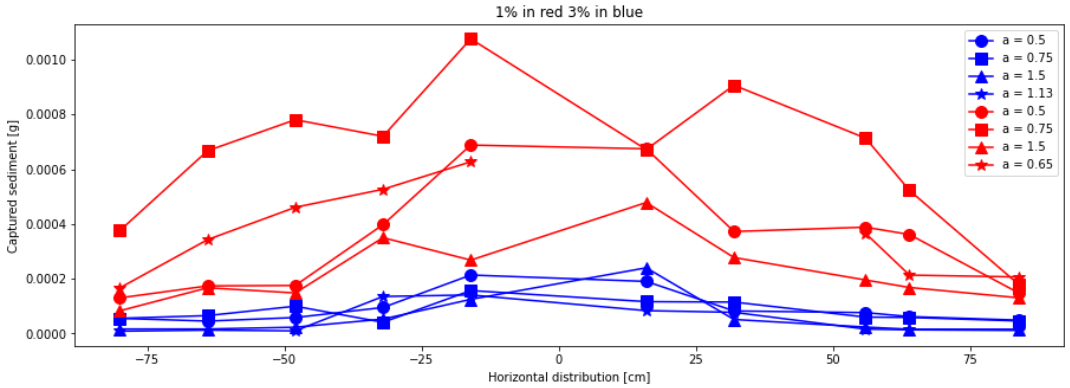

Figure 4.11: Sediment distribution for experimental sequence with 1% and 3% volumetric concentration

To make claims on the quantity of sediment captured during the experiments, the duration of the experiments has to be taken into account. The shorter experiments were finished after 11 seconds, whilst the longer experiments took up to a minute. The sediment flux is kept constant during the experiments and therefore an increase in experiment duration leads to a larger quantity of sediment being pumped into the setup. To investigate the difference in sedimentation for different experiments, the measured sedimentation can be compared to the total influx of sediment. By dividing the results in grams by the total influx of sediment in grams, a normalized value can be obtained.

4.5. Stationary experiments

Two experiments were conducted in which the cart had no velocity. One additional type of data that was gathered is the concentration measurements of the ADV. During the experiment the ADV measured the SNR value, which can be used to determine the concentration in the passing turbidity current. The obtained results do not show concentration measurements that are as expected. The measurements did not show a measurement over time that would indicate a turbidity current passing through the measurement area. One possible reason for this being that the ADV was positioned too high, and was not measuring the passing turbidity current. Visual data was obtained with the same method as for the non-stationary experiments. UVP data was gathered however, the position and direction of the probes were not altered, which led to the velocity profiles not being aimed in the direction of the turbidity current.

5

Analysis and discussion

In this chapter, the results provided in Chapter 4 will be analysed. Relevant trends will be gathered providing a basis to address the research questions. In the analysis the apparent trends will be provided. In the discussion the analysis results will be compared to existing research and probable explanations are provided. Other noteworthy observations or results will also be discussed.

5.1. General observations

For each type of result, some general observations could be made. One general observation that was made was that the temperature of the sediment mixture in the mixing tank increased when the same mixture was used for multiple experiments. One temperature measurement was conducted in which the temperature at the end of the day was 27 degrees Celsius (with 20 degrees as the original temperature). The increased temperature can be explained by the kinetic energy that was added to the sediment mixture by the pumps in the mixing tank. Assuming that the water used to be at room temperature, there is a difference of approximately 7 degrees Celsius, which would lead to a density difference of 1.9 kg/m^3, decreasing the overall negative buoyancy of the mixture. The smallest density difference occurring in the experiments is for the 0.5% runs in which a density difference of 7.3 kg/m^3 was used. For these experiments, the mixing time was lower which indicates that the temperature difference for these experiments would have been smaller. The experiment for which the 7 degrees difference was observed was using a 3% volumetric concentration, the density difference in this case is 44 kg/m^3. In this case the added buoyancy due to temperature is not expected to have led to significant differences in experimental results. It is also expected that the temperature in other experiments did not provide a substantial buoyancy difference. For future experiments it is however advised to measure the temperature for every experiment.

5.1.1. Velocity profiles

The quality of the velocity profiles differs for different experiments. For the experiments with a low concentration the quality decreased, this could either be due to a lack of a turbidity current occurring or due to the low concentration not being measured with sufficient quality by the UVP. Another observation for the velocity profiles is that not all profiles seem to be showing the table bottom at the same location. The UVP used in the experiments did not provide a clear location for the bottom which made estimating the location difficult. This problem was observed in other experiments conducted with the same UVP system and therefore it is expected that this was not due to a mistake in the experiment setup. The bottom location could be estimated by observing where the velocity starting going to zero and by using the dimensions of the test setup.

5.1.2. Cart velocity ratio

The previous chapters have all used the *a* to describe the cart velocity over buoyancy velocity ratio. However, the buoyancy velocity does not have a clear representation and cannot be calculated accurately. The ratio $\zeta = \frac{U_c}{U_D}$ can be calculated using measurements obtained during the experiments and

therefore gives a better representation of the results. In the text and plots, the *a* ratio will still be used to refer to specific experiments or when comparing to other research in which the *a* ratio is used.

5.2. Influence of source velocity

Two sets of experiments were designed to research the influence of the source velocity on the footprint and deposition of the sediment plumes. For two different volumetric concentrations, 1% and 3%, three experiments were conducted researching different ratios of source velocity over discharge velocity. These two sets of experiments were designed to maintain similarity in all aspects except for the source velocity. In this section, the results for both experiment sets will be analysed.

5.2.1. Video results

When analysing the video images obtained during these experiments, one trend that can be observed is that an increase of ζ, and thus an increase in source velocity, leads to smaller angles in the turbidity current at discharge. As observed in figures 5.1 and 5.2, the angle for experiment 9 starts similarly as for experiment 11, however in experiment 9, with $\zeta = 0.7$, impingement occurs, whereas for experiment 11, with $\zeta = 2.6$, no clear impingement occurs. For the experiments with a 1% volumetric concentration, similar results can be observed, with slower source velocities leading to earlier impingement, and this leading to a larger spreading angle. The video footage also shows that for the experiments with a high value of ζ, different behaviour can be observed. In the three experiments with high values for ζ, in the footage, no gravity current can be observed as can be seen in figure 5.4. Instead of the discharged sediment mixture bending down towards the table, the sediment mixture remains suspended. After the sediment mixture is discharged, dilution due to entrainment occurs, after which the sediment settles at low velocities. An observation for the experiments with high values of ζ also shows sediment being suspended into a higher part of the water column, reaching up to double the original discharge height as displayed in figure 5.5.

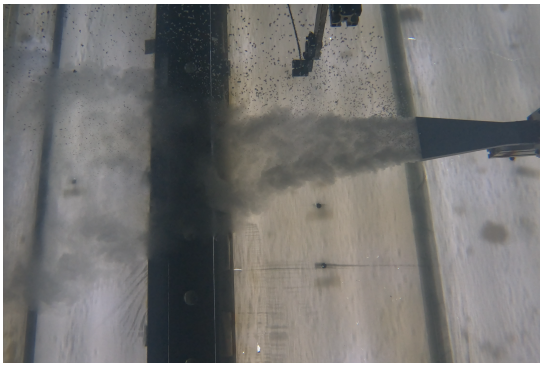

Figure 5.1: Mount view experiment 9, $\zeta = 0.71$

Figure 5.2: Mount view experiment 11, $\zeta = 2.63$

Figure 5.3: Side view experiment 9, $\zeta = 0,71$

Figure 5.4: Side view experiment 11, $\zeta = 2,63$

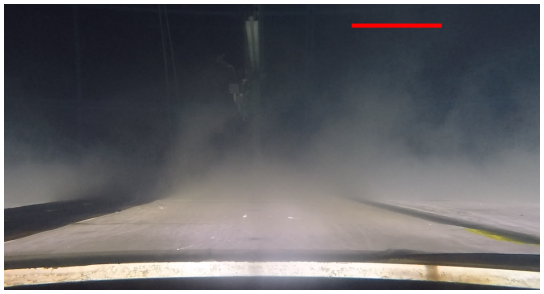

Figure 5.5: Suspended sediment experiment 3, 6 sec after discharge. Including marker for max height

5.2.2. Velocity profiles

The velocity profiles obtained during these experiments show a decrease in transverse turbidity current speed for the higher values of ζ. As can be observed in figure 5.8, there is a decrease in maximum velocity occurring at a higher value of ζ in experiment 11 and a decrease in the experiments for 1%. It can also be observed that for the 3% volumetric concentration experiments, at first, a trend can be observed with a slight increase as plotted in figure 5.8. It should also be noted that the quality of the measurements decreased for the highest and lowest values of ζ, with the measurements for $\zeta = 0.45$ and 0.58 at 0.5% concentration not obtaining any values. Observing the trends in figure 5.8 a difference can be observed for the 3% concentration experiments. The trend for the three lower values of ζ does not continue for the higher value of ζ. The video footage for this situation where $\zeta = 2.63$ shows that sediment remains suspended in the water column for a long time, compared to the experiments with lower values of ζ. In addition, the sediment plume was found to be higher in the situation with a higher cart velocity. For both concentrations, different phenomena can be observed in the situations with high values for ζ, where impingement does not occur after discharge. This leads to the sediment remaining suspended in the same location. The shapes of the turbidity current do not show a clear trend.

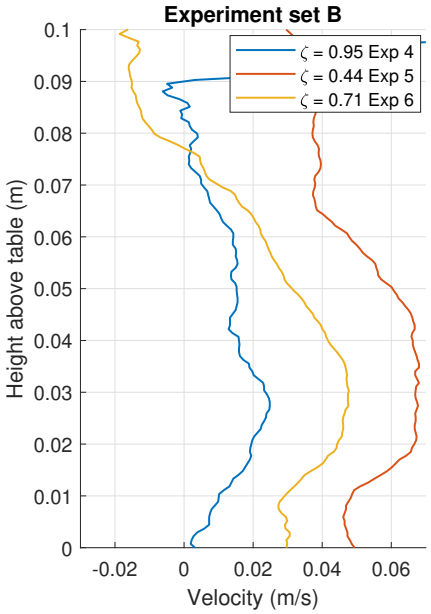

Figure 5.6: Velocity profiles for experiments with a concentration of 1%

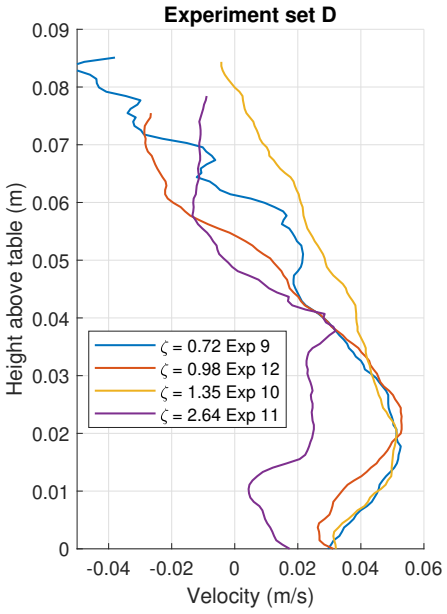

Figure 5.7: Velocity profiles for experiments with a concentration of 3%

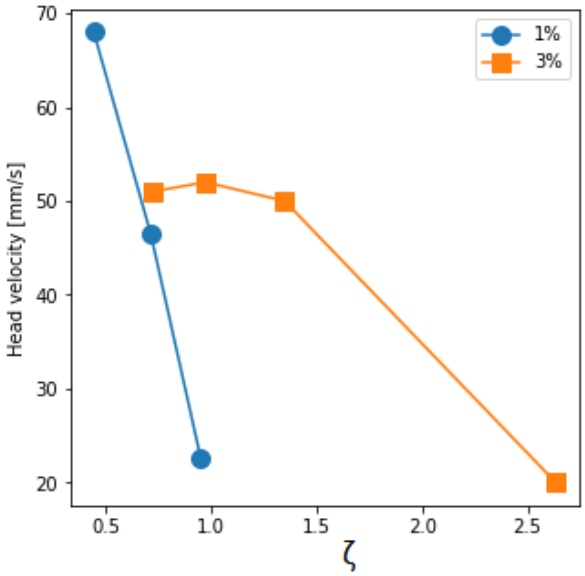

Figure 5.8: Turbidity current head velocity measurements

5.2.3. Sediment trap

The results obtained by the sediment trap do not provide any clear identifiable trends for an influence of the source velocity. The distributions of captured sediment, as displayed in figure 5.9, do not provide a clear link between the ζ ratio and the amount of sediment that gets captured by the sediment trap. For the experiments conducted with a 1% concentration, no clear trend can be observed for different ζ values. The experiments for 3% also do not show a clear trend. One observation that can be made is that the for the highest value of ζ, 2.6 at 3%, significantly less sediment is captured compared to the other experiments.

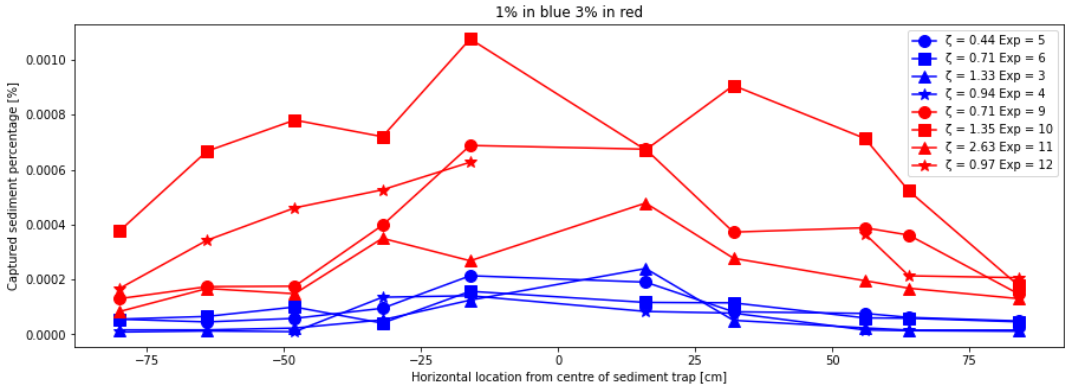

Figure 5.9: Sediment trap results for 1% in blue and 3% in red in percentage of total sediment influx

In figure 5.10 the total amount of sediment, m_s, divided by the total sediment influx is displayed for 1% and 3%. The total sediment influx, I_s was calculated using the discharge velocity, mixture concentration and experiment duration. In this plot it can be observed that the 3% concentration experiments had a higher percent of sediment settling in the sediment trap. For the 3 % concentration, it can also be observed that the higher ζ ratios show a larger percentage of sediment settling than the experiments with lower values of ζ, with the captured amount of sediment doubling. For the 1% concentration experiments a less significant increase can be observed for higher cart velocities.

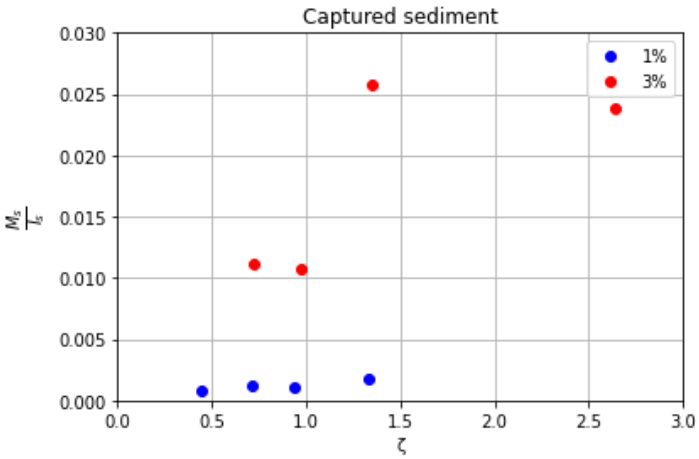

Figure 5.10: Total captured sediment for different values of ζ

5.3. Influence of concentration

For two values of *a*, 0.5 and 0.75, experiments were run using all volumetric concentrations, so 0.5% 1% and 3%. All experiments were conducted using the diffuser designed for 1%, and all experiments used the discharge velocity originally designed for the 1% volumetric concentration, so for these experiments, the sediment flux was not kept equal. Execution of these experiments allows for analysis of the influence of the volumetric concentration. A second comparison can be made between the two experimental sets in which different values of *a* were tested for two different concentrations.

5.3.1. Video footage

When comparing the video footage, a trend similar to the one found in the section on source velocity influence can be found, except now related to concentration. With an increase in concentration, the discharged mixture impinges on the table and starts spreading earlier. In figure 5.11 and 5.13, with 0.5% concentration, it can be observed that the discharged sediment does not impinge close to the discharge, however, a difference can be observed between this situation and what occurs in figure 5.14 with a 3% concentration. The experiments with a lower concentration showed a larger impingement length compared to the experiments with a higher concentration, and a smaller spreading angle. The impingement lengths and spreading angles for two sets of a values are plotted in figure 5.15. The results for the spreading angle show bigger differences for the different values of *a* than the impingement length, however the trend is similar.

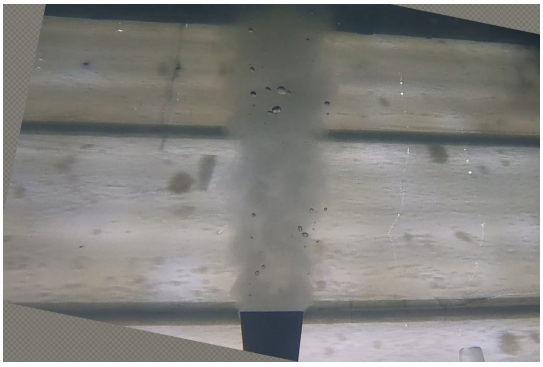

Figure 5.11: Mount view experiment 1, 0.5%

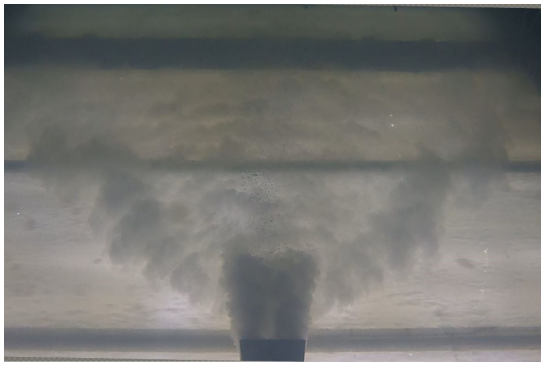

Figure 5.12: Mount view experiment 13, 3%

Figure 5.13: Side view experiment 1, 0.5%

Figure 5.14: Side view experiment 13, 3%

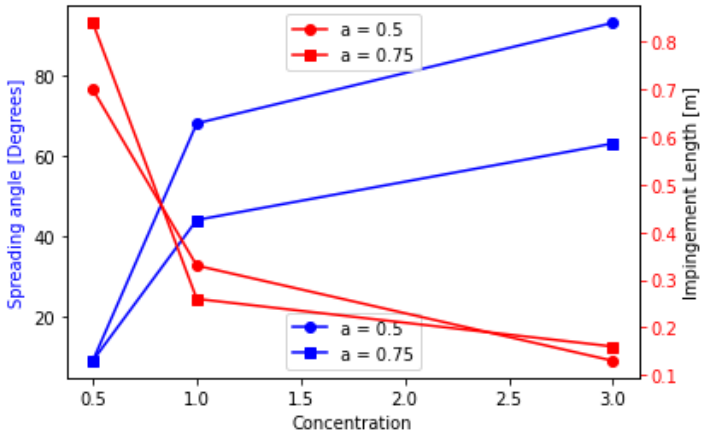

Figure 5.15: Spreading angle and impingement length for different concentrations

5.3.2. Velocity profiles

From the velocity profiles in figure 5.16 and 5.17, it can be observed that an increase in concentration leads to higher velocities. In figure 5.8, it can be observed that there are large differences between the velocity of the turbidity current head for different concentrations, both for the experiments where *a* is equal to 0.5 and for the experiments where *a* is equal to 0.75.

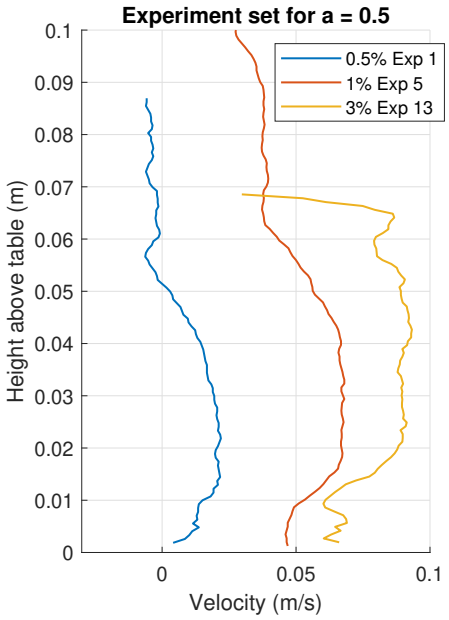

Figure 5.16: Velocity profiles for experiments a = 0.5

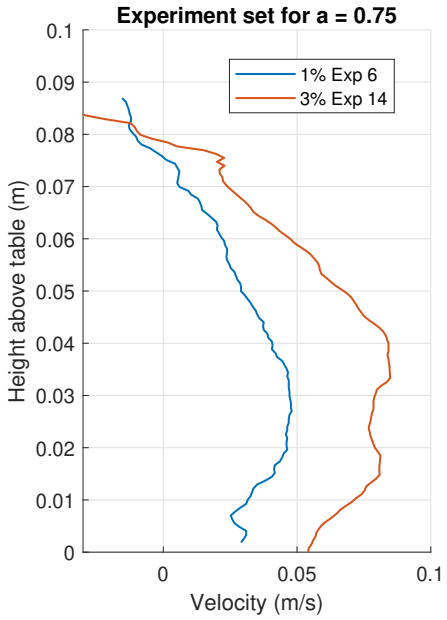

Figure 5.17: Velocity profiles for experiments a = 0.75

5.3.3. Sediment trap

The experiments conducted with different concentrations show minimal differences in the results obtained by the sediment trap. Two different comparisons can be made to analyse the concentration. In set B and D experiments were conducted for a = 0.5 and a = 0.75 where the concentration was the only varying input, and the diffuser, cart speed and discharge velocity were all constant. The experimental results for this data are provided in figure 5.18 in percentage of total sediment influx. Considering the total amount of sediment captured a clear trend can be observed with the higher concentrations leading to more capture sediment. No clear trend can be observed for the experiments with a = 0.5, only that the 3% concentration leads to the highest sedimentation, and in the experiments with a = 0.75, the 0.5% experiment led to the highest concentration. One of the main outliers in the experiment is the

0.5% concentration at *a* equal to 0.75.

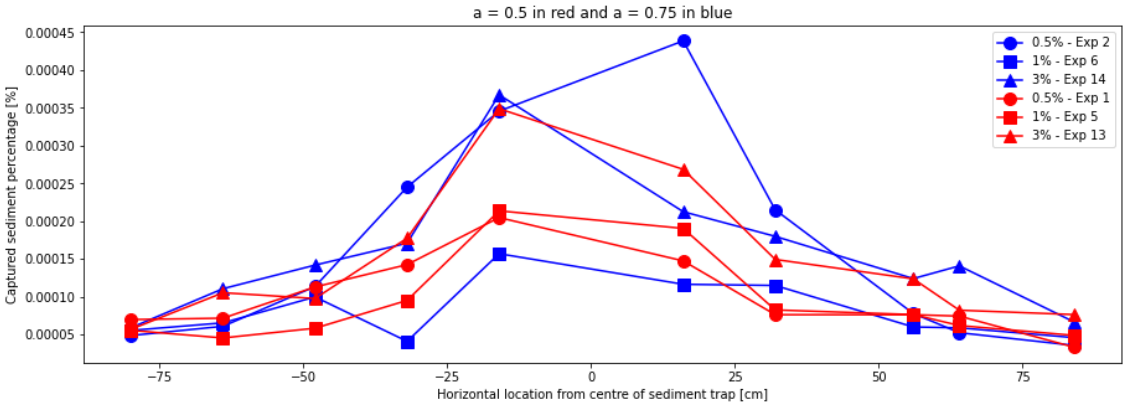

Figure 5.18: Sediment trap results for *a* = 0.5 and *a* =0.75 in percentages

When comparing the experimental sets for 1% and 3% where different diffusers were used, a more clear trend can be observed. All experiments with a 3% concentration had more sedimentation occurring compared to the 1% experiments. In figure 5.9 it can be observed that there is a difference of roughly factor 4 between the experiments with 1% and 3% concentration.

5.4. Influence of densimetric Froude number

To research the influence of the densimetric Froude number, four experiments, group E & F, were conducted wherein the source velocity and discharge velocity were changed so that the densimetric Froude at discharge was equal to 1, or 0.6. For all other experiments, the densimetric Froude number was equal to 1.58. These experiments were conducted mainly out of interest to research if different phenomena occurred.

5.4.1. Video footage

When looking at the experiments conducted with a densimetric Froude of 0.6 or 1 the video results show the same type of behaviour as for other experiments with lower source velocities. In the experiment for Fr = 0.6 at a concentration of 1% and 3% it can be observed that the flow is not fully homogeneous, with higher concentrations showing at the sides of the diffuser. For the experiments where the densimetric Froude is equal to 1, a clear outflow was realised. One comparison that can be made is between experiments where the densimetric Froude is equal to 1.58 and one where the densimetric Froude is 0.6. For experiments 5 and 8 the volumetric concentration and source velocity are equal, only the discharge velocity has been lowered significantly. The main difference that can be observed in this comparison is a change in impingement length, with the higher densimetric Froude leading to an impingement length of 0.33 m and the lower densimetric Froude leading to an impingement length of 0.08 m (see figure 5.19 and 5.20). A comparison between the stationary experiments and the experiments with low Froude number shows that in the stationary experiment the turbidity current moves in all directions (see figure 5.21, in the moving experiments the turbidity current does not move in the direction of cart movement.

Figure 5.19: Side view experiment 5, Fr = 1.58

Figure 5.20: Side view experiment 8, Fr = 0.6

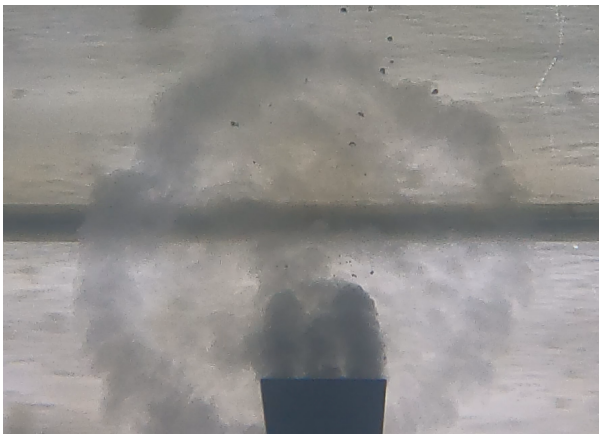

Figure 5.21: Stationary experiment for 3%

5.4.2. Velocity profiles

The comparison between experiments 5 and 8 also shows that the height of the turbidity current is different as can be seen in figure 5.22, with the lower densimetric Froude leading to a lower height. This can be observed in the velocity profile measurements ib figure 5.22. The experiment where the densimetric Froude is equal to 1.58 obtains a clear signal up to a height of 11.5 cm, whilst the lower densimetric Froude only measures up to a height of 7 cm.

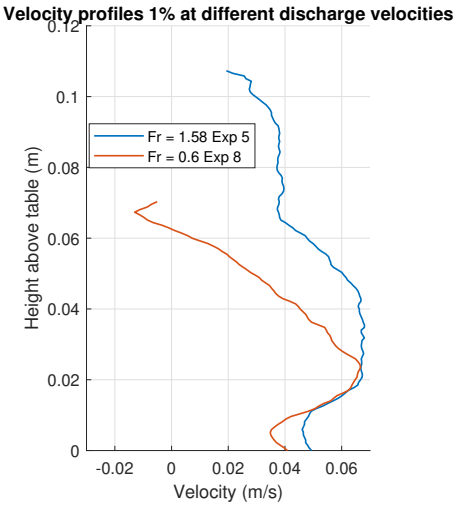

Figure 5.22: Velocity profiles at different Froude numbers

5.4.3. Sediment trap

When comparing the sedimentation profiles of experiment 5 and 8 a difference can be observed in the quantity of captured sediment. With the lower Froude number leading to a higher percentage of sediment settling close to the discharge. The observable assymetry for experiment 8 can be due to the outflow not being fully homogeneous.

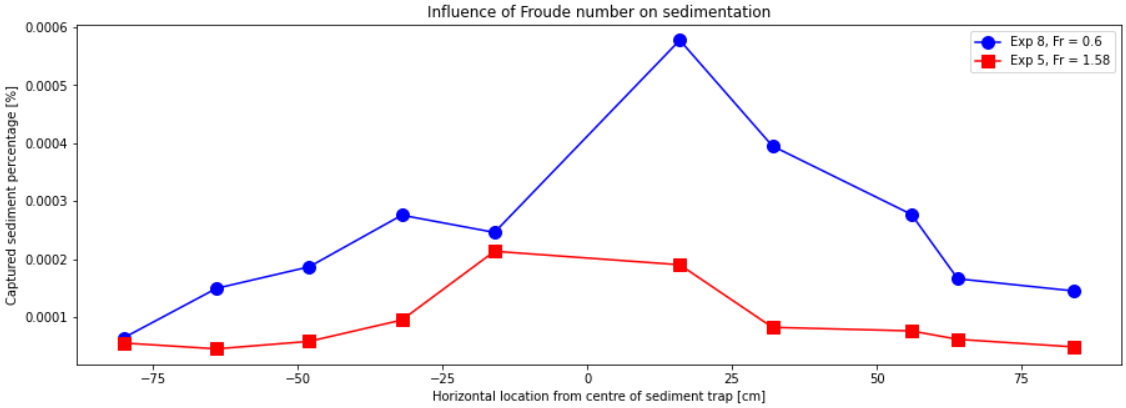

Figure 5.23: Sediment trap results for different Froude numbers

5.5. Discussion

5.5.1. High source velocities

All measurement types show a difference between the experiments with lower values of ζ, and the experiments where ζ was higher. The video data shows that for the experiments with high ζ the discharged sediment mixture has different behaviour that does not represent a clear turbidity current. The observed behaviour in the experiments with a higher source velocity could be explained by two phenomena. Firstly that a higher cart velocity will lead to a larger wake, in the top footage of these experiments a wake pattern can be observed that is similar to a von Karman vortex street as observed in figure 5.24.

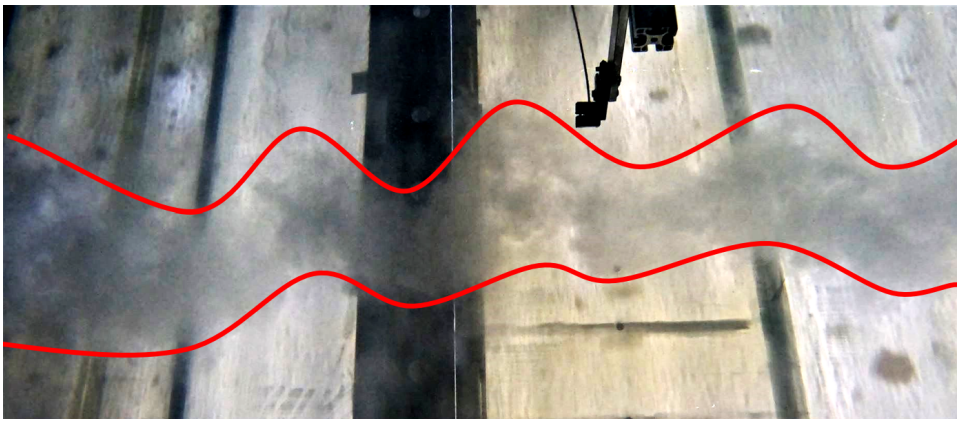

Figure 5.24: Vortex street with added outlines

The turbulence occurring has an alternating pattern that could be due to the wake created by the experimental setup. The Reynolds number for the flow around the test setup is in the order of 10^3 and therefore in the range where vortex shedding can occur. Hence, the appearance of the vortices is likely to be caused by this specific test setup and the scaling approach that was used. A second explanation for the turbulence could be the interaction of the turbulent jet discharged from the diffuser and the ambient fluid. The higher shear between the ambient fluid and the turbulent jet leads to more turbulence which then leads to an increased entrainment rate. Due to this entrainment, the sediment is diluted to low concentrations before it can impinge on the table and turn into a turbidity current. After entrainment, the sediment mixes in the water column, gradually diluting at extremely low velocities until it becomes

unobservable in the footage. The sediment trap captures minimal sediment for the experiments where this regime change is observable. It should also be noted that the sediment that has been captured in this experiment is not only sediment that was captured during the propagation of a turbidity current, but also for the slower settling in the case of higher source velocities. This difference has an impact on the quantity of sediment that was captured.

With the current set of experiments, the cart velocity at which this regime change starts occurring cannot be determined. The consequences of this regime change could have a big impact on the footprint and deposition of sediment. There are different ways in which this could have an impact:

- If the sediment mixture is diluted enough the induced velocity due to density differences can be lower than the velocity of the background current at the DSM site. In this case, the sediment plume will enter a passive transport phase which is governed by the velocity and direction of the ambient current. The sediment plumes resulting from this could be similar to the plume created by interaction of the SMT with the seabed.
- In DSM situations the sediment composition can lead to flocculation. The higher shear occurring between the jet and the ambient fluid, and the resulting turbulence will have an impact on the flocculation occurring. With an increase in shear, more flocculation will occur, which would likely lead to more sediment settling near the discharge location.

5.5.2. Low source velocities

In the experiments conducted at lower source velocities, the observed trends are largely as discussed by Oullion et al. (2021). With a higher source velocity, the spreading angle decreases, and with a higher volumetric concentration, the spreading angle increases. This larger spreading angle can be linked to the results from the UVP that show a higher transverse turbidity current velocity for higher concentrations. From the results obtained by the sediment trap, it can be concluded that a smaller percentage of sediment is captured for the experiments with a lower concentration. A likely reason for this is that the higher mixture density leads to a faster propagating turbidity current, which has an impact on the amount of sediment that is able to settle on the table positioned in the tank before it reaches the end of the table and is partly reflected higher into the water column by the tank wall, in which case part of the sediment might reflect back to the sediment trap, or is reflected downwards along the wall. In a DSM situation where there are no area constraints, this would lead to a larger turbidity current footprint. The sediment that has been captured does not show clear trends on the impact of the difference in cart velocity for the experiments in which the earlier mentioned regime change does not occur.

One difference that can be observed between these experiments and the results obtained by Oullion et al. is that at low cart velocities, the velocity of the turbidity current in the direction of the cart movement is not great enough to catch up with the cart. The experiments by Oullion et al. found a regime change at a = 0.63 between subcritical and supercritical flow. The experiments that were designed to be in this regime did not show the same behaviour. Even the experiments in which the discharge velocity was lowered to simulate a case in which the densimetric Froude was equal to 1 or 0.6 did not show this behaviour. Several potential reasons could explain this phenomenon:

1. One reason for the turbidity current catching up with the cart would be the high propagation speed of the front. Factors that increase the front velocity are concentration and the densimetric Froude number. Experiment 16 was conducted with a low Froude number, a high concentration and a low cart velocity to test whether the turbidity current caught up with the cart. In this situation, the input variables would be ideal for this test setup to simulate the turbidity current catching up with the cart; however, in this experiment, this behaviour was not apparent. Using the calculated U_b and measured cart velocity a can be calculated to be 0.24, which according to the results from Oullion et al. should lead to the gravity current moving ahead of the discharge. One possible reason for this different behaviour is that in the simulations by Oullion et al., the sediment mixture was discharged without any initial horizontal momentum. The experiments conducted in this research discharged the sediment mixture in a horizontal direction away from the cart with a certain discharge velocity. When the sediment mixture impinges on the table, the density difference has curved the momentum of the sediment mixture towards a vertical direction into the table. However, not all horizontal momentum is dissipated before impingement on the table. Due to this,

the spreading after impingement is not radial but is asymmetrical, with more sediment mixture spreading into the direction of the resulting momentum.

2. A second reason why this does not happen but might happen in DSM situations is that in a DSM operation, the SMT will create a larger, more turbulent wake. This wake is likely to have an impact on the impingement zone and, with that, might allow for faster turbidity current propagation towards the SMT. In order to research this situation, more research needs to be conducted into the influence of the wake on the near-field flow of the discharged sediment mixture. The exact impact of this on the footprint and sedimentation of the turbidity current is difficult to determine. However, it is expected that interaction between the turbidity current and the SMT will lead to different transport mechanisms than the turbidity current. For the setup used in this research the wake would not be representative for a real life DSM situation. In this setup the construction between the diffuser and cart created a wake over the entire height of the modular tank. As a result, the vertical aspects of the wake caused by the diffuser did not accurately represent a real-life scenario where fluid flows over the top of an SMT.

Lowering the discharge velocity might be beneficial as it decreases the horizontal momentum of the sediment particles. At higher discharge velocities the angle of impingement is smaller, leading to more energy being transferred into the turbidity currents in the direction of discharge as displayed in figure 5.5.2.

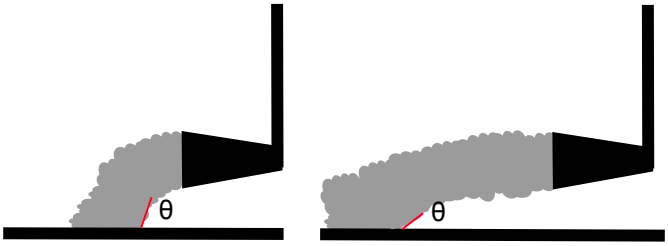

Figure 5.25: Impingement angle for a low discharge velocity (left) and a faster discharge velocity (right)

5.5.3. Richardson number

As mentioned in chapter 2 one way to describe the physics occurring after discharge is through the Richardson number. In figure 5.26 the Richardson numbers for the two experimental series of 1% and 3% have been plotted. The two experiments with the highest Richardson number are the experiments that were designed for the Froude number of 0.6. The high Richardson number indicates that the buoyancy of the discharged fluid is dominant over the momentum, which for these experiments, lead to a small impingement length. The experiments with a lower Richardson number all lead to a higher impingement length. In figure 5.26 the Richardson numbers for the two different experimental series show different trends. For the 1% concentration experiments, figure 5.26 shows an exponential decay. For the 3% concentration experiments, a different trend can be observed, with the lowest Richardson numbers leading to a smaller impingement length. Higher but still subcritical values show an increased impingement length, and then the supercritical value shows a decreased impingement length.

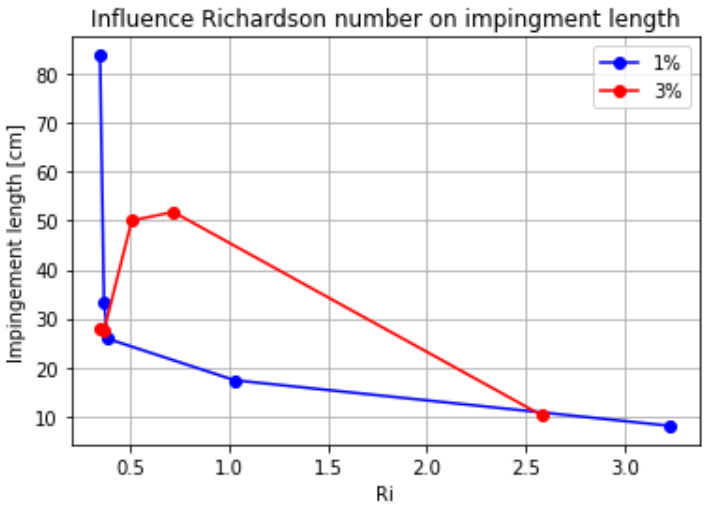

Figure 5.26: Impingement length and Richardson number

Whether the trends observed in figure 5.26 show an actual trend governed by the Richardson number can be doubted. The way in which the impingement length is defined in this research is using an Eulerian framework. In between the discharge and the impingement, the cart will have moved, this movement is currently included in the impingement length. Secondly, more data points are needed to observe an actual trend. However, the current results do indicate that this might be interesting for future research.

5.5.4. Scale effects

One notable aspect to consider is the potential influence of scale effects on the results. The size of the experimental tank, the dimensions of the moving cart, and the nature of the sediment mixture could all contribute to scale effects that might influence the behavior of the turbidity currents observed in the experiments. Part of the experiment that was not scaled correctly was the sediment size. The glass beads used were significantly larger than the sediment found in the CCZ. Actual sediment from the CCZ would have lower settling velocities, which would lead different settling behaviour. Another limiting factor of the experiments was the size of the tank and table used for the experiments. In all experiments the turbidity current would travel to the end of the table where it would be reflected upwards or downwards by the tank wall. This led to interference with the measured sedimentation from the turbidity current. The actual deposition area could also not be determined due to this size limitation.

5.5.5. Optimal SMT configuration

What the optimal SMT configuration would be can be answered in two parts, one part would be discussing whether DSM operations at higher velocities, with the discharged sediment mixture entering more of a passive transport phase would be best. Or whether operating the SMT at lower velocities, and with that leading to sediment transport by turbidity current would be optimal. The second part would be answering what operational characteristics would lead to the least plume dispersion.

Passive transport

To determine whether the observed passive transport will lead to less sediment plume dispersion is difficult. The sediment plume dispersion will be influenced by many different variables, of which many were not part of the scope of this research. Factors that will influence that, but were not part of this scope are:

- During DSM operations flocculation will occur in the sediment, this will have an impact on the settling characteristics of the discharged sediment mixture. For the experiments where a transition to passive transport was observed it is hypothesized that this is due to more turbulence occurring, either due to the wake of the SMT or due to the large velocity difference between the discharged jet and the ambient fluid. In both cases this turbulence would lead to a higher flocculation rate.

- Whether passive transport is likely to lead to more sediment plume dispersion depends on the characteristics of the ambient current in the deep sea. If the velocity of the background current is sufficiently high then it might take over as the dominant sediment transport mechanism.

Optimal turbidity current

For the situations in which the turbidity current is the dominating sediment transport mechanism the SMT characteristics can be changed to lead to different turbidity currents. More sedimentation close to the mining site is considered better as this leads to a lower footprint of the sediment plume. The experimental setup used in this research was not large enough to find the total footprint of the turbidity current, however the results obtained can give an indication on what parameters would have what influence on sediment plume dispersion. One result is that the Froude number at discharge did not have a large impact on the flow behaviour after discharge. Based on this results it might be possible to use a lower discharge velocity without risking that the turbidity current interacts with the SMT. A lower Froude number would lead to less initial energy added to the mixture at discharge and could therefore lead to less sediment dispersion, both in the direction of discharge and the transverse direction. Based on the results obtained using the sediment trap, showing that higher percentage of sediment settled near the discharge, it would be advised to use a higher volumetric concentration. For the source velocity the results show that an increase in velocity led to slower turbidity currents, and more sediment settling near the discharge. Therefore it is advisable to maintain a relatively high source velocity; however, the velocity should not be too high to prevent excessive sediment entry into passive transport.

6

Conclusion and recommendation

In this Chapter the results of the research will be used to provide an answer to the research questions posed in the introduction. The posed research questions are:

- What experimental setup would be optimal to investigate plume spreading in a moving source experiment using sediment particles?
- How will the ratio of source and discharge velocity impact the footprint and deposition of sediment plumes?
- How can modifying the source velocity, mixture concentration, and discharge velocity be used to reduce the plume dispersion in polymetallic nodule harvesting operations?

6.1. Experimental setup

The first research question was aimed at finding the optimal research setup to investigate plume spreading using a moving source. For this research, it was concluded that a Froude scaling would be used alongside several constraints to ensure similar physics occurring at the sediment discharge. Several physical aspects, such as flocculation, cannot be accounted for in this setup. That these physical aspects are missing make the experiments less representative for an actual DSM situation, however to research one aspect, in this case the influence of the source velocity, this is beneficial. The current approach has proven to lead to interesting results, however, improvements could be made to the setup that could lead to better results. Later in this chapter recommendations will be provided on how the improve the experimental setup.

6.2. Influence of source velocity

There is a large influence of the source velocity on the behaviour of the turbidity currents. Two distinctions can be made when looking at the influence of the source velocity. One focusing on the cases with higher velocities, and one focusing on lower velocities. For the higher range of source velocities, a new regime was observed in which a turbidity current cannot be observed, the sediment is suspended higher in the water column. In a real DSM situation this could lead to the sediment entering a passive transport phase dominated by the background current. Consequently, the deposition of sediment under such circumstances can spread over a broader area, contingent upon the characteristics of the background current.

For the lower cart velocities, a trend can be observed that an increase in cart velocity leads to a decrease in the spreading angle (β) and turbidity current velocity, which would lead to a smaller footprint. A second observation is that none of the experiments demonstrated the turbidity current advancing in front of the impingement zone. The main hypothesis for this is that the sediment particles had residual horizontal momentum from the horizontal discharge when impinging on the table. Factors that could influence this residual momentum are the mixture density and the proximity of the diffuser to the table. When the turbidity current does not advance in front of the impingement zone there will be no

interaction between the SMT and the turbidity current, leading to more predictable behaviour and less re-suspension by the SMT.

6.3. Optimal SMT configuration

What the optimal SMT configurations are can be answered in two parts, one part would be discussing whether DSM operations at higher velocities, with the discharged sediment mixture entering more of a passive transport phase would be optimal. The second part is whether operating the SMT at lower velocities and with that leading to sediment transport by a turbidity current would be better, and if so how this turbidity current can be changed to lead to reduce plume dispersion.

6.3.1. Passive transport

Determining whether the observed passive transport will lead to less sediment plume dispersion is hard. The sediment plume dispersion will be influenced by many different variables, of which many were not part of the scope of this research, such as fluctuation and influence of an ambient current.

If future research finds that the footprint and deposition in this regime would be better compared to a turbidity current, this could be used to change the design of the SMT. It is not yet clear if reaching the passive transport regime would be possible, and if it were possible at what velocity the vehicle would need to move. One main difference would be that the width of the SMT could be smaller to mine the same area. This is however dependent on if the collecting efficiency could be maintained for higher velocities.

6.4. Optimal turbidity current

For the situations in which the turbidity current is the dominating sediment transport mechanism, the SMT characteristics can be changed to lead to different turbidity current behaviour. Based on this research it is recommended to have a high source velocity, which will lead to lower transverse turbidity current velocities, leading to a smaller footprint. For the concentration, it is recommended to use a higher concentration when considering a constant sediment flux, which will lead to a higher percentage of sediment settling near the discharge.

6.5. Recommendations

During this research, several points for improvement were found and the results led to some interesting trends that could lead to new insights in future research. In this section recommendations will be provided, first recommendations for future research topics are given. After this practical recommendations regarding the experimental setup used in this research are provided.

6.5.1. Future research

These experiments were the first of its kind in that it included a moving discharge coupled with a sediment discharge. This first series of experiments found some new processes that had not been observed before and therefore might lead to new insights for the DSM industry. The experiments conducted in this research were constrained in time, equipment and knowledge. Based on the new knowledge several recommendations can be made for future experiments to obtain results that represent the actual DSM operations better or that can be used for research into potentially interesting topics.

One recommendation for future research would be to conduct experiments with a better sediment representation in a smaller test setup. In the current experiments glass beads were used which do not resemble the sediment that can be found in the CCZ. By using glass beads an important part of the physics influencing particle settling is also missing; flocculation. In future experiments a sediment type can be used that has similar cohesive properties. This could be either sediment obtained from actual mining sites in the CCZ or by using other cohesive sediment types. For this it is recommended to use a smaller, easier to operate, test setup.

A second recommendation for future research would be to conduct more research into the transition found between passive sediment transport and transport by a turbidity current. The current experimental results show a first indication of this transition happening however more research needs to be conducted on where this exact transition lays, and what impact this transition might have on the dispersion of sediment in DSM operations. The current setup could be used to research this transition by conducting the same type of experiments and extending the test matrix to research the range where the transition is expected to occur. A smaller, easier to handle, setup could also be used to research the transition and might allow for more types of measurement and shorter experiments.

A third recommendation would be to extend the measurements to also obtain concentration measurements of the turbidity currents. Obtaining concentration profiles of the turbidity currents at multiple locations could profile valuable data on the amount of sediment that settles over a distance. One possible method to research sedimentation could be to use higher quality cameras and a different table that allows for visual inspection of sedimentation on the table. Concentration profiles could either be conducted by taking samples from inside the tank, or by using equipment that measures signals that can be used to determine the concentration.

6.5.2. Practical recommendations

During the execution of the experiments multiple practical improvement points were found that would improve the accuracy and ease of similar experiments.

- The methods used to obtain a specific concentration of sediment mixture could be improved. During the experiments it was noticed that the setup used to keep the sediment homogeneously suspended in the mixing tank was not perfect and that over time sediment started accumulating at some locations of the bottom of the mixing tank. The concentration was measured minutes before commencement of the experiment. For future experiments a system should be used that either inputs more energy into the mixing tank, by for example adding more pumps, or the energy should be distributed differently so that the mixture is kept homogeneous. The concentration measurements could be conducted over the entire experiment by fixing the ADV in the mixing tank and taking measurements in front of the pump inlet.
- For future experiments action should be taken to prevent algea growth. Over time the clarity of the water in the modular flume started becoming blurry, leading to a decrease in the video footage quality. One proposed method would be to use sodium hypochlorite solution, as is used in the

TU Delft towing tank. Based on communication with the towing tank team one liter with a 12.5% solution would work for the modular flume.

- For the stationary experiments the procedure needs to be improved and the measurement setup should be altered. One problem for the stationary experiments was that the UVP could not obtain accurate velocity profiles due to the probes not being aligned with the flow direction. The concentration of the mixture at measurement location also influenced measurement quality and can be altered to improve velocity measurements. In future experiments the positioning of the probes could be altered or a different method for obtaining velocity could be implemented. Another improvement for the stationary experiments would be to place the ADV at a height where it would be able to obtain better concentration and velocity measurements of the turbidity current, as the location used in this research did not measure an area where the turbidity current passed through.
- A measurement device to obtain the exact velocity of the cart could be implemented. This would increase the accuracy and would remove the time needed to calculate the cart velocity manually
- Recording the flow velocity during the entire experiment should be done using the KATFLOW velocity meter to ensure that the discharge velocity is constant.
- To determine the impingement length a more precise method could be used that uses a Lagrangian approach instead of the currently used Eulerian frame. This would remove the influence of the cart velocity on the visually observed impingement length.
- Add markers to the diffusers to make recognizing the diffuser easier in the top and mounted view of experiments.

References

[1] Rahul Sharma, ed. *Deep-Sea Mining: Resource Potential, Technical and Environmental Considerations*. en. Cham: Springer International Publishing, 2017. ISBN: 978-3-319-52556-3 978-3-319-52557-0. DOI: 10.1007/978-3-319-52557-0. URL: http://link.springer.com/10.1007/978-3-319-52557-0 (visited on 12/08/2022).

[2] Xiaohong Wang and Werner E.G. Müller. "Marine biominerals: perspectives and challenges for polymetallic nodules and crusts". en. In: *Trends in Biotechnology* 27.6 (June 2009), pp. 375–383. ISSN: 01677799. DOI: 10.1016/j.tibtech.2009.03.004. URL: https://linkinghub.elsevier.com/retrieve/pii/S0167779909000754 (visited on 12/07/2022).

[3] *NORI and Allseas Lift Over 3,000 Tonnes of Polymetallic Nodules to Surface from Planet's Largest Deposit of Battery Metals, as Leading Scientists and Marine Experts Continue Gathering Environmental Data | The Metals Company*. en. Nov. 2022. URL: https://investors.metals.co/news-releases/news-release-details/nori-and-allseas-lift-over-3000-tonnes-polymetallic-nodules/ (visited on 07/30/2023).

[4] *Greenpeace confronts deep sea mining vessel to highlight threat to ocean*. en-US. Section: Oceans. Nov. 2022. URL: https://www.greenpeace.org/usa/news/greenpeace-confronts-deep-sea-mining-vessel-to-highlight-threat-to-ocean/ (visited on 12/15/2022).

[5] Catarina Demony, Helen Reid, and Catarina Demony. "France's Macron says deep-sea mining must not go ahead". en. In: *Reuters* (June 2022). URL: https://www.reuters.com/business/environment/frances-macron-says-deep-sea-mining-must-not-go-ahead-2022-06-30/ (visited on 12/15/2022).

[6] Karen McVeigh. "Germany calls for 'precautionary pause' before deep-sea mining industry starts". en-GB. In: *The Guardian* (Nov. 2022). ISSN: 0261-3077. URL: https://www.theguardian.com/environment/2022/nov/02/germany-calls-for-precautionary-pause-before-deep-sea-mining-industry-starts (visited on 12/15/2022).

[7] Tom Cassauwers. *Deep-sea mining: is it an environmental curse or could it save us? | Research and Innovation*. en. Aug. 2021. URL: https://ec.europa.eu/research-and-innovation/en/horizon-magazine/deep-sea-mining-it-environmental-curse-or-could-it-save-us (visited on 12/08/2022).

[8] Kathryn A. Miller et al. "An Overview of Seabed Mining Including the Current State of Development, Environmental Impacts, and Knowledge Gaps". en. In: *Frontiers in Marine Science* 4 (Jan. 2018), p. 418. ISSN: 2296-7745. DOI: 10.3389/fmars.2017.00418. URL: http://journal.frontiersin.org/article/10.3389/fmars.2017.00418/full (visited on 12/07/2022).

[9] Yoshio Masuda, Michael J. Cruickshank, and John L. Mero. "Continuous Bucket-Line Dredging at 12,000 Feet". en. In: *Offshore Technology Conference*. Houston, Texas: Offshore Technology Conference, 1971. DOI: 10.4043/1410-MS. URL: http://www.onepetro.org/doi/10.4043/1410-MS (visited on 12/08/2022).

[10] Blue Nodules. *Blue Nodules Summary - Deep sea mining*. Aug. 2020. URL: https://www.youtube.com/watch?v=pCus0hTsibc (visited on 12/15/2022).

[11] Keh-Sik Min and Jae-Yong Shim. "Conceplual Design of a Hybrid Pick-up Device for Deep O..an Mining". en. In: (1997).

[12] A.M. Lang et al. *Blue Nodules Deliverable report D3.4 Report describing the process flow overview*. Tech. rep. Blue Nodules, Jan. 2021. URL: https://blue-nodules.eu/download/public_reports/public_reports/Blue-Nodules-688975-D3.4-Report-describing-the-process-flow-overview-FINAL.pdf (visited on 12/08/2022).

[13] Diva J. Amon et al. “Assessment of scientific gaps related to the effective environmental management of deep-seabed mining”. en. In: *Marine Policy* 138 (Apr. 2022), p. 105006. ISSN: 0308597X. DOI: 10.1016/j.marpol.2022.105006. URL: https://linkinghub.elsevier.com/retrieve/pii/S0308597X22000537 (visited on 11/17/2022).

[14] Rob Williams et al. “Noise from deep-sea mining may span vast ocean areas”. In: *Science* 377.6602 (July 2022). Publisher: American Association for the Advancement of Science, pp. 157–158. DOI: 10.1126/science.abo2804. URL: https://www.science.org/doi/full/10.1126/science.abo2804 (visited on 12/12/2022).

[15] Daniel O. B. Jones, Diva J. Amon, and Abbie S. A. Chapman. “Mining Deep-Ocean Mineral Deposits: What are the Ecological Risks?” en. In: *Elements* 14.5 (Oct. 2018), pp. 325–330. ISSN: 1811-5217, 1811-5209. DOI: 10.2138/gselements.14.5.325. URL: https://pubs.geoscienceworld.org/msa/elements/article/14/5/325/559104/Mining-DeepOcean-Mineral-Deposits-What-are-the (visited on 11/17/2022).

[16] Tanja Stratmann et al. “Abyssal plain faunal carbon flows remain depressed 26 years after a simulated deep-sea mining disturbance”. en. In: *Biogeosciences* 15.13 (July 2018), pp. 4131–4145. ISSN: 1726-4189. DOI: 10.5194/bg-15-4131-2018. URL: https://bg.copernicus.org/articles/15/4131/2018/ (visited on 12/12/2022).

[17] Philip Weaver and David Billett. “Environmental Impacts of Nodule, Crust and Sulphide Mining: An Overview”. In: May 2019, pp. 27–62. ISBN: 978-3-030-12695-7. DOI: 10.1007/978-3-030-12696-4_3.

[18] J.O. Rodriguez. *Small scale testing of crawler outlet diffusers for plume reduction of offshore mining*. Tech. rep. Sept. 2019. (Visited on 11/22/2022).

[19] B K Blankenaar. *The deep sea mining horizontal discharge plume*. en. Tech. rep. TU Delft, June 2020.

[20] Yannick Wijmans. “Horizontal negatively buoyant jets in deep sea mining”. en. PhD thesis. TU Delft, Nov. 2021.

[21] Thomas Peacock and Raphael Ouillon. “The Fluid Mechanics of Deep-Sea Mining”. en. In: *Annual Review of Fluid Mechanics* 55.1 (Jan. 2023), annurev–fluid–031822–010257. ISSN: 0066-4189, 1545-4479. DOI: 10.1146/annurev-fluid-031822-010257. URL: https://www.annualreviews.org/doi/10.1146/annurev-fluid-031822-010257 (visited on 11/17/2022).

[22] Raphael Ouillon et al. “Gravity currents from moving sources”. en. In: *Journal of Fluid Mechanics* 924 (Oct. 2021), A43. ISSN: 0022-1120, 1469-7645. DOI: 10.1017/jfm.2021.654. URL: https://www.cambridge.org/core/product/identifier/S0022112021006546/type/journal_article (visited on 11/15/2022).

[23] G. Shanmugam. “Shanmugam, G. 2020. Gravity flows: Types, definitions, origins, identification markers, and problems. Journal Indian Association of Sedimentologists, Vol. 37, Issue 2, p. 61-90.” In: (Jan. 2020), pp. 61–90.

[24] R. A. Bagnold. “Auto-Suspension of Transported Sediment; Turbidity Currents”. In: *Proceedings of the Royal Society of London. Series A, Mathematical and Physical Sciences* 265.1322 (1962). Publisher: The Royal Society, pp. 315–319. ISSN: 0080-4630. URL: https://www.jstor.org/stable/2414168 (visited on 01/25/2023).

[25] HJS Fernando. *Handbook of Environmental Fluid Dynamics, Volume One*. en. Dec. 2012. ISBN: 978-1-4398-1669-1. URL: https://learning.oreilly.com/library/view/handbook-of-environmental/9781439816691/ (visited on 07/26/2023).

[26] Mohamed Elerian, Cees van Rhee, and Rudy Helmons. “Experimental and Numerical Modelling of Deep-Sea-Mining-Generated Turbidity Currents”. en. In: *Minerals* 12.5 (May 2022). Number: 5 Publisher: Multidisciplinary Digital Publishing Institute, p. 558. ISSN: 2075-163X. DOI: 10.3390/min12050558. URL: https://www.mdpi.com/2075-163X/12/5/558 (visited on 07/26/2023).

[27] Frank M. White and Rhim Yoon Chul. *Fluid mechanics*. eng. Eighth edition in SI units. McGraw-Hill series in mechanical engineering. New York, NY: McGraw-Hill education, 2016. ISBN: 978-981-4720-17-5.

[28] Jasim Imran et al. “Froude scaling limitations in modeling of turbidity currents”. en. In: *Environmental Fluid Mechanics* 17.1 (Feb. 2017), pp. 159–186. ISSN: 1573-1510. DOI: 10.1007/s10652-016-9488-6. URL: https://doi.org/10.1007/s10652-016-9488-6 (visited on 12/13/2022).

[29] Hugo B. Fischer et al. *Mixing in Inland and Coastal Waters*. en. Google-Books-ID: ki9wPH2j1EcC. Academic Press, 1979. ISBN: 978-0-12-258150-2.

[30] Hai-Bo Chen. “TURBULENT BUOYANT JETS AND PLUMES IN FLOWING AMBIENT ENVIRONMENTS”. en. In: (1991).

[31] Mijanur R. Chowdhury and Firat Y. Testik. “A review of gravity currents formed by submerged single-port discharges in inland and coastal waters”. en. In: *Environmental Fluid Mechanics* 14.2 (Apr. 2014), pp. 265–293. ISSN: 1573-1510. DOI: 10.1007/s10652-014-9334-7. URL: https://doi.org/10.1007/s10652-014-9334-7 (visited on 01/04/2023).

[32] Carlos Muñoz-Royo et al. “An in situ study of abyssal turbidity-current sediment plumes generated by a deep seabed polymetallic nodule mining preprototype collector vehicle”. en. In: *Science Advances* 8.38 (Sept. 2022), eabn1219. ISSN: 2375-2548. DOI: 10.1126/sciadv.abn1219. URL: https://www.science.org/doi/10.1126/sciadv.abn1219 (visited on 11/17/2022).

[33] Philip J. W. Roberts, Adrian Ferrier, and Greg Daviero. “Mixing in Inclined Dense Jets”. en. In: *Journal of Hydraulic Engineering* 123.8 (Aug. 1997), pp. 693–699. ISSN: 0733-9429, 1943-7900. DOI: 10.1061/(ASCE)0733-9429(1997)123:8(693). URL: https://ascelibrary.org/doi/10.1061/%28ASCE%290733-9429%281997%29123%3A8%28693%29 (visited on 02/07/2023).

[34] Ilias G. Papakonstantis and George C. Christodoulou. “Spreading of round dense jets impinging on a horizontal bottom”. en. In: *Journal of Hydro-environment Research* 4.4 (Dec. 2010), pp. 289–300. ISSN: 1570-6443. DOI: 10.1016/j.jher.2010.07.001. URL: https://www.sciencedirect.com/science/article/pii/S1570644310000699 (visited on 01/29/2023).

[35] Robert M. Dorrell and Andrew J. Hogg. “Length and Time Scales of Response of Sediment Suspensions to Changing Flow Conditions”. en. In: *Journal of Hydraulic Engineering* 138.5 (May 2012), pp. 430–439. ISSN: 0733-9429, 1943-7900. DOI: 10.1061/(ASCE)HY.1943-7900.0000532. URL: https://ascelibrary.org/doi/10.1061/%28ASCE%29HY.1943-7900.0000532 (visited on 01/29/2023).

[36] Mathew G. Wells and Robert M. Dorrell. “Turbulence Processes Within Turbidity Currents”. en. In: *Annual Review of Fluid Mechanics* 53.1 (Jan. 2021), pp. 59–83. ISSN: 0066-4189, 1545-4479. DOI: 10.1146/annurev-fluid-010719-060309. URL: https://www.annualreviews.org/doi/10.1146/annurev-fluid-010719-060309 (visited on 11/17/2022).

[37] S. Altinakar, W. H. Graf, and E. J. Hopfinger. “Weakly depositing turbidity current on a small slope”. In: *Journal of Hydraulic Research* 28.1 (Jan. 1990). Publisher: Taylor & Francis _eprint: https://doi.org/10.1080/00221689009499147, pp. 55–80. ISSN: 0022-1686. DOI: 10.1080/00221689009499147. URL: https://doi.org/10.1080/00221689009499147 (visited on 01/29/2023).

[38] Octavio E. Sequeiros, Rodrigo Mosquera, and Francisco Pedocchi. “Internal Structure of a Self-Accelerating Turbidity Current”. en. In: *Journal of Geophysical Research: Oceans* 123.9 (2018). _eprint: https://onlinelibrary.wiley.com/doi/pdf/10.1029/2018JC014061, pp. 6260–6276. ISSN: 2169-9291. DOI: 10.1029/2018JC014061. URL: https://onlinelibrary.wiley.com/doi/abs/10.1029/2018JC014061 (visited on 01/29/2023).

[39] M. Ashraful Islam and Jasim Imran. “Vertical structure of continuous release saline and turbidity currents”. en. In: *Journal of Geophysical Research: Oceans* 115.C8 (2010). ISSN: 2156-2202. DOI: 10.1029/2009JC005365. URL: https://onlinelibrary.wiley.com/doi/abs/10.1029/2009JC005365 (visited on 01/29/2023).

[40] G. Postma and M. J. B. Cartigny. “Supercritical and subcritical turbidity currents and their deposits–A synthesis”. en. In: *Geology* 42.11 (Nov. 2014), pp. 987–990. ISSN: 0091-7613, 1943-2682. DOI: 10.1130/G35957.1. URL: https://pubs.geoscienceworld.org/geology/article/42/11/987-990/131469 (visited on 02/03/2023).

[41] Octavio E. Sequeiros. “Estimating turbidity current conditions from channel morphology: A Froude number approach”. en. In: *Journal of Geophysical Research: Oceans* 117.C4 (2012). _eprint: https://onlinelibrary.wiley.com/doi/pdf/10.1029/2011JC007201. ISSN: 2156-2202. DOI: 10.1029/2011JC007201. URL: https://onlinelibrary.wiley.com/doi/abs/10.1029/2011JC007201 (visited on 02/03/2023).

[42] G V Middleton. “Sediment Deposition from Turbidity Currents”. In: *Annual Review of Earth and Planetary Sciences* 21.1 (1993). _eprint: https://doi.org/10.1146/annurev.ea.21.050193.000513, pp. 89–114. DOI: 10.1146/annurev.ea.21.050193.000513. URL: https://doi.org/10.1146/annurev.ea.21.050193.000513 (visited on 01/26/2023).

[43] R. E. Burns. “Assessment of environmental effects of deep ocean mining of manganese nodules”. en. In: *Helgoländer Meeresuntersuchungen* 33.1-4 (Mar. 1980), pp. 433–442. ISSN: 0017-9957, 1438-3888. DOI: 10.1007/BF02414768. URL: http://link.springer.com/10.1007/BF02414768 (visited on 01/27/2023).

[44] Mohamed Elerian et al. “Near-Field Analysis of Turbidity Flows Generated by Polymetallic Nodule Mining Tools”. en. In: *Mining* 1.3 (Nov. 2021), pp. 251–278. ISSN: 2673-6489. DOI: 10.3390/mining1030017. URL: https://www.mdpi.com/2673-6489/1/3/17 (visited on 12/06/2022).

[45] Sape A. Miedema. “Dredging Engineering: Special Topics”. en. In: *TU Delft OPEN Textbooks* (June 2019). ISBN: 9789463661744. URL: https://textbooks.open.tudelft.nl/textbooks/catalog/view/22/47/144-1 (visited on 01/27/2023).

[46] Wilford Gardner. “Sediment trap dynamics and calibration: a laboratory evaluation.” In: *Journal of Marine Research* 38 (Jan. 1980), pp. 17–39.

[47] Willord D Gardner. “Field assessment of sediment traps”. en. In: *Journal of Marine Research* (Sept. 1997).

[48] *Sediment Traps*. en-US. URL: https://mclanelabs.com/sediment-traps/ (visited on 01/17/2023).

[49] Boudewijn Decrop et al. “EXPERIMENTAL INVESTIGATION OF NEGATIVELY BUOYANT SEDIMENT PLUMES RESULTING FROM DREDGING OPERATIONS”. en. In: (2012), p. 10.

[50] Yu Dai et al. “Numerical analysis on hydrodynamic characteristics of a deep-sea mining vehicle under three typical motions | Elsevier Enhanced Reader”. en. In: (Feb. 2021). DOI: 10.1016/j.oceaneng.2021.109446. URL: https://reader.elsevier.com/reader/sd/pii/S0029801821008519?token=196DE0CE1BCCDEDC291FA0CA253ECBE8857128F16C32CF0B60040243D72C2448ADBCE0FA6592D60FBA46E19A94763DBE&originRegion=eu-west-1&originCreation=20230109105711 (visited on 01/09/2023).

[51] A. Roshko. “Perspectives on bluff body aerodynamics”. en. In: *Journal of Wind Engineering and Industrial Aerodynamics* 49.1-3 (Dec. 1993), pp. 79–100. ISSN: 01676105. DOI: 10.1016/0167-6105(93)90007-B. URL: https://linkinghub.elsevier.com/retrieve/pii/016761059390007B (visited on 01/12/2023).

[52] I. P. Castro and A. G. Robins. “The flow around a surface-mounted cube in uniform and turbulent streams”. en. In: *Journal of Fluid Mechanics* 79.2 (Feb. 1977), pp. 307–335. ISSN: 0022-1120, 1469-7645. DOI: 10.1017/S0022112077000172. URL: https://www.cambridge.org/core/product/identifier/S0022112077000172/type/journal_article (visited on 01/12/2023).

[53] Ayan Kumar Banerjee and Santosh Kumar Singh. “Parametric investigation of spatio-temporal variability of submerged body hydrodynamics | Elsevier Enhanced Reader”. en. In: (Feb. 2022). DOI: 10.1016/j.apor.2022.103152. URL: https://reader.elsevier.com/reader/sd/pii/S0141118722001018?token=6102FE2DB637092646111C3AD0E480DE734A1E61E2FC4957D4341E0E4B5A4001D9348D7205C9148CF46397AD85B56129&originRegion=eu-west-1&originCreation=20230112094248 (visited on 01/12/2023).

[54] J.F. Derakhshandeh and Md Mahbub Alam. “A review of bluff body wakes | Elsevier Enhanced Reader”. en. In: (Apr. 2019). DOI: 10.1016/j.oceaneng.2019.04.093. URL: https://reader.elsevier.com/reader/sd/pii/S0029801818307418?token=F9B4CA4528391C41AE722631ADCB33FFE46DDE493579D86F4EC870043A31267CCDD9DABA7CCE961980A9FD9D4AD322DA&originRegion=eu-west-1&originCreation=20230109123739 (visited on 01/09/2023).

[55] Claudio Mannini, Ante Soda, and Gunter Schewe. “Unsteady RANS modelling of flow past a rectangular cylinder: Investigation of Reynolds number effects | Elsevier Enhanced Reader”. en. In: (May 2010). DOI: 10.1016/j.compfluid.2010.05.014. URL: https://reader.elsevier.com/reader/sd/pii/S0045793010001271?token=9E292E1E6DF197C1F4963ED36EAB1748178A386D1547DE8057D17E77AB825A4A732C5B005F322C7B44EC2A5B320D563E&originRegion=eu-west-1&originCreation=20230208132924 (visited on 02/08/2023).

[56] Metflow. *UVP-Duo Manual*. Jan. 2002.

[57] Remo Cossu and Matthew Wells. “A comparison of the shear stress distribution in the bottom boundary layer of experimental density and turbidity currents | Elsevier Enhanced Reader”. en. In: (Oct. 2011). DOI: 10.1016/j.euromechflu.2011.09.006. URL: https://reader.elsevier.com/reader/sd/pii/S0997754611000926?token=438A356BBCDD3BDD86CD770A6A64D69600C297C7A855F39EDA62100D868CB7FBC1BB0A0F9F2286587BD5E26647842655&originRegion=eu-west-1&originCreation=20230130151232 (visited on 01/30/2023).

A

Video capture results

A.1. Mounted view

For this view some pictures are tilted due to the camera moving during the experiments. These pictures have been rotated to give the original perspective.

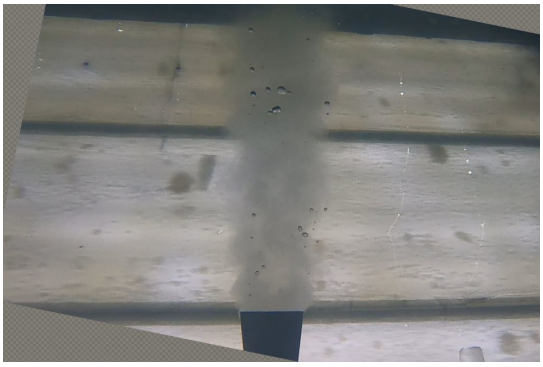

Figure A.1: Mounted view Experiment 1

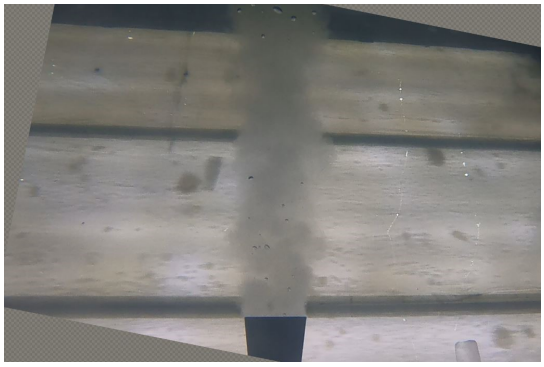

Figure A.2: Mounted view Experiment 2

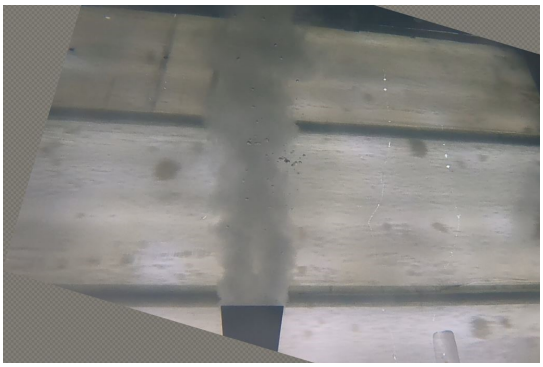

Figure A.3: Mounted view Experiment 3

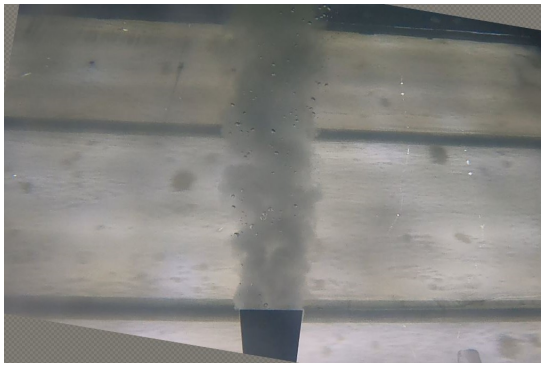

Figure A.4: Mounted view Experiment 4

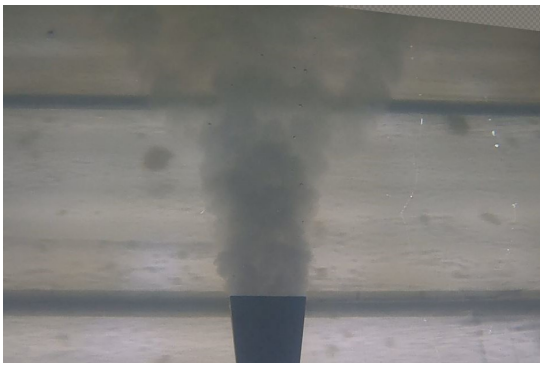

Figure A.5: Mounted view Experiment 5

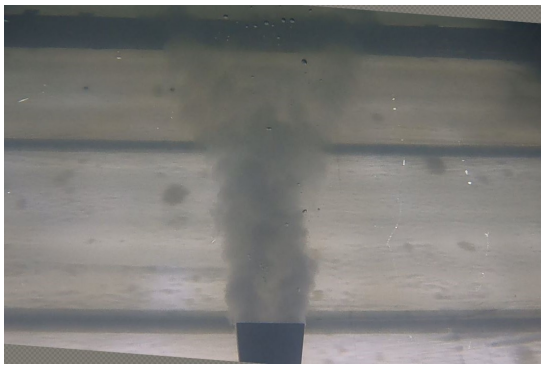

Figure A.6: Mounted view Experiment 6

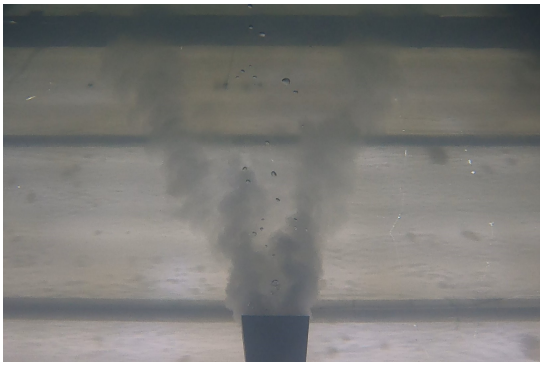

Figure A.7: Mounted view Experiment 7

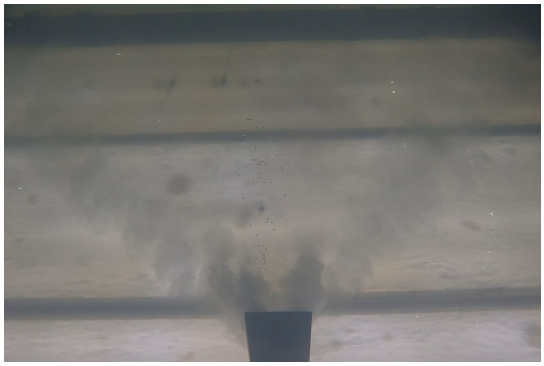

Figure A.8: Mounted view Experiment 8

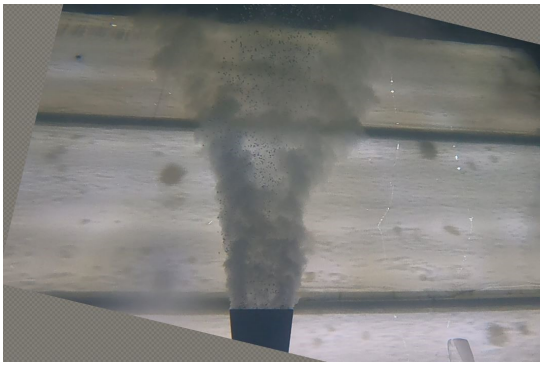

Figure A.9: Mounted view Experiment 9

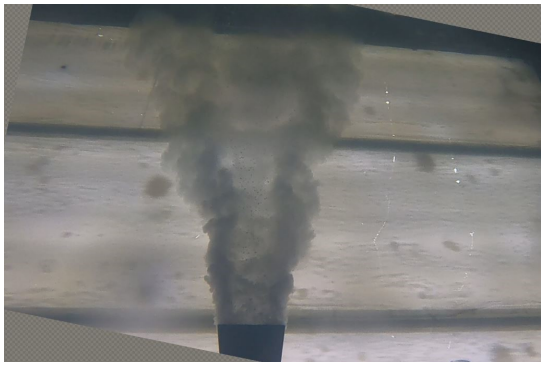

Figure A.10: Mounted view Experiment 10

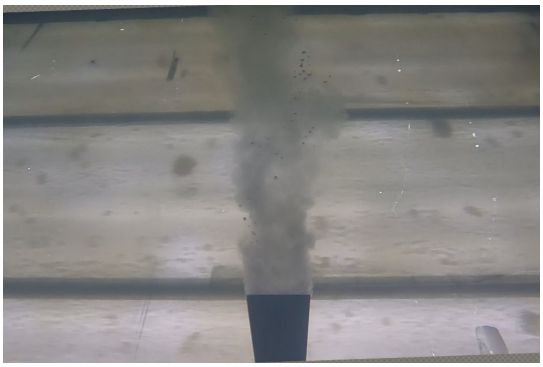

Figure A.11: Mounted view Experiment 11

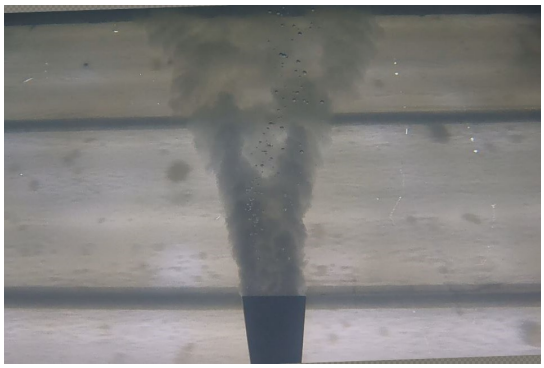

Figure A.12: Mounted view Experiment 12

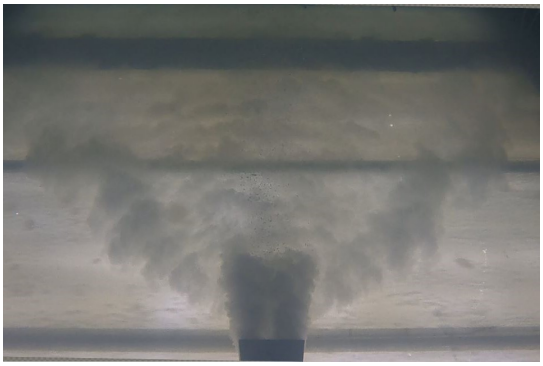

Figure A.13: Mounted view Experiment 13

Figure A.14: Mounted view Experiment 14

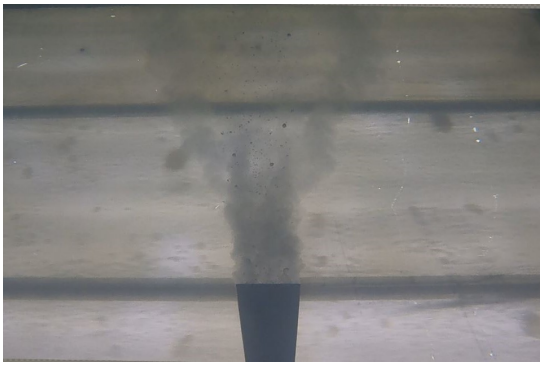

Figure A.15: Mounted view Experiment 15

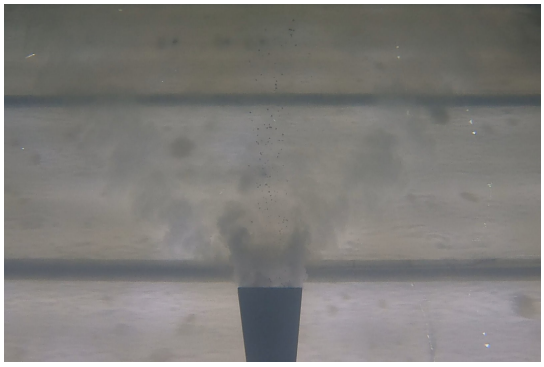

Figure A.16: Mounted view Experiment 16

A.2. Top view

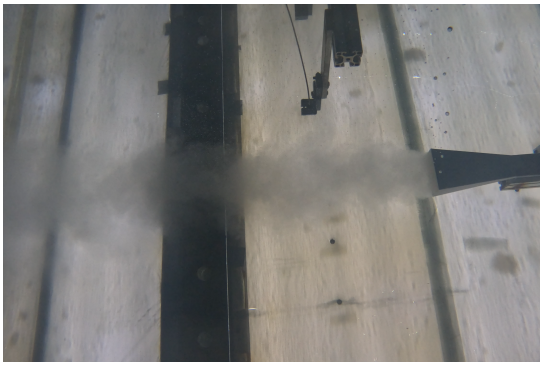

Figure A.17: Top view Experiment 1

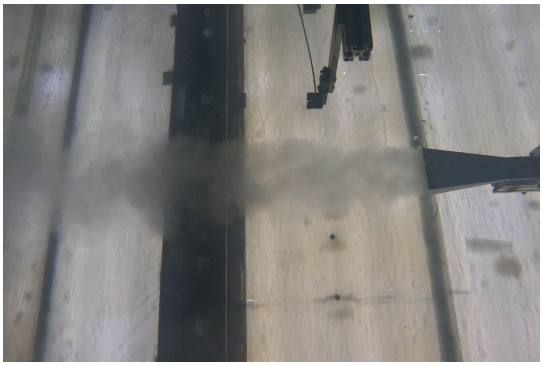

Figure A.18: Top view Experiment 2

Figure A.19: Top view Experiment 3

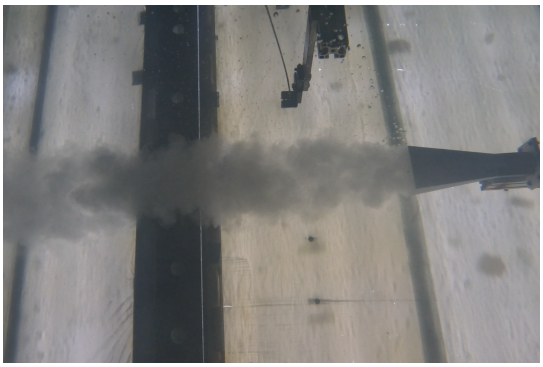

Figure A.20: Top view Experiment 4

Figure A.21: Top view Experiment 5

Figure A.22: Top view Experiment 6

Figure A.23: Top view Experiment 7

Figure A.24: Top view Experiment 8

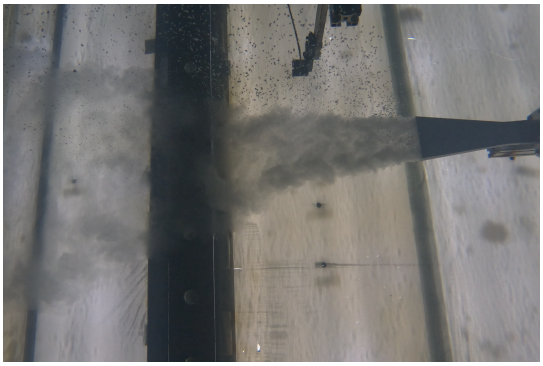

Figure A.25: Top view Experiment 9

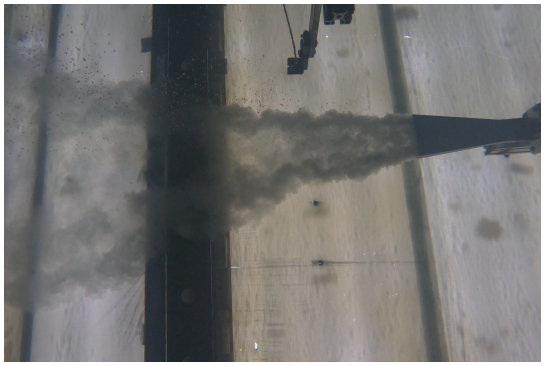

Figure A.26: Top view Experiment 10

Figure A.27: Top view Experiment 11

Figure A.28: Top view Experiment 12

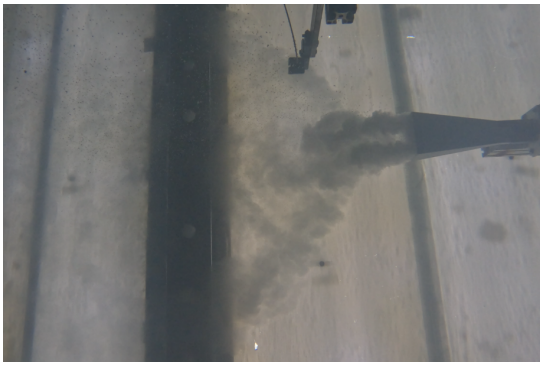

Figure A.29: Top view Experiment 13

Figure A.30: Top view Experiment 14

Figure A.31: Top view Experiment 15

Figure A.32: Top view Experiment 16

A.3. Side view

Figure A.33: Side view Experiment 1

Figure A.34: Side view Experiment 2

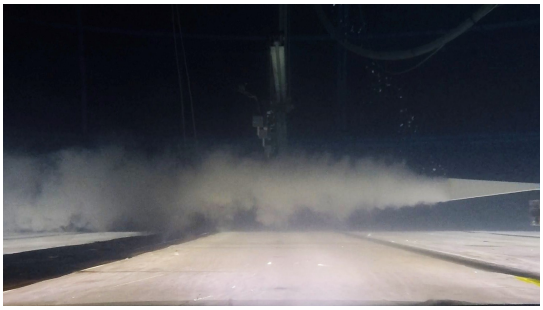

Figure A.35: Side view Experiment 3

Figure A.36: Side view Experiment 4

Figure A.37: Side view Experiment 5

Figure A.38: Side view Experiment 6

Figure A.39: Side view Experiment 7

Figure A.40: Side view Experiment 8

Figure A.41: Side view Experiment 9

Figure A.42: Side view Experiment 10

Figure A.43: Side view Experiment 11

Figure A.44: Side view Experiment 12

Figure A.45: Side view Experiment 13

Figure A.46: Side view Experiment 14

Figure A.47: Side view Experiment 15

Figure A.48: Side view Experiment 16

B

Sediment trap results

In this appendix the results obtained by the sediment trap will be provided. Two types of data will be provided, first the raw data will be provided as obtained from the balance. Secondly the normalized values will be given, which were calculated by dividing the captured sediment with the total amount of sediment influx during the experiment. Several data points are missing due to errors in the measurement process, these values have been removed and replaced with a ”-”.

	Irregular <– Sediment trap –>Regular									
Position [cm]	-80	-64	-48	-32	-16	16	32	56	64	84
1	0,023	0,023	0,037	0,046	0,067	0,048	0,025	0,025	0,024	0,011
2	0,005	0,006	0,012	0,026	0,037	0,047	0,023	0,008	0,006	0,004
3	0,006	0,006	0,008	0,018	0,042	0,081	0,017	0,008	0,005	0,005
4	0,004	0,006	0,005	0,067	0,069	0,041	0,038	0,008	0,007	0,006
5	0,066	0,054	0,070	0,113	0,254	0,226	0,098	0,091	0,074	0,058
6	0,039	0,046	0,070	-	0,110	0,082	0,081	0,042	0,041	0,032
7	0,023	0,055	0,089	0,095	0,220	0,124	0,051	0,068	0,060	0,022
8	0,040	0,092	0,114	0,169	0,151	0,353	0,242	0,170	0,102	0,089
9	0,041	0,055	0,056	0,126	0,218	0,214	0,118	0,123	0,115	0,047
10	0,097	0,172	0,201	0,185	0,277	0,173	0,233	0,184	0,135	0,046
11	0,008	0,016	0,014	0,033	0,026	0,046	0,026	0,019	0,016	0,012
12	0,059	0,122	0,164	0,187	0,223	-	-	0,130	0,076	0,074
13	0,130	0,239	0,222	0,403	0,792	0,610	0,339	0,281	0,187	0,174
14	0,079	0,148	0,190	0,229	0,492	0,285	0,241	0,166	0,189	0,089
15	0,011	0,030	0,033	0,049	0,113	0,110	0,097	0,037	0,034	0,014
16	0,027	0,052	0,082	0,156	0,179	0,263	0,170	0,102	0,084	0,035
17	0,078	0,216	0,314	0,569	0,743	0,710	0,677	0,603	0,435	0,330
18	0,211	0,430	0,547	0,720	0,816	0,774	0,531	0,445	0,327	0,230

Table B.1: Sediment trap data in grams

	Irregular <– Sediment trap –>Regular									
Position	-80	-64	-48	-32	-16	16	32	56	64	84
1	0,070	0,072	0,113	0,143	0,205	0,148	0,076	0,076	0,075	0,033
2	0,049	0,061	0,114	0,245	0,346	0,439	0,215	0,078	0,053	0,036
3	0,017	0,017	0,023	0,053	0,125	0,240	0,051	0,024	0,016	0,016
4	0,009	0,013	0,010	0,135	0,141	0,084	0,078	0,016	0,014	0,012
5	0,056	0,046	0,059	0,095	0,214	0,191	0,083	0,077	0,062	0,049
6	0,056	0,066	0,100	-	0,157	0,117	0,115	0,060	0,059	0,046
7	0,039	0,093	0,150	0,158	0,368	0,207	0,085	0,114	0,100	0,037
8	0,065	0,150	0,187	0,276	0,246	0,577	0,395	0,277	0,166	0,145
9	0,130	0,174	0,176	0,398	0,688	0,675	0,373	0,389	0,362	0,148
10	0,376	0,667	0,781	0,720	1,076	0,672	0,907	0,714	0,523	0,178
11	0,083	0,167	0,148	0,350	0,268	0,479	0,278	0,196	0,168	0,130
12	0,167	0,343	0,461	0,527	0,627	-	-	0,366	0,213	0,207
13	0,057	0,105	0,098	0,178	0,349	0,269	0,149	0,124	0,082	0,077
14	0,059	0,111	0,142	0,171	0,367	0,213	0,180	0,124	0,141	0,067
15	0,027	0,075	0,082	0,121	0,281	0,275	0,243	0,091	0,084	0,034
16	0,081	0,159	0,249	0,473	0,545	0,800	0,516	0,309	0,256	0,105

Table B.2: Normalized sediment trap data in ‰

C

Velocity profiles

In this appendix the velocity profiles gathered with the UVP will be provided. The profiles have been plotted in their subgroup. For experiments 1, 2 and 3 no accurate velocity profiles could be obtained.

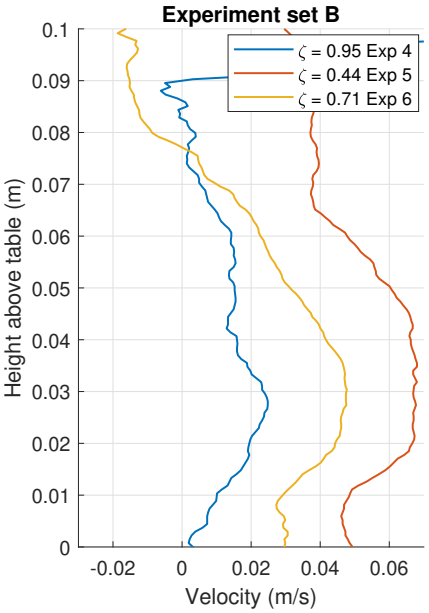

Figure C.1: Velocity profiles Set B

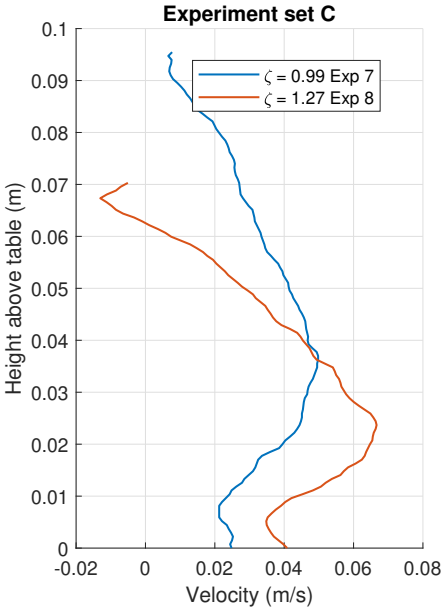

Figure C.2: Velocity profiles Set C

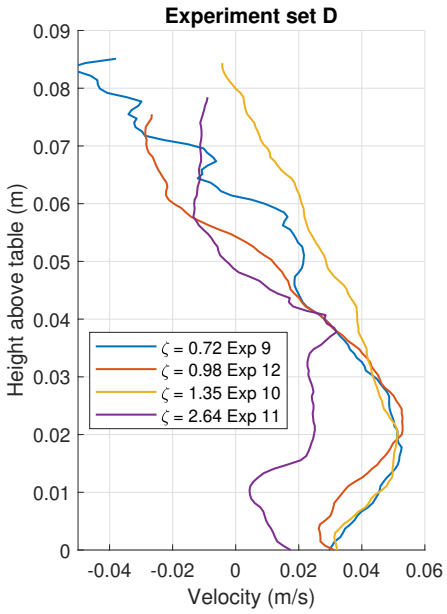

Figure C.3: Velocity profiles Set D

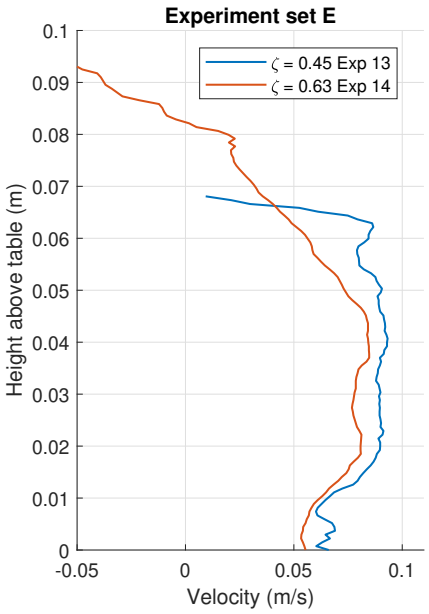

Figure C.4: Velocity profiles Set E

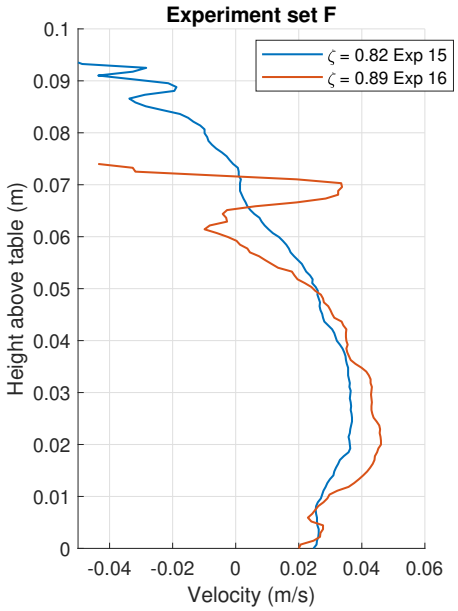

Figure C.5: Velocity profiles Set F